

Die approbierte Originalversion dieser Dissertation ist an der Hauptbibliothek der Technischen Universität Wien aufgestellt (<http://www.ub.tuwien.ac.at>).

The approved original version of this thesis is available at the main library of the Vienna University of Technology (<http://www.ub.tuwien.ac.at/englweb/>).



TECHNISCHE
UNIVERSITÄT
WIEN

VIENNA
UNIVERSITY OF
TECHNOLOGY

PhD Thesis

Dissertation

PHOTOPOLYMERS FOR BONE TISSUE ENGINEERING

ausgeführt zum Zwecke der Erlangung des akademischen Grades eines Doktors der
technischen Wissenschaften unter der Leitung von

Ao. Univ. Prof. Dr. Robert Liska

Institut für Angewandte Synthesechemie

Technische Universität Wien

von

Monika Schuster

9925298

Margaretenstrasse 56/2/20

A-1050 Wien

Wien, am 19.5.2008

An dieser Stelle möchte ich meinem Betreuer Robert Liska meinen tiefen Dank ausdrücken. Seine Ideen, seine Motivation und Unterstützung haben maßgeblich zu meiner gesamten Arbeit beigetragen.

Bei Herrn Heinrich Gruber möchte ich mich für die Aufnahme unter „seinen Makromolekülen“ und sein fortlaufendes Interesse an meiner Arbeit bedanken.

Herrn Franz Varga und Frau Claudia Turecek von LBIO, Hanusch-KH, Herrn Günter Weigel von der Universitätsklinik für Chirurgie, Herrn Günter Russmüller und Herrn Christian Schopper von der Universitätsklinik für Mund-, Kiefer- und Gesichtschirurgie, Herrn Volker Schmid von Joanneum Research Weiz, sowie Herrn Jürgen Stampfl vom Institut für Werkstoffkunde und Materialprüfung an der TU Wien möchte ich für die hervorragende Zusammenarbeit danken. Mein spezieller Dank gilt Robert Inführ, Christian Heller und Stefan Baudis für die Anfertigung unzähliger 3D Strukturen und für ebenso unzählige fruchtbare Gespräche. Äußerst positive und ertragreiche Zusammenarbeit fand auch mit Martina Sandholzer und Christian Slugovc vom Institut für Chemie und Technologie organischer Stoffe der TU Graz statt, die ich dankend erwähnen möchte.

Bei all meinen „Qualpraktikanten“, allen voran Alex aus Spanien, der sehr lange bei mir „gedient“ hat, möchte ich mich herzlich bedanken. Sie alle haben einen wichtigen Beitrag zu dieser Arbeit geleistet.

Finanzielle Unterstützung fand meine Arbeit einerseits beim FWF (N-703), andererseits bei der Österreichischen Akademie der Wissenschaften im Rahmen eines Doc-fForte Stipendiums, wofür ich mich herzlich bedanken möchte.

Mein Dank gilt auch allen Kolleginnen, Kollegen und Mitarbeitern des Instituts, die mich in meiner Arbeit unterstützt haben, nie um einen kompetenten Ratschlag verlegen waren und stets um eine angenehme Arbeitsatmosphäre bemüht waren.

Mein ganz spezieller Dank richtet sich schließlich an meine Eltern, die mir das Studium ermöglicht und mich immer vorbehaltlos unterstützt haben, sowie an Andi, Vreni, Roni, Deen und alle anderen, für ihre liebevolle Unterstützung, Motivation und ihren unerschütterlichen Glauben an mich.

ABSTRACT

Wouldn't it be good to be able to make a bone implant, even one with complex individual geometry, only a few hours after a computer tomography of the injured site has been made? Rapid Prototyping techniques and in particular Stereolithography, a computerized fabrication technique that works with layer-by-layer photopolymerization, offer great possibilities for the fabrication of medical devices in any conceivable shape to copy nature's designs and architecture. Although efforts have been made in the development of biodegradable polymers that serve as temporary tissue replacement until healing is completed, only few of the existing materials are processable by Stereolithography. Furthermore, many of these polymers are based on polyesters (e.g. poly(lactic acid)) that follow an autocatalytic hydrolytic degradation mechanism which is disadvantageous for larger implantation sites as they can appear in orthopedic surgery.

The purpose of this research project was the development of a new liquid acrylate-based monomer formulation for the fabrication of cellular bone replacement materials using Stereolithography. Potential components were systematically tested regarding their reactivity, biocompatibility and mechanical properties. To introduce biodegradability, an enzymatic gelatin hydrolysate was modified with methacrylic groups to obtain a photopolymerizable crosslinker with an enzymatically cleavable backbone. Further modifications had to be carried out in order to improve the compatibility with the remaining monomer formulation. Finally different test objects were constructed.

KURZFASSUNG

Wäre es nicht wünschenswert, wenige Stunden nach der Computer Tomographie Aufnahme eines verletzten Knochengewebeteils ein Patienten-individuelles Implantat bereitstellen zu können, egal wie komplex die Geometrie auch sein mag? Rapid Prototyping Techniken und im speziellen Stereolithographie, ein computerisiertes Fertigungsverfahren das auf schichtweiser Photopolymerisation beruht, bietet großartige Möglichkeiten medizinische Implantate in jeder denkbaren Form herzustellen und natürliche Strukturen nachzubauen. Obwohl großer Aufwand in der Entwicklung bioabbaubarer Polymere betrieben wurde und wird, die als zeitweiliges Stützmaterial während der Heilung beschädigten Gewebes dienen, sind doch nur wenige dieser neuen Materialien mittels Stereolithographie verarbeitbar. Des Weiteren basieren viele dieser Polymere auf Polyester Strukturen (z.B. Polymilchsäure) und folgen einem autokatalytischen, hydrolytischen Abbaumechanismus, der sich bei größeren Defekten, wie sie in der orthopädischen Chirurgie auftreten können, nachteilig auswirkt.

Ziel und Zweck dieser Arbeit war die Entwicklung einer neuen Acrylat-basierten Monomer Formulierung für die stereolithographische Herstellung zellulärer Knochenersatzmaterialien. Potentielle Komponenten wurden systematisch bezüglich ihrer Photoreaktivität, Biokompatibilität und mechanischen Eigenschaften getestet. Um Bioabbaubarkeit zu induzieren wurde ein enzymatisches Gelatinehydrolysat herangezogen und mit methacrylischen Gruppen versehen. Auf diese Weise wurde ein enzymatisch spaltbarer Vernetzer gewonnen. Weitere Modifikationen waren notwendig um die Kompatibilität dieses Vernetzers mit der übrigen Monomer Formulierung zu gewährleisten. Schlussendlich konnten zelluläre Test-Strukturen mittels Stereolithographie hergestellt werden.

Table of Contents

Introduction	3		
1 Bone	3		
2 Biomaterials	8		
3 Rapid Prototyping of tissue engineering scaffolds	15		
Objective	22	Experimental	
State of the art	24		
Results and Discussion	31		81
1 Basis Monomer.....	31		81
1.1 Synthesis of gelatin derivatives.....	32		81
1.1.1 Gelatin hydrolysate – methacrylate (GM)	81		
1.1.2 Gelatine hydrolysate – PEG-methacrylate (GPMM).....	83		
1.1.2.1 Preparation of monomehtacrylate-PEG-acid	83		
1.1.2.2 Preparation of monomethacrylate-PEG-NHS.....	84		
1.1.2.3 Preparation of GPMM.....	85		
1.1.3 Gelatin hydrolysate – PEG, methacrylate (GPM and GP4M).....	86		
1.1.3.1 Preparation of monomethyl-PEG-acid.....	86		
1.1.3.2 Preparation of monomethyl-PEG-NHS	87		
1.1.3.3 Modification of GH with monomethyl-PEG-NHS.....	88		
1.1.3.4 Preparation of GPM and GP4M.....	89		
1.1.4 Gelatin hydrolysate – linolic amide, methacrylate (GLM).....	91		
1.1.4.1 Preparation of linolic acid NHS ester	91		
1.1.4.2 Modification of GH with linolic acid	92		
1.1.4.3 Preparation of GLM.....	93		
1.2 Testing	40	94	
1.2.1 GPC and MALDI-TOF	40	94	
1.2.2 Compatibility with acrylic monomers	41	94	
1.2.3 Cytotoxicity.....	42	95	
2 Reactive Diluents.....	44	95	
2.1 Selection of monomers.....	44	95	
2.2 Testing.....	47	96	

2.2.1	Photoreactivity	48	96
2.2.2	Mechanical Properties.....	51	97
2.2.3	Biocompatibility.....	55	99
3	Additives.....	58	101
3.1	Photoinitiators	58	101
3.1.1	Low molecular weight photoinitiators.....	59	101
3.1.2	Development of migration stable photoinitiators	60	101
3.1.2.1	General Investigations on the photoreactivity of eosin..	61	101
3.1.2.2	Preparation of macromolecular photoinitiators.....	65	101
3.1.2.3	Characterization of macromolecular photoinitiators.....	67	102
3.1.2.3.1	Photoreactivity	67	102
3.1.2.3.2	Migration Stability	69	102
3.1.2.3.3	In vitro LD50	72	102
3.2	Further Additives.....	72	
3.2.1	Fillers	72	
3.2.2	Absorbers	73	
4	3D-Structuring	73	103
4.1	Digital light processing	74	103
4.2	Micro-Stereolithography	77	104
4.3	Two Photon Absorption Polymerization.....	79	104
Materials and Methods		105	
Conclusion		107	
Abbreviations		110	
Appendix I		112	
Appendix II		123	
References		124	

Introduction

1 Bone

Bone is a dynamic tissue with a unique capacity to heal and remodel without leaving a scar. It performs several integral functions in the maintenance of body systems, such as protection of vital organs, providing support and site for muscle attachment for locomotion, generation of red and white blood cells for immunoprotection and oxygenation of other tissues, retaining reserve stores of calcium, phosphate, and other important ions, and providing housing to hematopoietic stem cells in the bone marrow.^{1,2} Therefore pathologies of bone can be very serious, affecting a wide range of body functions. Bone deficiencies can result from abnormal development, tumors or general trauma.

Tissues in general are not purely made up of cells, the smallest individual unit of every living matter, but rather are a combination of specific cells and extracellular matrix. Tissues can roughly be categorized as epithelial, muscle, nervous, and connective tissues. Together with cartilage, ligament, and tendon, bone belongs to the group of connective tissues, which have relatively small numbers of cells and much more extracellular matrix than other tissues.¹ Most of the outstanding properties of bone are related to its extracellular matrix constitution and its hierarchical organization. It is composed of an organic phase, an inorganic biomineral phase occupying approximately half of the extracellular space by volume, and water. The organic part of bone consists of 90% type I collagen, a fibrillar (structural) protein providing the framework for the skeletal structure and being concerned with the matrix calcification. The remaining 10% are made up of other proteins, polysaccharides, and glycoproteins. The bone mineral is a highly substituted biological analogue of the mineral hydroxyl apatite (HA) with the base composition $\text{Ca}_5(\text{PO}_4)_3\text{OH}$ and a hexagonal crystal structure. These crystals appear as nanometer-scale plates (20-80 nm long and 4-5 nm thick) and fuse in both directions, laterally and longitudinally, forming long and broad sword-blade structures. Together with collagen fibrils these crystals organize first into parallel ordered layers (lamellae) and then into higher-order cylindrical structures called osteons, through which a central neurovascular canal is running (Haversian

canal). Due to the local orientation variations of the collagen fibrils and mineral plates, the elastic response of bone is anisotropic. The tubular structure at larger length scales reinforces this anisotropy, resulting in an elastic modulus along the long axis of femoral cortical bone that is 1.5 times the transverse value.¹

At a structural level, bone is arranged in two architectural forms: trabecular, also called cancellous or spongy bone (20% of the total skeleton) and cortical or compact bone (80% of the total skeleton).³ Both have approximately the same material density, but trabecular bone is macroscopically porous with a relative density of less than 0.7, making its modulus and ultimate compressive strength around 20 times inferior to that of cortical bone. In a whole bone, such as the femur, both types of bone are present, with cortical bone forming a protective shell around the porous trabecular bone (Figure 1).

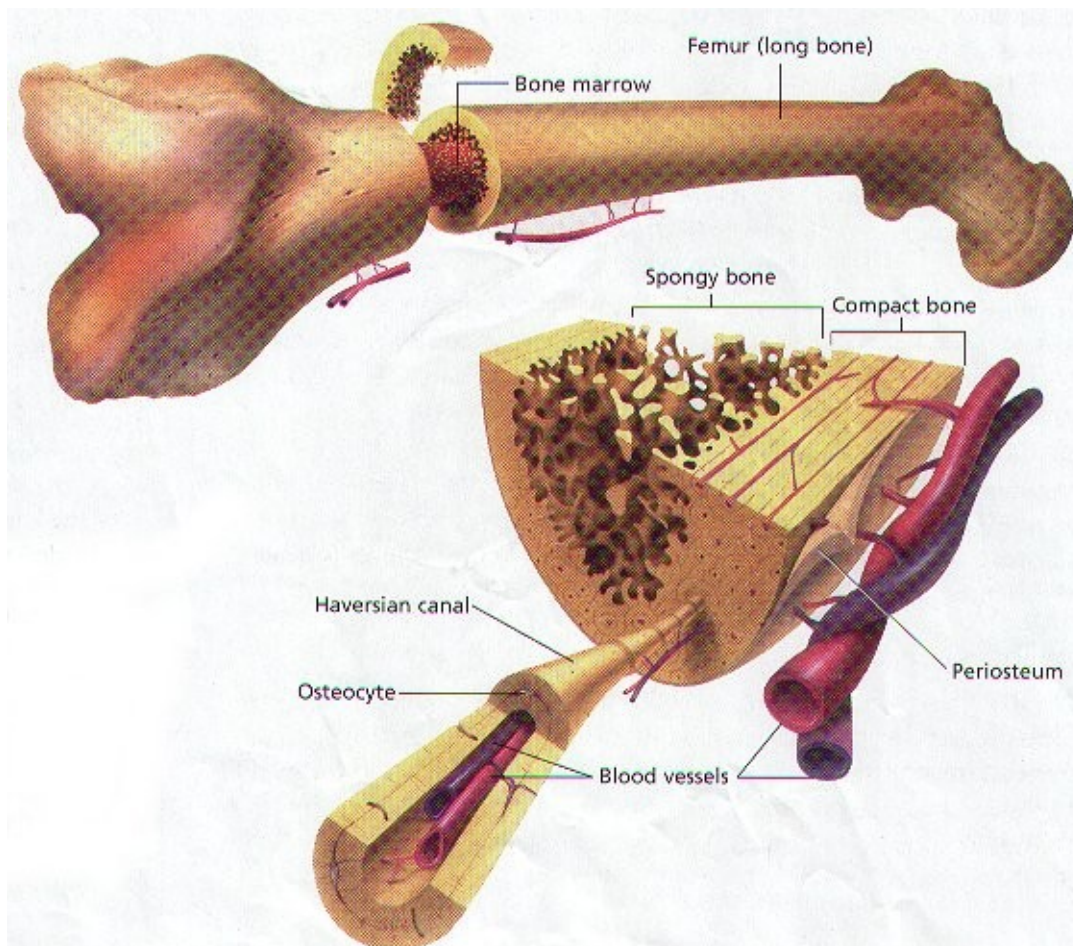


Figure 1: Architecture of bone

The elaboration, maintenance, and resorption of this remarkable tissue result from the interaction of three types of cells: osteoblasts, osteoclasts and osteocytes. Osteoblasts

and osteocytes are involved in bone formation and maintenance, including deposition and mineralization, while osteoclasts are the major resorptive cells of bone. Bone is, in general, dynamic and systematically remodeling (2-5% of cortical bone per year)¹ via the action of these cells.

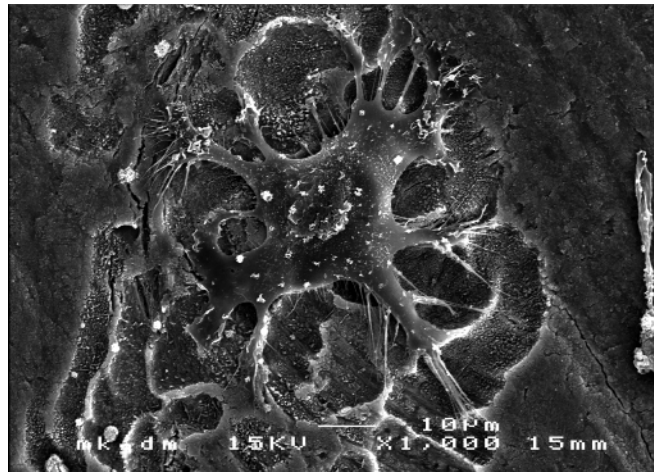


Figure 2: Osteoclast adhering to the surface

They respond to a variety of signals including chemical, mechanical, and electrical signals. Cracks – due to single fracture events or due to accumulated fatigue damage – can and do heal. There are lingering questions about how bone cells can determine which areas of tissue to remodel. One factor that has been identified as potentially important in bone regulation, remodeling, and biomineralization is that the bony material itself is piezoelectric: extrinsic mechanical loading results in the generation of an electrical charge.¹ Research is ongoing in this exciting area.

In the United States there are more than one million cases of skeletal defects each year (as for 2004) that require bone-graft procedures to achieve union.^{3,4} Current clinical practice for bone replacement usually involves an autologous or allogenic bone transplant, or as an alternative, metals or ceramics. Autologous bone graft, that is, bone taken from another part of the patient's own body, has been the gold standard of bone replacement for many years because it provides osteogenic cells as well as essential osteoinductive factors (promoting the differentiation of immature progenitor cells down an osteoblastic lineage)⁴ needed for bone healing and regeneration. Usually it is taken from the patient's iliac crest. However, applications are restricted, mainly due to the limited amount of autograft material that is available as well as to possible donor site morbidity (reported recently to be as high as 44%).⁴ Also the bone might not be of

sufficient quality, especially if a systemic condition affects bone quality. As an alternative, allografts, bone taken from another body, can be used. But in this case there is always exists the risk of disease transmission and immune response to the foreign matter. Other materials used as bone grafts are metals and ceramics, both of which have other disadvantages. Metals, for instance, although providing immediate mechanical support at the site of the defect, exhibit poor overall integration with the tissue at the implantation site, and can fail because of infection or fatigue loading. On the other hand ceramics have very low tensile strength and are brittle, and therefore they cannot be used in locations of significant torsion, bending, or shear stress.

This situation has led to substantial interest in creating artificial bone-like materials for use in the body. As a result of such increasing interest, the field of tissue engineering has emerged, “an interdisciplinary field of research that applies the principles of engineering and the life sciences towards the development of biological substitutes that restore, maintain, or improve tissue function.”³ In contrast to classic approaches, it is based on an understanding of tissue formation and regeneration, and aims to induce new functional tissues, rather than just implant new spare parts. In basic tissue engineering approaches, cells are seeded onto a porous scaffold material optimized for cellular attachment, proliferation, and synthetic activity. Additionally, factors intended to encourage the synthesis of extracellular matrix are applied, such as growth factors or signaling molecules (Figure 3).

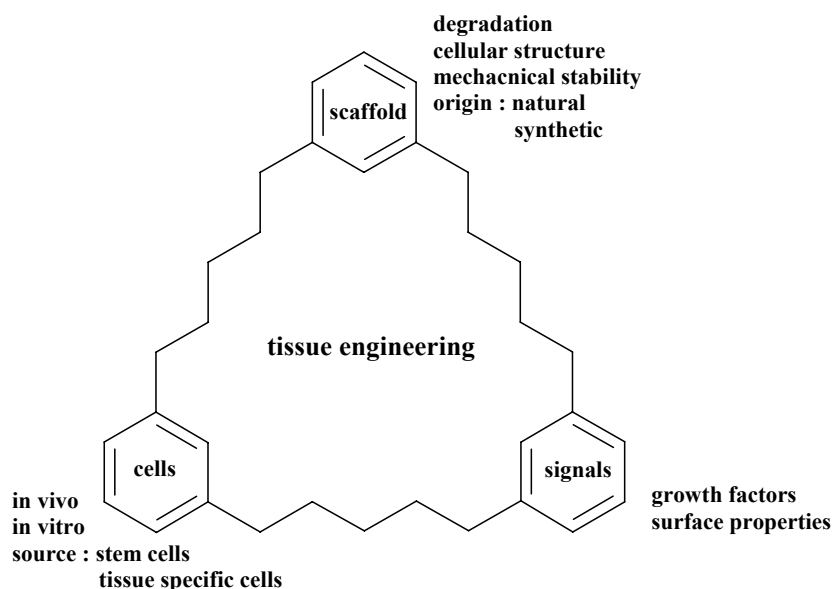


Figure 3: Principle of tissue engineering

Most tissue engineering scaffolds are designed to be resorbable, such that the newly synthesized extracellular matrix gradually replaces the artificial scaffold. In this way, the scaffold provides initial mechanical support as well as a three-dimensional structure for promotion of cell-activity. The most promising results are obtained with biomaterials that best imitate the normal physiological environment of the cells. To mimic a living system a multi-scale approach is beneficial, since nature often derives properties from hierarchical structures.⁵ On the macro-scale (10^{-1} to 10^{-3} m) the size and shape of the scaffold must fit to the anatomical defect, allowing for integration with adjacent tissue and generating properly sized new tissue. Mechanical stability is necessary to afford sufficient hold. Controllability on the micro-scale (10^{-3} to 10^{-6} m) is valuable to mimic microscopic cellular tissue structure. The inclusion of sufficiently sized open pores with good interconnectivity is essential for diffusion of nutrients and metabolic wastes throughout the scaffold. Ingrowth of bone material is found for pore sizes around 100 μm .⁶ Nano-scale (10^{-6} to 10^{-9} m) structural features (surface topography) provide the most significant influence on cell functions.⁵ Surface properties include stiffness, charge, polarity and chemistry, among others. Cells that adhere to a surface investigate the surface stiffness by application of contractile forces.⁶ Controversial results have been published regarding the influence of the surface charge. Lee *et al.*⁵ found that positively charged surfaces support better osteoblast adhesion, while Mikos *et al.*⁴ stated that anionic surface groups result in adsorption of fibronectin (a protein of the extracellular matrix in bone tissue), furthermore inducing integrin-binding by osteoblast-like cells and subsequently mineral deposition by these cells. Finally the biomaterial must degrade along with the reconstruction of the newly built tissue. The degradation products must not affect the tissue regeneration and remodeling process.

Scaffolds for bone tissue engineering are often constructed to release bone morphogenic proteins. Those are biologically active molecules capable of inducing new bone formation. Surface modifications with immobilized adhesion supporting peptides are also widely used. For instance the RGD sequence (Arg-Gly-Asp) is a peptide that is responsible for the cell adhesive integrin-ligand interaction between many cells and multiple extracellular matrix proteins, including fibronectin and fibrinogen, also present in bone tissue.

The objective of the present project is the development of a new scaffold material for bone tissue engineering. Therefore a short overview of existing biomaterials shall first be presented.

2 Biomaterials

Dealing with a complex and sensitive biological system such as the human body, the development of a material for tissue engineering is extremely challenging and the requirements are manifold. Biocompatibility is a prerequisite. The material should not evoke a sustained inflammatory or toxic response upon implantation in the body. Degradation times must match the healing and regeneration process of the replaced tissue, and lead to non-toxic degradation products, which are able to be metabolized and cleared from the body. In addition, the mechanical properties must be viable, both initially and during degradation.

Among biomaterials currently under investigation one can find ceramics as well as polymers. Composite systems combining the advantages of both seem to be a promising choice, in particular for hard tissue replacements. A good overview is provided by Laurencin *et al.*¹² and other research groups.^{3,6,21,7}

A common characteristic of ceramics and bioactive glasses is the time-dependent modification of the surface that occurs upon implantation. The surface forms a biologically active hydroxy carbonate apatite layer which provides a bonding interface with tissues. This phase is chemically and structurally equivalent to the mineral phase in bone, providing interfacial bonding there.⁷ Bioactive glasses usually contain SiO₂, Na₂O, CaO, and P₂O₅ and in addition to their bone-bonding capability, they have been found to support enzyme activity, vascularization, foster osteoblast adhesion, growth and differentiation, and induce the differentiation of mesenchymal cells into osteoblasts.^{8,9} Their serious drawback is their low fracture toughness and mechanical strength, especially in a porous form (Table 1). Nevertheless a bioactive glass (45S5 Bioglass®) has found medical application as bone filler material (Novabone™). Around 60 wt% of bone consists of a biological equivalent to HA and therefore it is evident why HA and related calcium phosphates, e.g. β-tricalcium phosphate (β-TCP), have been intensively investigated as the major component of scaffold materials

for bone tissue engineering. As expected, calcium phosphates exhibit excellent biocompatibility due to their close resemblance to bone mineral. Although osteoinductivity could not be demonstrated, they are at least osteoconductive, encouraging the ingrowth of surrounding bone. Furthermore, calcium phosphates, no matter of which form, always support the attachment, differentiation and proliferation of osteoblasts and mesenchymal cells.⁷ But their relatively slow biodegradation and in particular their inferior mechanical properties limit their application in engineering of new bone tissue, especially at load-bearing sites. Development of composite scaffold materials is attractive since advantageous properties of ceramics and polymers can be combined in order to suit the mechanical and physiological demands of the host tissue more closely.

Table 1: Mechanical properties of bone and selected ceramic biomaterials

Material	Compressive strength	Tensile strength	Elastic modulus	Fracture toughness
	[MPa]	[MPa]	[GPa]	[Mpa \sqrt{m}]
Cortical bone	130 - 180	50 - 151	12 - 18	6 - 8
Cancellous bone	4 - 12	-	0.1 - 0.5	-
Hydroxyapatite	> 400	~ 40	~ 100	~ 0.1
porous Hydroxyapatite (82-86%)	0.21 - 0.41	-	$0.83 - 1.6 \times 10^{-3}$	-
45S5 Bioglass®	~ 500	42	35	0.5 - 1
Porous Bioglass® (>90%)	0.2 - 0.4	-	-	-

Among biodegradable polymers one can distinguish between two different types. Natural-based materials are one category, including polysaccharides and proteins as well as chemically modified natural polymers. Synthetic biodegradable polymers make up the second category.

Natural polymers were the first biodegradable materials to be used clinically. However, their rate of degradation is strongly dependent on the site of implantation and the availability of enzymes, and it can also significantly change if chemical modifications have been performed on the polymer. Nevertheless natural polymers possess several inherent advantages such as bioactivity, the ability to present receptor-binding ligands to cells, susceptibility to cell-triggered proteolytic degradation, and natural remodeling. But the inherent bioactivity has its own downsides, including strong immunogenic responses associated with most of the natural polymers, possibility of disease transmission, and complexities concerning their purification.

Synthetic biomaterials on the other hand are generally biological inert; they have more predictable properties and the unique advantage of being able to be designed with property profiles tailored for specific applications. Depending on the mode of degradation, polymeric biomaterials can be further classified into hydrolytically and enzymatically degradable polymers. Most of the natural-based polymers undergo enzymatic degradation.

Natural polymers can be divided into proteins and polysaccharides. Being a major component of the natural tissues, proteins and other amino acid derived polymers are a preferred biomaterial for sutures, haemostatic agents, scaffolds for tissue engineering, and drug delivery vehicles. *Collagen* is the most abundant protein present in the human body, being the major component of skin and other musculoskeletal tissues. Due to its enzymatic degradability (by collagenases and metalloproteinases), unique physico-chemical, mechanical, and biological properties, collagen has been extensively investigated for biomedical applications.^{10,11} Several collagen-based materials are currently on the market. Thus haemostatic agents (Sulzer-Spine®, CoStasis®, Floseal®), wound-dressings (Biobrane®, Alloderm®), drug delivery for antibiotics (Sulmycin®, Septocoll®) and biodegradable synthetic bone grafts (Collagraft®) have been approved by the United States Food and Drug Administration (FDA).¹² Also its degradation product gelatin is widely used in biomedical applications. It has been employed for coatings and microencapsulating various drugs¹³ and for preparing biodegradable hydrogels.^{14,15} The major sources of collagen currently used for biomedical applications are bovine or porcine skin or bovine or equine Achilles tendons. One disadvantage of these collagen-based biomaterials, which is a limiting factor for the wide-spread clinical application, is their mild immunogenicity.¹² The use of recombinant gelatin as reported by Sutter *et al.*¹⁴ can circumvent this problem, but the treatment is remarkably more cost-intensive.

Elastin is another important structural protein in the human body, namely in vascular and lung tissue. It is responsible for the unusual elastic properties of these tissues. Elastin and artificial polypeptides with the amino acid sequence VPGXG, which recurs quite often in natural elastin, have been considered as drug delivery devices and as potential biomaterials for cartilage tissue engineering.¹²

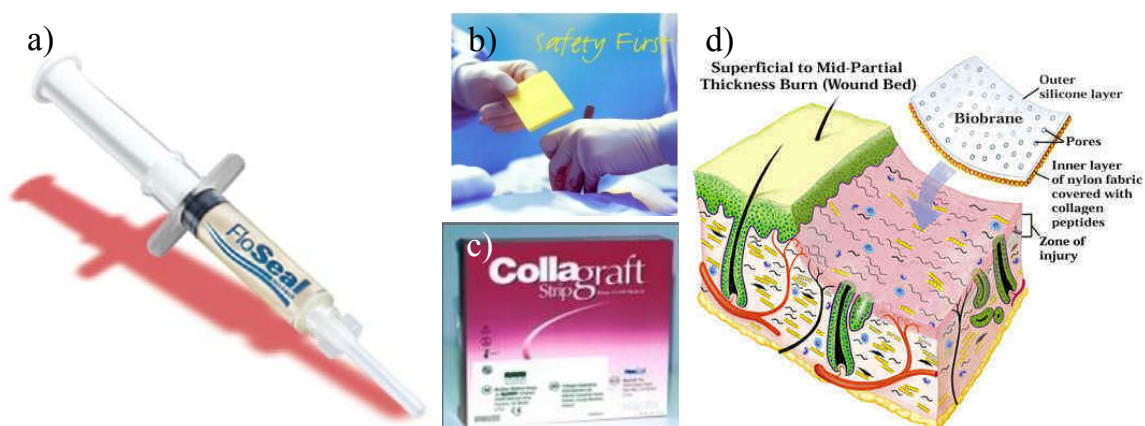
A highly preferred biodegradable material is *albumin*, a protein present in the blood plasma. Studies have shown that almost every tissue in the human body is able to degrade albumin. Up to now investigations include applications as drug and gene delivery system and as surgical adhesives.¹⁶

Fibrin is one of the earliest biopolymers used as biomaterial. This is due to the excellent biocompatibility, biodegradability, injectability and the presence of several extracellular matrix proteins, such as fibronectin, which favorably affects cell adhesion and proliferation. Various fibrin sealant products are being used clinically worldwide for hemostasis and tissue sealing applications.¹²

Homopolymers of *natural and synthetic poly(amino acids)* such as poly(γ -glutamic acid), poly(L-glutamic acid) and poly(aspartic acid) have been the subject of several investigations in the past years, but to the author's knowledge no biomaterial based on such a polymer has reached the market up to now.

A polysaccharide of human origin that has extensively been studied for biomaterials applications is *hyaluronic acid*.^{17,18} It is a member of the glycosaminoglycon family and can be found in virtually every tissue in vertebrates. Since hyaluronic acid is produced by cells during early wound healing, this polymer has been investigated for wound dressing applications and entered the market as HYAFF®. A viscous formulation of this protein (OSSIGEL®) is undergoing late stage clinical trial as a synthetic bone graft to accelerate bone fracture healing.¹²

In addition to the glycosaminoglycans present in the human body, other types of polysaccharides have also raised interest as biodegradable polymeric materials. The most prominent along them are the cationic polymer *chitosan*, which originates from crustacean skeletons, and the anionic polymer *alginate acid*, derived from brown algae. Both have been used as drug delivery devices.¹⁹ Applications as wound dressing are also under investigation.¹²



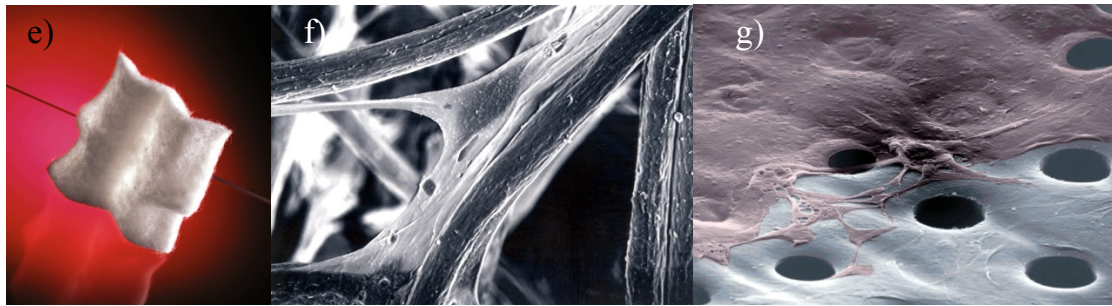


Figure 4: a) FloSeal®, b) Septocoll®, c) Collagraft®, d) Bioderm® e) Hyaff®, f) and g) cells on Hyaff®

In contrast to natural polymers, *synthetic polymers* can be produced under controlled conditions and therefore exhibit in general predictable and reproducible mechanical and physical properties. Another advantage is their lower risk of immunogenicity and infections. Most of the synthetic biodegradable polymers degrade by hydrolytic cleavage of labile bonds in the backbone, e.g. esters, anhydrides, carbonates, etc.

Poly(α -esters) comprise the earliest and most extensively investigated class of biodegradable polymers. They can be synthesized from a variety of monomers via ring opening and condensation polymerization routes. Among these, *poly(α -hydroxy acids)* including poly(lactic acid) (PLA), poly(glycolic acid) (PGA) and copolymers thereof (Figure 6), are well-established and can be found in many different medical products. The first biodegradable synthetic suture called DEXON® that was approved by the FDA in 1969 was based on PGA.¹² PLA is a chiral molecule and therefore three possible polymers exist: poly(L-lactic acid), poly(D-lactic acid) and racemic poly(D,L-lactic acid). Poly(L-lactide) is a partially crystalline polymer with a relatively high elastic modulus (4.8 GPa) and hence has been considered for load-bearing applications, such as orthopedic fixation devices (BioScrew®, Bio-Anchor®). With its amorphous character, the racemic polymer has less mechanical strength and higher degradation rates. Hence its use as a drug delivery vehicle is preferred. Copolymers of glycolic and lactic acid mark the second generation of surgical sutures with optimized mechanical properties and degradation rates (Vicryl®, PANACRYL®).¹²

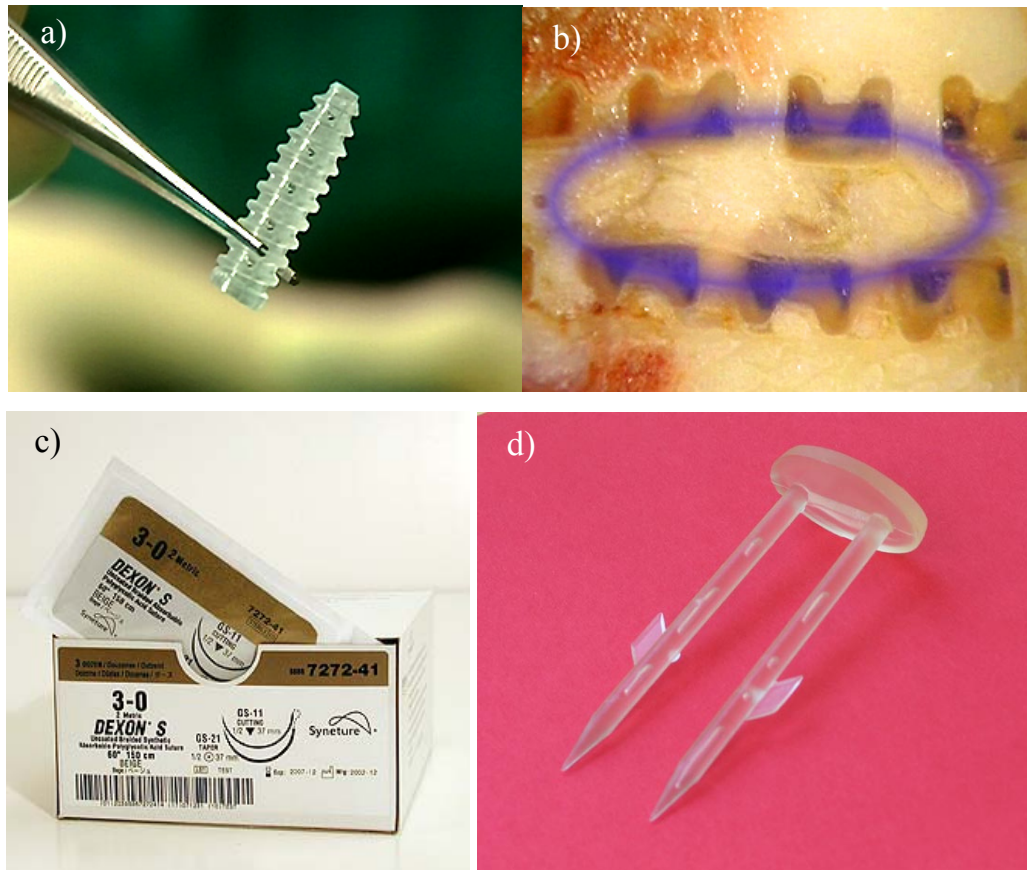


Figure 5: PLA screw a) before implantation and b) in vivo; c) DEXON® suture and d) Bio-Anchor®

Poly(ε-caprolactone) (PCL) is a semicrystalline polyester that is of great interest as it can be obtained by ring opening polymerization of a relatively cheap monomer. Due to its slow degradation, high permeability to many drugs, and non-toxicity, PCL has been investigated as a long-term drug delivery vehicle (Capronor®).

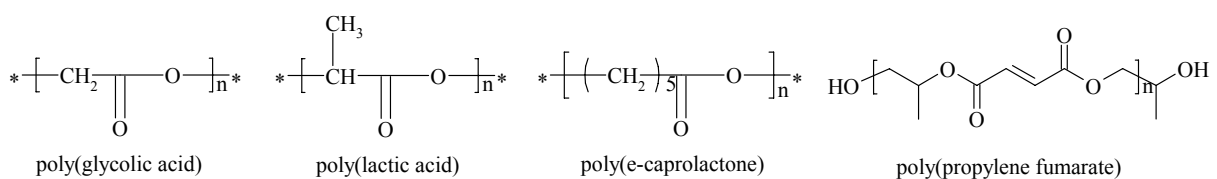


Figure 6: Chemical structures of biodegradable polyesters

A high-strength biodegradable polymer is the co-polyester *poly(propylene fumarate)* (PPF). Its unique feature is the presence of unsaturated double bonds along the backbone that can be used for crosslinking and hence improving mechanical properties. Injectable formulations that solidify *in vivo* are promising candidates for bone tissue engineering.²⁰

All of these polyester materials undergo a *bulk erosion* process which can cause scaffolds to fail prematurely. Thick samples can lead to heterogeneous degradation, faster inside than at the exterior. This is due to easier diffusion of soluble oligomers from the surface into the external medium and therefore reduced acidity at the surface, compared to autocatalytic degradation in the bulk due to acidic end groups. In addition, abrupt release of these acidic degradation products can cause a strong inflammatory response.^{7,21} These problems concerned with hydrolytic bulk degradation are to a certain extent diminished with *surface eroding polymers*. Among these, *poly(trimethylene carbonate)* (Figure 7) is an elastomeric biomaterial that seems to be a promising candidate for soft tissue engineering. A flexible suture material (Maxon®) has already entered the market. Also poly(hydroxy alkanates) produced by certain microorganisms evince a surface erosion mechanism. Poly(3-hydroxy butyrate) and copolymers with 3-hydroxyvalerate are being investigated for orthopedic applications and drug delivery systems.²² However, the drawbacks of these materials are their limited availability and time-consuming extraction procedures from bacterial cultures. Polymers also known to show surface erosion are poly(anhydrides), poly(ortho-esters) and poly(phosphazenes). These polymers have been intensively investigated as drug delivery vehicles.⁷

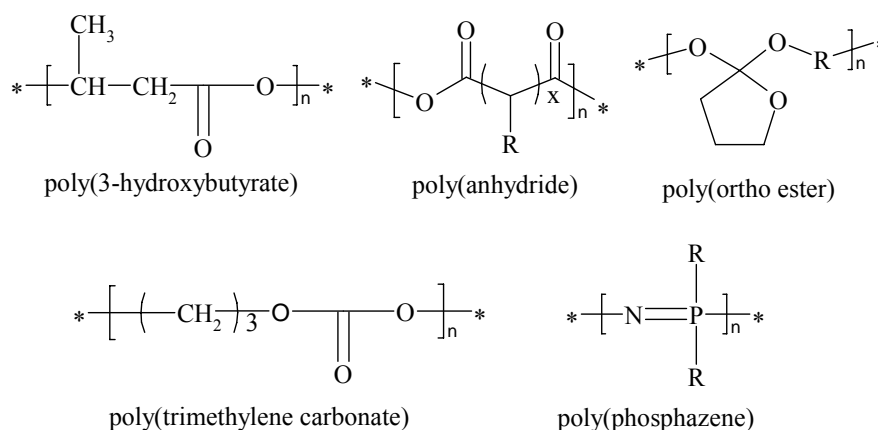


Figure 7: Chemical structures of biodegradable polyesters

Another class of biodegradable polymers having only carbon-backbones are *poly(alkyl cyanoacrylates)*. Their uniqueness consists in the instability of the carbon-carbon sigma bond on the polymer backbone causing hydrolytic sensitivity that can be attributed to the high inductive activation of methylene hydrogen atoms by electron

withdrawing neighbouring groups. Poly(alkyl cyanoacrylates) are among the fastest degrading polymers, having degradation times ranging from few hours to few days. Dermabond® (2-octyl cyanoacrylate) has been approved by the FDA as tissue adhesive.¹²

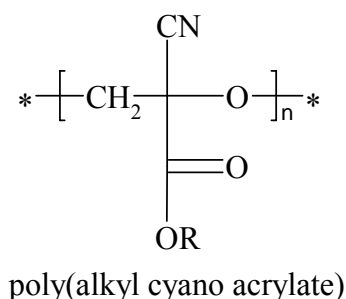


Figure 8: Chemical structure of a biodegradable polymer with C-backbone

3 Rapid Prototyping of tissue engineering scaffolds

Conventional methods for manufacturing scaffolds, such as solvent casting and particulate leaching, gas foaming or fiber bonding, all possess some inherent limitations. They offer little capability to precisely control pore size, pore geometry, pore interconnectivity, spatial distribution of pores, and construction of internal channels within the scaffold. One of the milestones in tissue engineering has been the development of 3D scaffolds that guide cells to form functional tissue. Recently, mouldless manufacturing techniques, known as Solid Free-Form Fabrication (SFF), or Rapid Prototyping (RP), have been successfully used to fabricate complex scaffolds. Leong *et al.*²³ provided a good overview of existing methodologies. Unlike conventional machining, which involves constant removal of materials, SFF builds objects by selectively adding materials, layer by layer, as specified by a computer program.

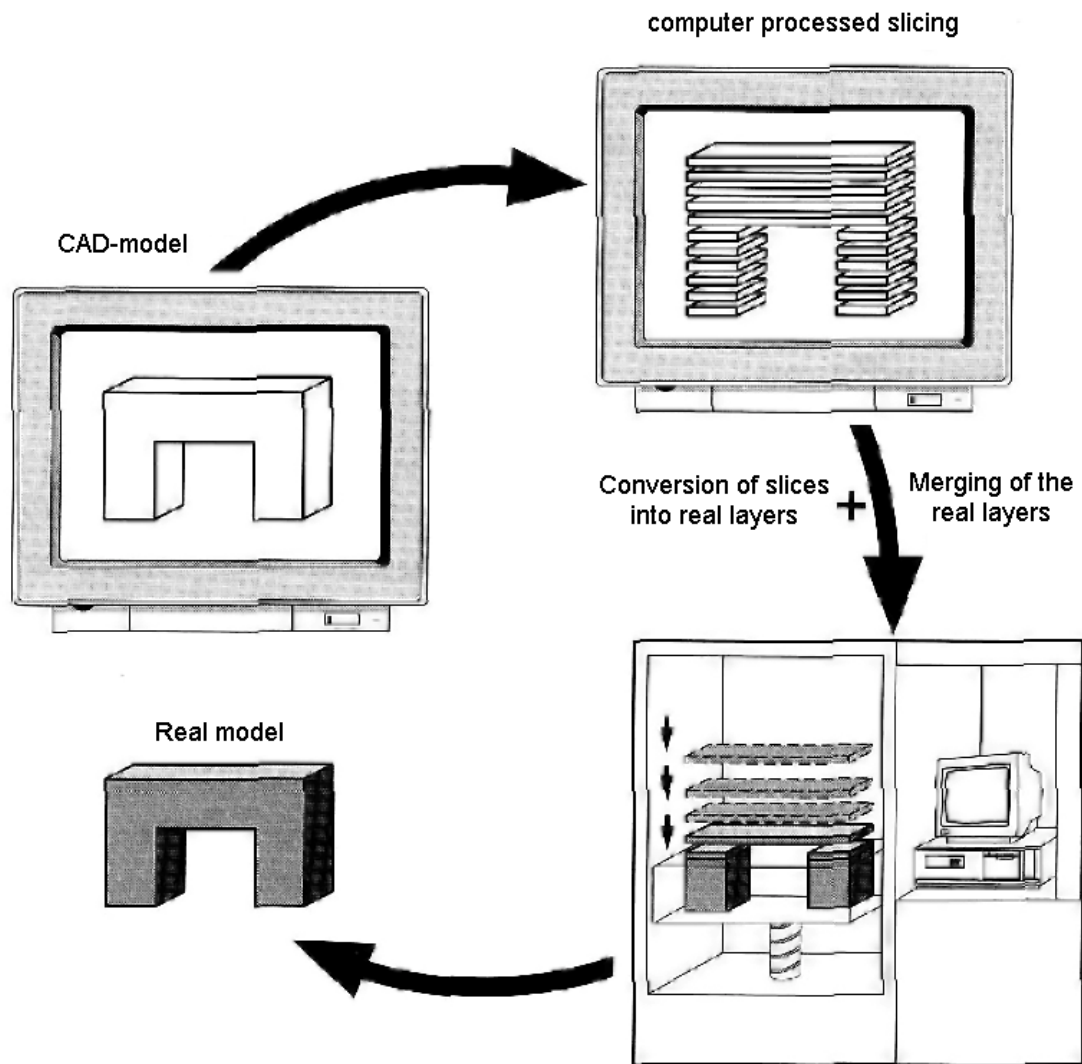


Figure 9: Principle of 2 1/2 D -RP

Over the past 25 years more than 20 RP systems have been developed and commercialized with a focus on the rapid manufacturing of prototypes for non-biomedical applications. Although the application of SFF for scaffold fabrication is not yet widespread, its immense potential for producing scaffolds with highly complex macro- and microstructures is widely recognized and is receiving vast interest and attention from many researchers. Direct utilization of computer-aided design (CAD) models as inputs allows one to incorporate patient-specific data and to realize complex geometries. In contrast to conventional methods for scaffold fabrication, high throughput, high resolution, and high repeatability can be achieved.

To give an overview of existing methodologies and possible usage for tissue engineering, different SFF techniques will now be discussed. According to their

manufacturing principles, RP methods can be divided into three different categories, melt and dissolution deposition techniques, particle bonding techniques, and methods based on photopolymerization.

In a typical *melt-dissolution deposition system*, each layer is created by extrusion of a strand material through an orifice while it moves across the plane of the layer cross-section. The material cools, solidifying itself and fixing to the previous layer. Successive layer formation, one atop another, forms a complex 3D object. Porosity in the horizontal XY plane is created by controlling the spacing between adjacent filaments. The vertical Z gap is formed by depositing the subsequent layer of filaments at an angle with respect to the previous layer. In that way porous structures can be built. A representative system using the concept of melt extrusion is *fused deposition modeling (FDM)*. In a typical FDM unit the material is fed and melted in a heated liquefier head and extruded through a nozzle directly onto the building platform following a programmed path. The layer thickness is varying in proportion to the nozzle diameter. FDM is restricted to the use of thermoplastic materials with good melt viscosity. The operating temperature of the system is too high to incorporate biomolecules into the scaffold, hence limiting the possibilities for tissue engineering. Other drawbacks of FDM are the poor interconnectivity of pores in Z direction, due to the fabrication process, and the need of support materials for overhanging and complex structures, which carries the risk of material contamination.²³ Some variations of the FDM process are *precision extruding deposition (PED)*, *3D fiber-deposition technique*, and *precise extrusion manufacturing (PEM)*. Some biodegradable thermoplasts like PCL have successfully been fabricated into scaffolds using FDM or a related method.^{23,24} Nevertheless, the melt process is generally undesirable from the perspective of scaffold bioactivity because of the elevated temperatures involved. This limitation motivates researchers to replace the melting process with one of dissolution. Such systems developed include *low-temperature deposition manufacturing (LDM)*, *multinozzle deposition manufacturing (MDM)*, *pressure-assisted microsyringes (PAM)* and *robocasting*. The processing temperature can be lowered to 0°C with LDM, and MDM, which is an improved version of LDM using more jetting nozzles and therefore enhances the range of materials that can be used. Biomolecules have been successfully incorporated, as shown by the work of Yana *et al.*²⁵ who integrated bone morphogenic

protein. A remarkable capacity of PAM is the high resolution of this method, being on a cellular scale ($20\mu\text{m}$).²⁶ Robocasting is able to lay down a highly concentrated colloidal suspension to fabricate 3D scaffolds. In general, scaffolds prepared by the methodologies described so far are meant to serve as hard tissue replacements. Landers and Mühlhaupt²⁷ have developed an aqueous system, the 3D bioplotter, to meet the demand for fabrication of hydrogels useful in soft tissue engineering. The key feature of this method is the 3D dispensing of liquids and pastes into a liquid medium with matched density. The material solidifies in the medium after bonding to the previous layer. No support structures are needed since the liquid medium compensates for gravity.

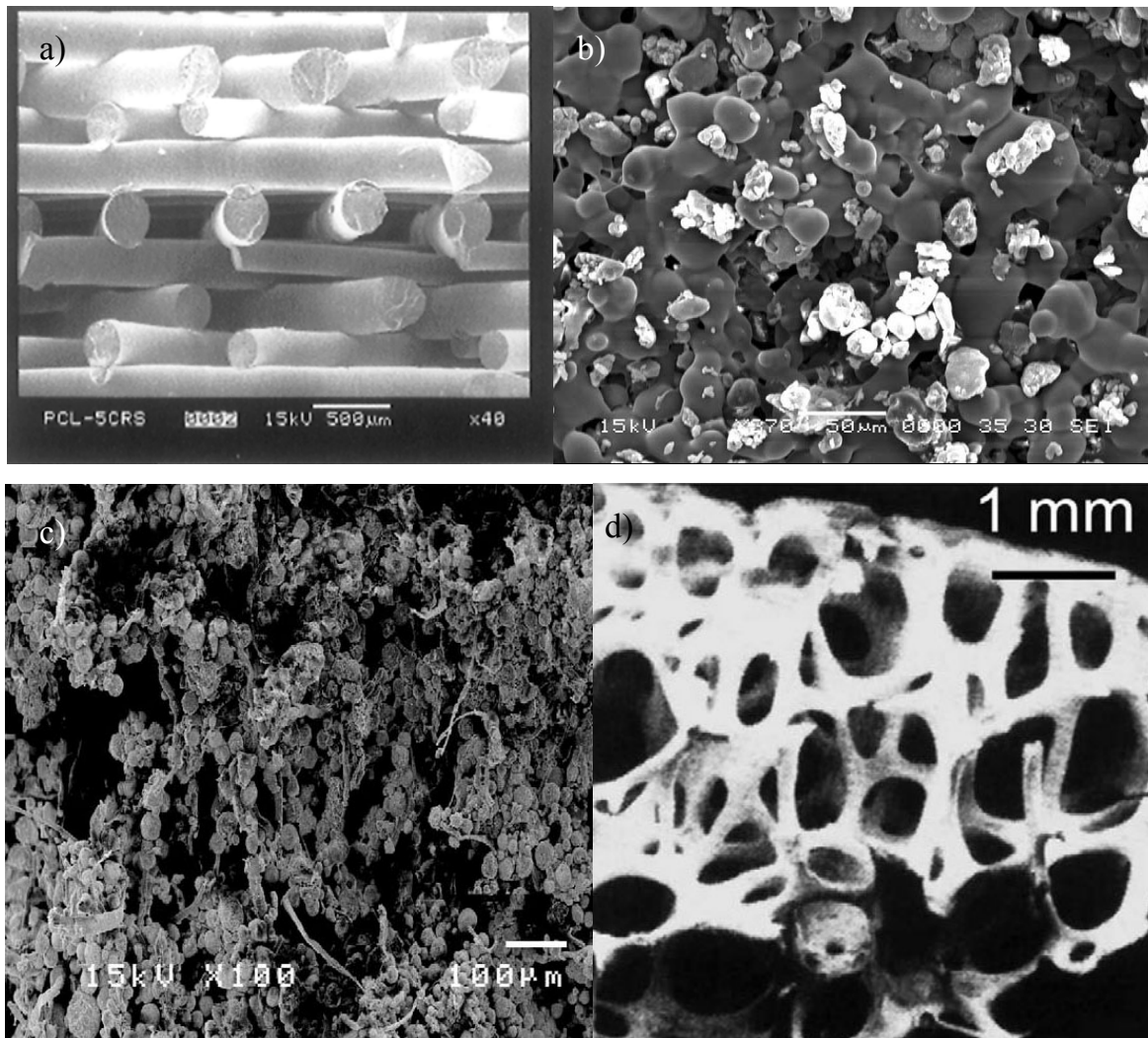


Figure 10: Cellular scaffolds prepared by a) FDM²¹ b) SLS²⁶ and c) 3DP²³ compared to d) cancellous bone⁷

In *particle bonding techniques*, particles are selectively bonded in thin layers of powder material by ink-jet printing of a binder compound. During fabrication, the object is supported by and embedded in the unprocessed powder, which allows for shaping complex and overhanging features. After completion of all layers the structure is removed from the bed of unbound powder. In the case of cellular structures the removal of internal unbound powder might be difficult. In principle, every powder material can be used, no matter if it's a single compound powder, or a blend of materials. Also surface-coated particles can be applied. Resolution is defined by the diameter of the nozzle and the particle size. The latter also limits the size of macropores that can be built. A rough surface and microporosity arise from the space between the granules of powder and are features that favor cell adhesion and viability.²⁶ *Three-dimensional printing (3DP)* employs ink jet printing technology for processing a wide range of powder materials, including polymers, ceramics and metals. The versatility and simplicity of 3DP made it one of the most investigated SFF techniques in tissue engineering and drug delivery applications.²⁴ Since this system operates at room temperature, processing of temperature sensitive materials such as biological or pharmaceutical agents can be conducted. However, when polymer powders are intended to be used, 3DP relies heavily on the use of organic solvents as binders. Although the work of Hutmacher²⁸ *et al.* demonstrated the feasibility of water as a binder, when used for biopolymers such as starch, dextran and gelatin, the constructed scaffold is water-soluble in the first place and necessitates post-processing to make it waterproof, again requiring organic solvents. *Selective laser sintering (SLS)* is another well-established particle bonding technique that uses a deflected CO₂ laser beam to scan over the powder surface and selectively sinter polymer or composite materials. The interaction with the laser beam causes an elevation of the powder temperature just beyond the glass transition temperature, which causes particle surfaces in contact to deform and fuse together. Ceramic scaffolds for tissue engineering were successfully built by Porter *et al.*²⁹ who used calcium polyphosphate and a photocurable epoxyresin for fabricating bioresorbable skeletal implants. After SLS processing, the green part was sintered and the binder burned out. High temperatures during this post-processing step again prohibit incorporation of biomolecules. Typical pore sizes (micropores) encountered by SLS are rather small

(<50 μm)²³ and vary over a wide range due to the dependence on the particle size of the powder and the compaction pressure exerted onto the powder bed during deposition of powder layers. Resolution is also limited by the diameter of the laser beam that is typically 400 μm .³⁰ Due to the Gaussian distribution of the laser energy and the nature of powder bonding, sharp corners and clear boundaries are difficult to achieve. The diffusion of the laser heat causes unwanted bonding of neighboring powder.

The third group of SFF systems is based on the *photopolymerization*^{89,31} of photocurable resins that is initiated by radiation energy. Three different principles have been realized in RP machines up to now. *Stereolithography (SL)* is based on the use of a UV laser that is vector scanned over the top of a bath containing a photosensitive resin. Layer-by-layer photopolymerization forms the 3D structure. Resolution is determined by the laser spot size (that can be as small as 10 μm , as was measured with REM at the Institute of Materials Science, Vienna University of Technology) and by the layer thickness which is itself dependent on the penetration depth and can be influenced by additives with appropriate absorption characteristics (20 μm could be achieved). The second technique using photopolymerization is *digital light processing (DLP)*, where in contrast to SL, illumination of a whole layer is performed at once. Through a micro-mirror array the light is transmitted into the bottom of a resin tank where the photopolymerization takes place on the lower surface of a movable z-stage. Although it's a relatively simple and cheap technique, no biomaterials have been prepared by this method so far due to the lack of photopolymerizable biodegradable materials. *Two photon absorption (TPA)* polymerization employing femto-second laser pulses is the third and only real 3D technique. The resin is transparent for the used laser wavelength and only at the focal point, where the photon intensity is high enough, can solidification occur. Feature resolutions below the diffraction limit of the used light are therefore possible. This method has recently been used to fabricate structures of an organic-inorganic hybrid material (ORMOCER®) that were investigated as potential scaffolds for different kinds of cells, including osteoblasts and endothelial cells (cells in blood vessels).³²

Photocuring in biomedical industry is currently used to a greater extent for the creation of anatomical models for surgical planning or teaching, and sparse for the fabrication of implants. That is because photopolymerizable biomaterials are rather new in tissue

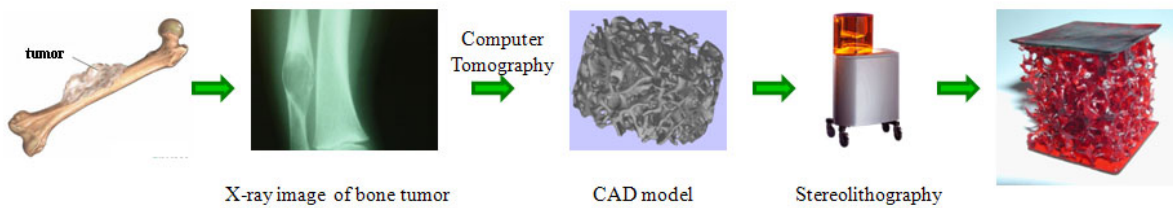
engineering and comparably little has been published about them. Materials that have the required biodegradability and biocompatibility, mechanical stability and other prerequisite properties for scaffold applications are under investigation, but to the author's knowledge none of them has reached the medical market up to now.

Objective

Increasing life expectancy, resulting in larger numbers of injuries and diseases, creates a need for tissue replacement materials that can serve as temporary substitutes until healing is completed. This is especially true for bone tissue engineering, where mechanical support is needed while an injured site - after fracture or removal of a bone tumor - rebuilds itself.

Rapid Prototyping (RP) has become increasingly interesting as a manufacturing method for the fabrication of cellular scaffolds for tissue engineering applications. Special emphasis has been put on methods based on fused deposition modelling and 3D printing. Due to a lack of available resins, stereolithography (SL) has been used only to a small extent up to now, even though RP methods based on photopolymerization offer several advantages. In contrast to other RP-techniques, all processing steps take place at room temperature. This enables the incorporation of temperature sensitive materials (e.g. growth factors) into the material. Furthermore, lithographic methods are capable of producing parts with excellent feature resolution and small layer thicknesses. Furthermore, photosensitive resins can be tailored fairly easily with regard to their biological and mechanical properties. By choosing various monomers the biocompatibility and biodegradability can be tuned, and by changing the degree of crosslinking the elastic modulus and the strength of the final product can be varied over several orders of magnitude.

Although the development of new biomaterials has been an ongoing process since the late 1960s and numerous useful materials have been found, relatively few achievements can be observed within the group of biodegradable photopolymers. Therefore the intention of the present project has been the development of a new resin for the SL fabrication of cellular structures that can be used as bone replacement materials. The figure below shows the planned overall pathway from the detection of a diseased site to the fabrication of an adequate implant.



Rather than being one single substance, such a resin will reasonably consist of several compounds fulfilling different purposes. Biocompatibility and biodegradability of the material as a whole is a prerequisite. Therefore every single component must meet the requirements. The suggested composition of a monomer formulation for the desired application would be:

- 1) An enzymatically cleavable basis monomer (based on gelatin), providing more than one photoreactive moiety to act as crosslinker
- 2) Reactive diluents to adjust network density and mechanical properties
- 3) A non-toxic photoinitiator with adequate absorption characteristics
- 4) Several additives, required either by the fabrication process (such as absorbers) or by the desired application (such as additional fillers for further improvement of the mechanical stability)

The project includes the synthesis and evaluation of an adequate basis monomer and the systematic testing of commercially available photocurable monomers regarding their applicability as reactive diluents. This involves cell culture tests, as well as investigations of mechanical properties and photoreactivity. Furthermore, an appropriate photoinitiator has to be found. And finally a monomer formulation must be designed and optimized to be able to build some test structures using SL.

State of the art

Photopolymerization is a widely explored technology that has recently been recognized to have great potentialities in the biomedical field. Contact lenses are one example for successful medical photopolymer applications. Numerous clinical applications benefit from the ability to form biomaterials *in situ*. Poly(methyl methacrylate) (PMMA) bone cements are commonly used to secure various implant prostheses in orthopedics. PMMA is dissolved in liquid methyl methacrylate monomer to form a viscous solution that can be injected *in vivo* and polymerized via redox or thermal initiation. In dentistry, a formulation of dimethacrylate monomers with ceramic fillers is cured *in vivo* by photoinitiated polymerization to form composite restorative materials. These materials have excellent properties with respect to mechanics but are non-degradable.³³

With advances in synthetic chemistry, novel multifunctional monomers and macromers have been synthesized that form degradable polymers via radical polymerization. An overview is given by Burdick et al.³⁴ These materials can potentially be used as injectable biomaterials, although certain challenges have to be met. Unreacted monomer can have significant effects on mechanical properties and biocompatibility. But in general, complete double bond conversion is almost never attained due to severe restrictions on the mobility of the reacting molecules. An additional concern with radical polymerizations *in vivo* is the temperature increase during the exothermic reaction. However, some materials have been reported to be successfully cured *in vivo* without severe damage to the surrounding tissue.³⁵ Besides the possibility of *in vivo* curing, the use of photopolymerizable materials also opens the gates to the custom-designed fabrication of implants, copying nature's design and architecture, by means of Stereolithography (SL).²⁴ Feature resolutions from the mm to the nm range are not a major challenge nowadays. One of the main goals of tissue engineering is the delivery of living cells to the damaged tissue. Water-soluble macromers, which form highly hydrated polymers upon curing, have been used for photoencapsulation of living cells.³⁶

Some general statements can be made about biodegradable networks that are formed upon the photopolymerization of different monomers and macromers. In Figure 11 four typical networks and their degradation mechanisms are shown.

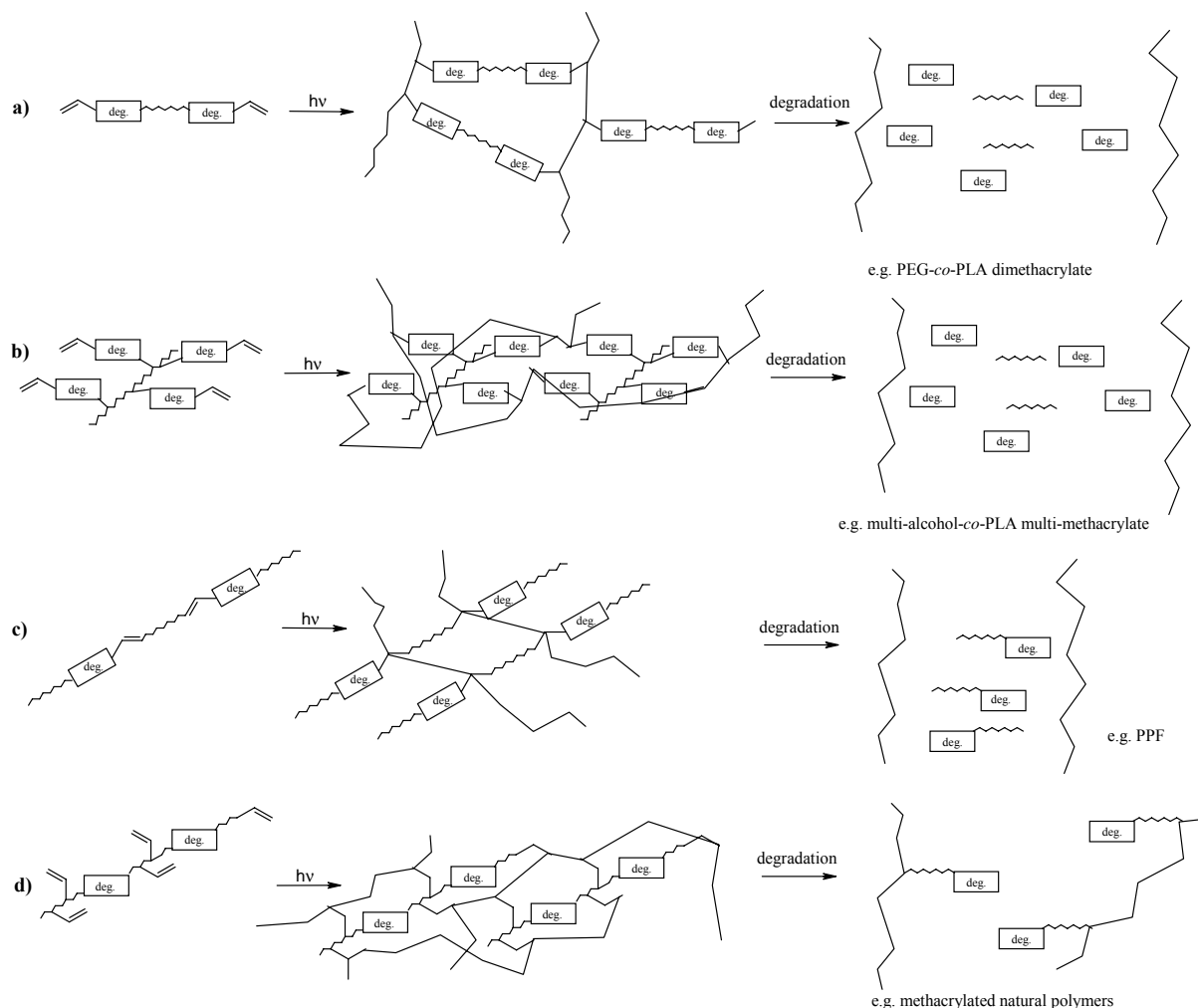


Figure 11: Schematic network formation and degradation of different biodegradable photopolymers

The first example shows an oligomer that is first endcapped with degradable groups and further modified with photopolymerizable moieties. Upon hydrolytic or enzymatic degradation three different products are formed: the original core oligomer, the degradable units and the kinetic chains formed upon photopolymerization (e.g. poly(acrylic acid) (PAA)). As another possibility (Figure 11 b) the photoreactive groups can be found along the oligomer backbone linked through degradable units. Degradation products similar to those in example 1 occur. Additionally, the photoreactive groups may be located along the oligomer backbone as shown in Figure 11 c. Kinetic chains and segments of the starting oligomer occur as degradation

products. Finally (Figure 11 d) the oligomer itself can be degradable and possess photoreactive moieties as side chains. In this situation, the network cleaves along the backbone releasing kinetic chains that probably incorporate segments of the starting oligomer. All degradation products must be non-toxic and water soluble in order to be metabolized or eliminated through the liver or the kidneys. The unproblematic excretion of water soluble polymers like PEG, poly(vinyl alcohol) (PVA) or PAA has been reported.^{37,68}

Biodegradable photopolymers can be roughly divided into purely synthetic and modified natural materials. Further classifications concern their mode of degradation, whether hydrolytically or enzymatically.

Within the class of purely ***synthetic polymers***, PEG has a long history of use in biomaterials. Due to its extreme hydrophilicity, which decreases the adsorption of proteins, it can be used to alter the interaction of materials with tissues and cells. Specific cell attachment can be achieved by incorporation of specific signaling molecules, while avoiding attachment of other cells at the same time. Additionally, the end groups on PEG chains are easily modified through a variety of reactions, e.g. modification with (meth)acryloyl chloride leads to photopolymerizable products. (Meth)acrylated PEG chains of various length have been used for many applications including the encapsulation of chondrocytes for cartilage regeneration,³⁸ osteoblasts for bone tissue engineering,³⁹ vascular smooth muscle cells⁴⁰ and mesenchymal stem cells.⁴¹ For example the group around R. B. Wicker⁴² have successfully prepared three dimensional poly(ethylene glycol) dimethacrylate (PEGDM) hydrogel constructs with encapsulated cells. PEG hydrogels like these are non-degradable, but degradable units can easily be introduced between the PEG chain and the photoreactive moiety. Oligomers of α -hydroxy acids have been used to synthesize biodegradable macromers. Anseth *et al.*⁴³ were among the first to synthesize *methacrylate endcapped oligo-esters*, which made processing by light-induced curing possible and opened the door to stereolithographic tissue engineering. Typically the synthesis of such macromers employs a PEG chain of desired length that serves as initiator for the ring opening polymerization of d,l-lactide, glycolide or ϵ -caprolactone. Subsequently the hydroxyl end groups are modified with (meth)acryloyl chloride to form a photopolymerizable macromer. Alterations in the oligomer chemistry lead to changes in mechanical

properties and degradation behavior.^{43,44} To summarize it can be said that longer PEG chains lead to more flexible materials, and the rate of mass loss decreases as hydrophobicity increases. Instead of difunctional PEG chains, tri- or multifunctional alcohols were also used as cores for such macromers.^{45,46} Depending on the chemical composition and the water content these hydrogels typically show elastic moduli between 1 and 8 kPa,⁴⁷ which is in the range of natural soft tissues.

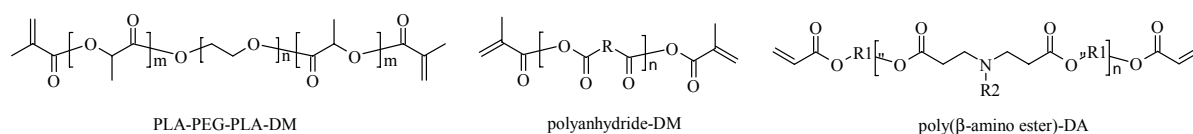


Figure 12: General structures of synthetic photocrosslinkable polymers

Also *anhydrides*, such as sebacic acid or carboxyphenoxy propane, have been modified with methacrylic groups to obtain injectable materials for bone regeneration.⁴⁸ In general, the densely crosslinked networks formed from multifunctional anhydride monomers degrade via a surface erosion mechanism, with mass loss only at the exposed zones at the surface. Therefore structural integrity is maintained for longer degradation periods than in polymers that degrade throughout their bulk.

Anderson *et al.*⁴⁹ synthesized and characterized a large library of *poly(β-amino ester)s* with acrylate end groups using various amines and diacrylates via a simple synthetic process with no byproducts. The general structure of these macromers is shown in Figure 12. Hydrolytic degradation of these cured materials results in bis(β-amino acid)s, diols and PAA kinetic chains. The polymers exhibit a wide range of degradation times (from days to months) and mechanical properties (elastic moduli ranging from 3 MPa to 500 MPa) depending on their chemical structure.

Another three dimensional macromer photopolymerization was done by T. Matsuda *et al.*⁵⁰ with *acrylate endcapped poly(ε-caprolactone-co-trimethylene carbonates)*, resulting in scaffolds that showed surface-eroding properties both *in vitro* and *in vivo*. To improve the mechanical stability of a bone replacement material, HA can be used. V. K. Popov *et al.*⁵¹ were able to fabricate cellular structures using a monomer formulation containing oligocarbonate dimethacrylate and up to 30 wt% HA. *In vivo* experiments showed the formation of new bone around the implant.

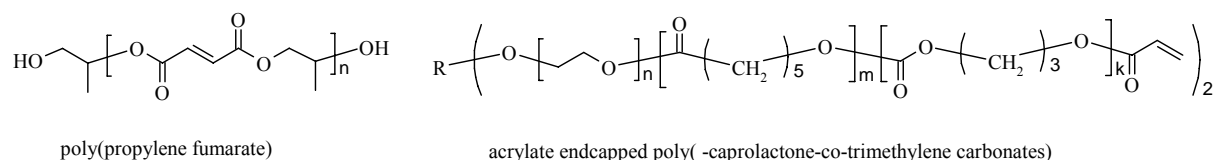


Figure 13: General structures of synthetic photocrosslinkable polymers

Poly(propylene fumarate)s (PPFs) are linear polyesters consisting of repeat units with multiple ester groups and unsaturated carbon-carbon double bonds. Networks are formed via photoinitiated crosslinking of these double bonds. Compressive moduli of up to 150 MPa can be achieved.⁵² Hydrolytic degradation leads to fumaric acid and propylene glycol, which are cleared from the body via metabolic pathways.⁵³ M. N. Cooke *et al.*⁵⁴ were among the first that have published the stereolithographic fabrication of a biodegradable scaffold for bone tissue engineering. They used a resin consisting of diethyl fumarate and PPF. Significantly worse photoreactivity compared to acrylates and therefore slower building speed is an issue of concern.

However, all of these polyester based materials have one big drawback. Their hydrolytic and autocatalytic degradation mechanism can result in large amounts of free acid in the tissue, depending on the size of the implant and on the site in the human body. That change in pH can cause a strong inflammatory response and lead to fracture due to implant failure.^{7,21} Therefore a different degradation mechanism is desirable. From the viewpoint of chemical linkages only amide bonds provide an alternative. Because of their analogy to natural macromolecules such as peptides they can be cleaved by certain enzymes, proteases, and lead to pH-neutral degradation products.

The logical consequence would be the use of polyamides as biomaterials, but unfortunately they cannot be degraded by enzymes because of their high crystallinity due to the relatively small repeating units and strong interchain interactions compared to peptides.⁵⁵ Hence, peptides themselves or short synthetic amino acid sequences can be used as building blocks. Both strategies have been followed and documented in literature.

Short synthetic amino acid sequences have been topic of numerous investigations. Thus, many papers have been published on PEGDA hydrogels containing short peptide sequences.^{56,57,58} Anseth *et al.*⁵⁹ report that PEGDA hydrogels with additional

RGD (Arg-Gly-Asp) and PHSRN (Pro-His-Ser-Arg-Asn) sequences improve osteoblast adhesion, spreading, and focal contact formation. Although these results seem somehow promising for bone tissue engineering, one big drawback of these PEG-based materials is their hydrogel character, leading to poor mechanical properties.

Other groups follow strategies using relatively small amino acid containing monomers, like Mühlhaupt *et al.*⁶⁰ who prepared lysineurethane dimethacrylate (Figure 14). In contrast to peptide based macromers, which can only be cured in aqueous solution, this powder-like monomer can be photo-cured in a molten stage. The mechanical properties are therefore much better than those of hydrogels and are in a reasonable range for a bone replacement material (Young's modulus at 37°C: 3180 MPa). Tests with osteoblasts showed promising adhesion and growth of the cells. Anyway, such a monomer cannot be used with conventional SL since this technique works only with fast curing monomer formulations that are liquid at room temperature.

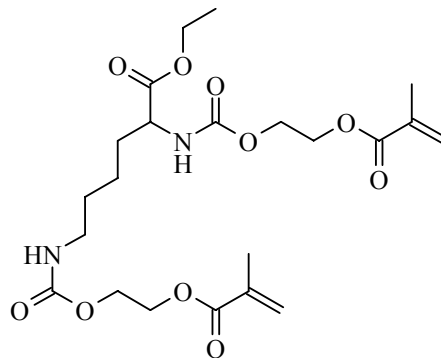


Figure 14: Lysineurethane dimethacrylate

A number of different ***natural proteins*** such as collagen, gelatin, albumin and fibrin have been modified either with small polymerizable groups, e.g. methacrylic anhydride,⁶¹ glycidyl methacrylate⁶² or vinyl-functionalized azlactones,⁶³ or with high molecular weight compounds such as PEGDA.⁶⁴ Also enzymatically degradable polysaccharides such as hyaluronic acid and chitosan have been modified with (meth)acrylic groups to yield photopolymerizable materials.^{65,66} In every case, polymers of the modified proteins and polysaccharides - usually as copolymer with PEGDA - were formed in the presence of water, resulting in soft and flexible hydrogels.

The aim of this project is the development of a monomer formulation that is suitable for SL and leads to a biocompatible and biodegradable polymer that mimics the mechanical properties of natural bone. Hydrogel-based materials like those mentioned above are excluded because of their poor mechanical stability. Moreover, all the discussed peptide-based materials are not suitable since they can only be cured in an aqueous solution due to their solid state and insolubility in non-aqueous media. In this project the synthesis of a new peptide macromer with improved compatibility with organic media will be presented.

Results and Discussion

The aim of the present research project is the development of an acrylate-based formulation for the stereolithographic shaping of a cellular bone implant. To tune the material properties with regard to processability and biocompatibility, as well as mechanical and degradation properties, several components such as *crosslinkers*, *reactive diluents*, *fillers*, and *initiators* have been investigated. To overcome the problem of uncontrolled hydrolytic cleavage of polymers containing esters, biodegradability is introduced by a multi-acrylated *crosslinker* that can be cleaved enzymatically in vivo. The use of a modified peptide is planned. Biodegradation should then lead to scission along the peptide chains leaving small peptides and non-cytotoxic⁶⁷ oligo-(meth)acrylates that can be excreted by body fluids.⁶⁸ Processing properties of the formulation and the network density of the polymer can be tuned by *reactive diluents*. Soluble *filler* materials are applied to tune the viscosity for an optimum resolution of the stereolithographic shaping process. Optimal *photoinitiators* and *fillers* for advanced mechanical properties must also be determined and implemented.

1 Basis Monomer

The key issue of the present project is the development of a new peptide macromer with improved compatibility towards organic media. Taking a clue from natural bone, the decision for the right starting material fell on a commercial gelatin hydrolysate (GH), an enzymatic degradation product of porcine collagen. Although a molecular mass distribution between 0 and 6000 g/mol led to analytical difficulties later on, it seemed to be an appropriate material for fundamental investigations and might or should be replaced in future projects by artificial peptide sequences containing RGD, which fulfill the same purpose, namely to enhance bone cell adhesion, spreading, and proliferation and act as enzymatically cleavable crosslinker.

GH provides two different reactive groups for chemical modification. One anchorage point is the free amino group on lysine units (0.38 mmol/g gelatin)⁶⁹ that provides an excellent spot to introduce various molecule fragments via typical amine reactions. For

example the reaction of gelatin with methacrylic anhydride is reported to yield a photopolymerizable peptide at very mild conditions.⁶² The other way is the modification of free acidic groups of glutamic acid and aspartic acid units (1,27 mmol/g gelatin). Koepff *et al.*⁶⁹ report the derivatization of gelatin with glycidylmethacrylate that reacts with both amino and acidic groups, and leads to polymerizable gelatin as well.

In the following section the synthesis of different gelatin derivatives and their characterization in terms of organo-compatibility and toxicity is described.

1.1 Synthesis of gelatin derivatives

Free primary amino groups on lysine units and free acidic groups on glutamic acid and aspartic acid units were used for the introduction of photopolymerizable groups and moieties that enhance the compatibility with organic media. In these investigations a commercial enzymatic GH was used because lower molecular weights are favored due to better solubility. Dialysis was always performed prior to use, so that only peptide fragments with molecular weights between 3500 and 6000 were used for derivatization. In a first attempt GH was modified with an isocyanate bearing a methacrylate group (Figure 15), supposing that the amino groups of lysine should easily react with this compound. After 4 hours of reaction time at 40°C in DMSO unexpectedly no product could be isolated.

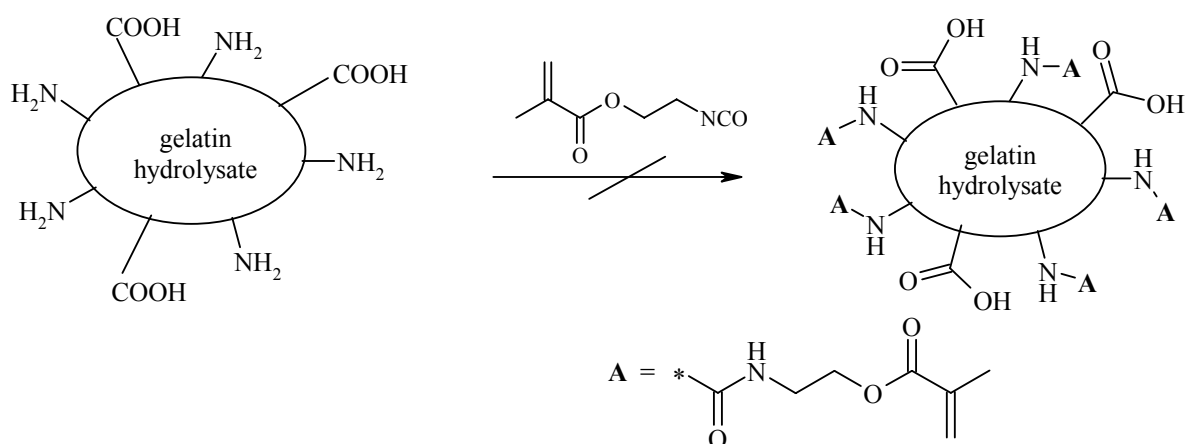


Figure 15: The reaction of GH with an isocyanate

As an alternative GH was modified with glycidylmethacrylate according to Koepff *et al.*⁶⁹ (Figure 16). The basic aqueous reaction mixture containing GH and 5 eq of glycidylmethacrylate was stirred at 40°C overnight.

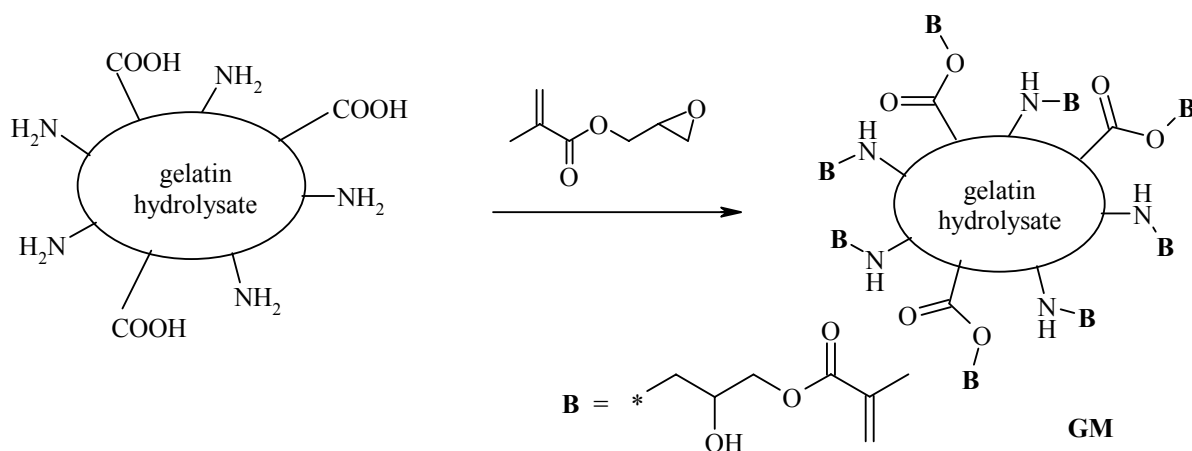


Figure 16: Reaction with glycidylmethacrylate

To determine the degree of conversion acidimetric titration of free acidic and amino groups with 0.01M KOH or 0.01M HCl was used. The values of unreacted GH differed from those found for gelatin in literature, which indicates a changed amino acid composition after enzymatic degradation and dialysis and/or that not all functional groups are available for titration and reaction due to aggregation effects. An amount of 0.360 mmol acidic groups per gram GH was found (phenolphthalein as indicator). Titration with methyl red as indicator, having an indicator range from 4.4 to 6.2, resulted in 0.105 mmol/g primary amino groups of lysine. A quantitative conversion of the amino groups could be observed, while acidic groups reacted only to 35%.

Alternatively, the signals of the methacrylic protons in NMR spectra were used to calculate the degree of conversion. That was done assuming that the NMR signal at 0.9 ppm belongs to all CH₃ moieties present in the GH (Figure 17).

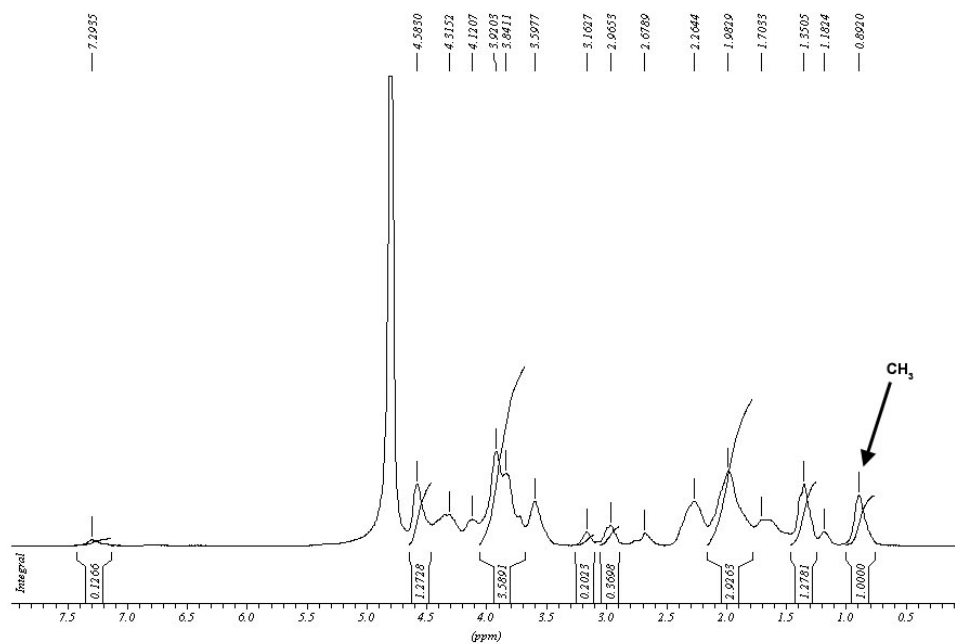


Figure 17: NMR spectrum of GH

Porcine gelatin has a content of 0.465 mmol/g CH₃ groups originating from valine, leucine, and isoleucine. The amount of these amino acids will presumably change during enzymatic degradation and dialysis. To roughly determine the final concentration of CH₃ groups in dialyzed GH, NMR spectra with phenol as internal standard were measured (Figure 18).

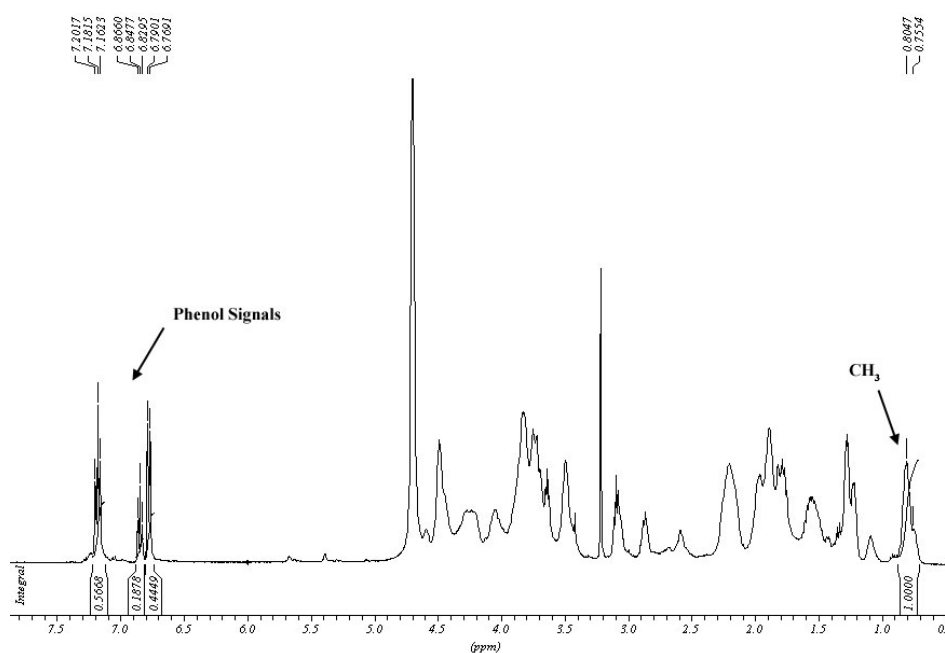


Figure 18: NMR spectrum of GH with phenol as internal standard

The calculation resulted in 0.288 mmol/g CH₃ groups. With that value the amount of methacrylic groups for GM (Figure 19) was calculated to be 0.245 mmol/g.

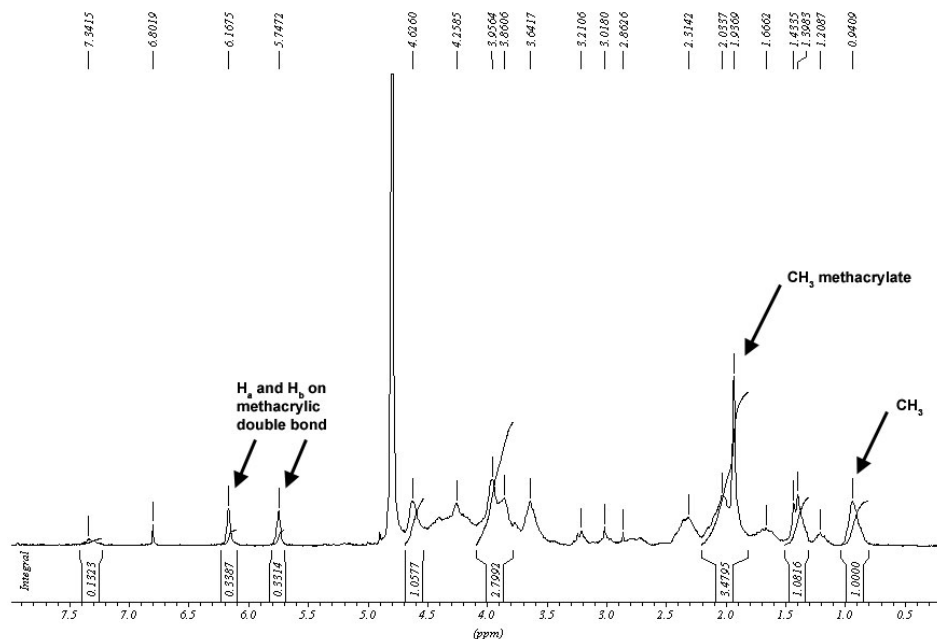


Figure 19: NMR spectrum of GM

GM prepared in that way was isolated as a yellow, water-soluble solid. Therefore it can only be used in water-borne monomer formulations. Solutions of pure GM in water form brittle hydrogels when exposed to light. Hence, the use of reactive diluents is necessary to lower network density and increase the mechanical stability. The use of water in monomer formulations is somehow problematic, since shrinkage and evaporation will very likely occur and the mechanical properties decrease significantly. Further modifications of GH to increase the monomer tolerance and lower the amount of water or even avoid it entirely were attempted.

One strategy that was followed was the temporary modification of the peptide backbone. Since hydrogen bonds formed by the amide backbone hinder the solubility in organic solvents, modification was intended in such a way that it can easily be cleaved in vivo. It is expected that due to sterical hindrance only those spots on the peptide backbone can react where two relatively small amino acids like glycine are next to each other. It is known that the primary structure of collagen is composed of repeating triplets of (glycine-X-Y)_n, where X and Y are often proline and hydroxyproline. Modifications might be possible next to those glycine units. As a model reaction GM was reacted with methyl iodide. This small molecule could react

with the backbone of the protein and yielded a product that was readily soluble in ethanol. Unfortunately also the methacrylic double bonds were modified under these conditions to the Michael addition products. The same kind of reaction was tried with different acid chlorids, such as acryloyl chloride, benzoyl chloride, fatty acid chlorides, but no conversion could be observed. The reason for that is most probably the sterical hindrance.

As an alternative to the backbone modification, the introduction of slightly more hydrophobic parts should enhance the monomer compatibility. PEG chains were chosen to cover the free amino and acidic groups, which could subsequently be endcapped with acrylic groups. Similar to modifications of polyamides (NH)⁷⁰ and cellulose (OH)⁷¹ GH was reacted with ethylene oxide. The gas was condensed (bp. 10°C) and added to a suspension of GH in DMF. The reaction was conducted in a “Berghof” autoclave at 50°C for 24h. At least the amino and hydroxyl groups present in GH should be able to open the epoxide and start the ring opening polymerization. The resulting terminal OH groups were thought to be further modified, but no product could be found in the first reaction step.

The introduction of PEG was also tried by another route. The carboxylic groups in proteins can generally be substituted by activation with dicyclohexylcarbodiimide and reaction with amines. Wong *et al.*⁷² reported the successful derivatization of ferritin with long-chain aliphatic amines, while Libera *et al.*⁷³ used PEG-chains with a primary amino group on one end. Both groups report an enhanced solubility in organic solvents. Analog reactions with GH were less successful. The reaction with dodecylamin didn't work at all, while the yields of the modification with PEG-NH₂ were too low to be useful (10%).

Another approach was the use of a prefabricated reagent, having both a PEG chain and a methacrylic group (Figure 20).

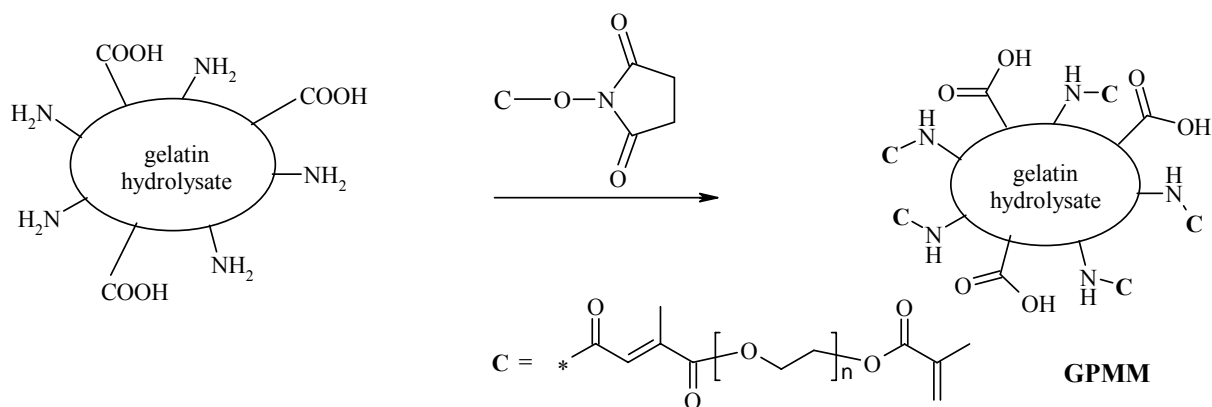


Figure 20: Reaction with PEG-Methacrylate

Here PEG-mono-methacrylate was reacted with maleic anhydride and further activated with N-hydroxysuccinimide (NHS). Finally GH was modified with those activated esters. NMR spectroscopy showed a relatively low value of 0.028 mmol/g methacrylic groups. In contrast to the reaction with glycidylmethacrylate, only lysine amino groups were able to react and therefore less methacrylic groups per gram gelatin can be found in GPMM. In addition, lower conversion of the free amino groups was observed. Furthermore, free acidic groups decreased the miscibility with organic media. Hence, derivatization of both, free amino and acidic groups, was undertaken.

Because of the two different reactive sites on GH – amino and acidic groups – introduction of two different moieties is possible with selective reagents. Higher reactivity of amino groups compared to carboxy groups suggests a first reaction step, where the amines are modified. Several examples of NHS activated esters can be found in literature^{74,75} that can easily react with lysine NH₂ without modification of the acidic sites. In that way hydrophobic moieties might be introduced that enhance the tolerance towards organic media. In a second step the carboxylic groups can be modified with glycidylmethacrylate to introduce the polymerizable moiety.

A promising approach for the introduction of PEG chains was the reaction with NHS activated esters thereof. For that PEGs with molecular weights of 1000 and 4000 were primarily modified with maleic anhydride and subsequently activated with NHS (Figure 21). GH could be converted with these products under mild conditions in very good yields (>90%). The reaction of the remaining carboxylic groups with glycidylmethacrylate resulted in polymerizable gelatin derivatives (GPM and GP4M).

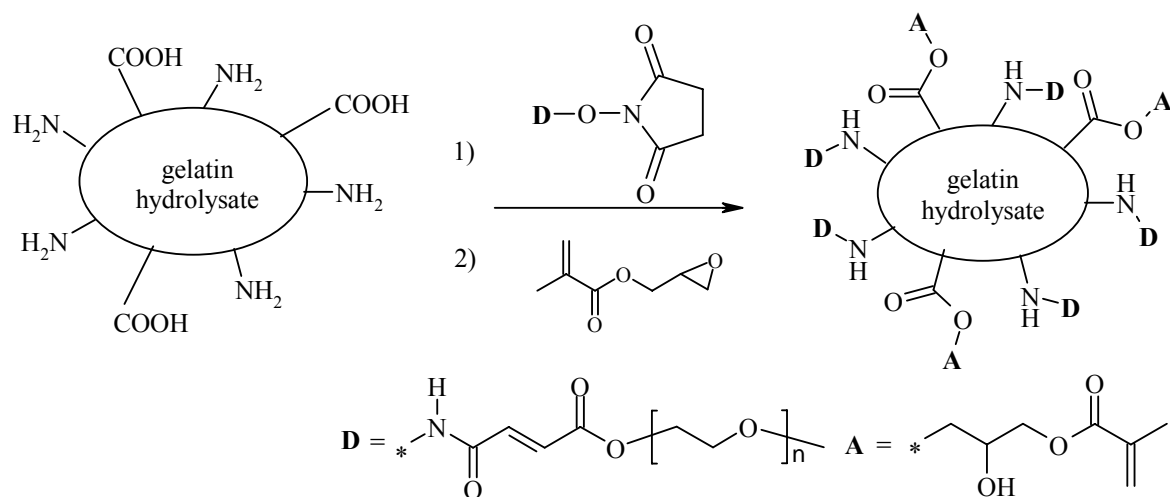


Figure 21: Additional modification with PEG

The use of polypropylene glycol (PPG) instead of PEG led to a yellow solid that formed a white milk-like dispersion in water. Solubility was only given in DMSO and the product was therefore not useful.

Another possible kind of hydrophobic moiety that is also a natural substance would be a fatty acid. Linolic acid and caprylic acid were activated with NHS and stirred with GH in water-free DMSO for 24h. Conversion of amino groups was again determined by titration with 0.01M HCl, which showed complete conversion. In a second step methacrylate groups were introduced as described above (Figure 22). During this reaction fatty acids seemed to fall off again, because titration of the amino groups afterwards indicated a conversion of less than 10%. In the NMR spectra no fatty acid could be observed as well. Nevertheless, at least a small amount of fatty acid must have been in the product, perhaps only as physical mixture, since the aqueous solution of GLM tended to intensive foaming, in contrast to all other GH derivatives.

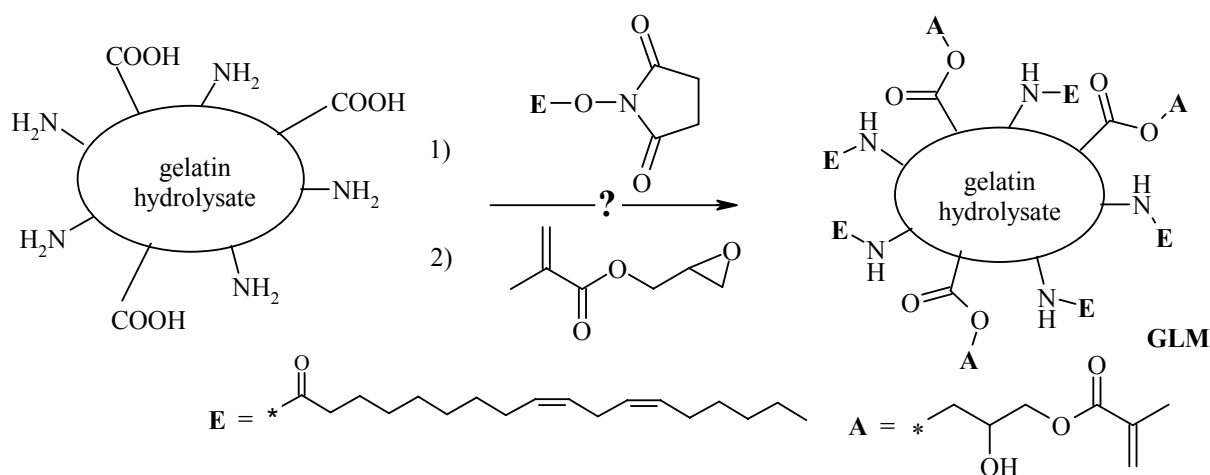


Figure 22: Additional modification with linolic acid

As a summary of this chapter the tables below show all synthesized GH derivatives.

Table 2: GH derivatives (substituents in mmol/g)

product	modification according to NMR [mmol/g]		modification according to titration [mmol/g]	
	methacrylic groups	other groups	modified COOH	modified NH ₂
GM	0.245	-	0.136	0.105
GPMM	0.028	-	- ^{*)}	-
GPM	0.009	0.206	0.212	0.105
GP4M	0.065	0.132	0.328	0.105
GLM	0.068	0	0.258	0.008

^{*)} no data available

Table 3: GH derivatives (conversion in %)

product	conversion according to NMR ^{**) [%]}		conversion according to titration [%]	
	COOH	NH ₂	COOH	NH ₂
GM	53		35	>90
GPMM	-	27	- ^{*)}	-
GLM	18	0	70	7
GPM	<10	200	56	>90
GP4M	18	125	89	>90

^{*)} no data available

^{**) relating to the amount of free amino and acidic groups determined by titration}

Both NMR spectroscopy and titration have their faults and imperfections. Nevertheless, the results can be used to compare the different derivatives and estimate the real degree of conversion. In general, amino groups seemed to be modified more or

less completely. One exception is the GH derivative with the fatty acid (GLM), where amino groups are almost unmodified, maybe due to decomposition of the product during the second reaction step or during storage. Acidic groups were less reactive, as expected. High amounts of PEG in the NMR spectra may indicate an incomplete isolation of the products from the reagents. But some additional physically bound PEG chains are no problem in terms of biocompatibility. Only reproducibility and analysis of these substances become rather complicated.

1.2 Testing

Besides the NMR and acidimetry described above, also MALDI-TOF and GPC served to identify and confirm the synthesized GH derivatives. Further investigations included compatibility tests with acrylic monomers and cytotoxicity measurements.

1.2.1 GPC and MALDI-TOF

No appropriate standard materials were available for the *GPC measurements*. Therefore PEGs were used to calibrate the system, well-aware that the results have to be interpreted with care. Measurements indicated that the molecular weights (MW) of modified GHs, namely GLM (280000), GPM (104000), GP4M (120000) were higher than that of GH itself (78000), indicating that the desired modification had taken place. In the spectra of GPM and GP4M a second peak was observed, probably resulting from unbound PEG chains that could not be completely removed. But in both cases the retention time was significantly different to GH, so that PEG chains must be covalently bound to the protein.

Also *MALDI-TOF measurements* were performed to verify the modification of GH. Fortunately the dialysis for the purification of the products was incomplete, so that peptide fragments below 3500 g/mol were available that could be observed with MALDI-TOF. Comparing the spectra of GH and GM it could be seen, that glycidylmethacrylate has been bound between one and three times on peptide fragments below 3500 g/mol. In Figure 23 a detail of the GH and GM spectra is shown. The GH spectrum has been shifted to higher values that correspond to an addition of two molecules glycidylmethacrylate per peptide molecule (+284.13 Da).

Numerous matching peaks indicate the successful modification of GH with glycidylmethacrylate. Additional spectra can be found in the appendix.

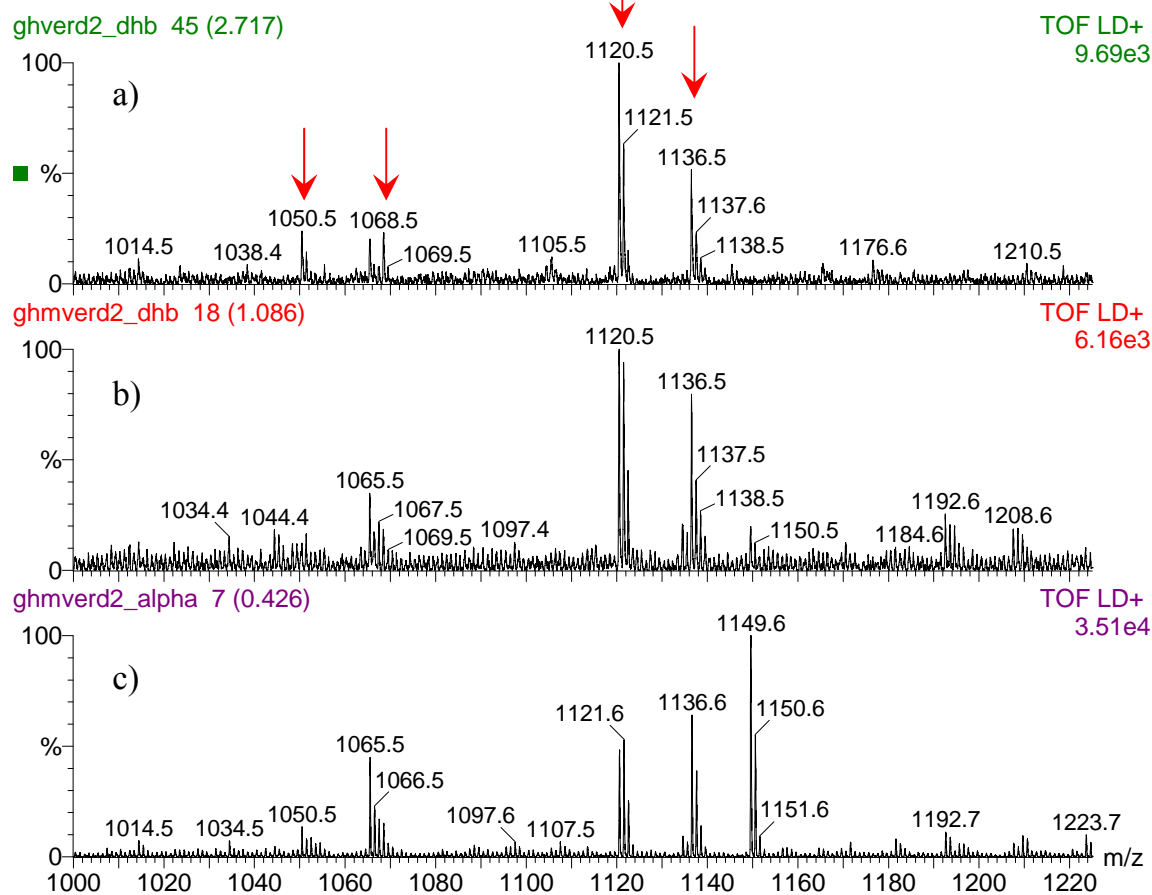


Figure 23: MALDI-TOF spectra: a) GH spectrum shifted +284,13Da (corresponding to two-fold addition of glycidylmethacrylate; b) GM in DHB and c) GM in α -cyanocinnamic acid (red arrows indicate matching peaks)

In GLM no linolic acid could be found, which matches the results from NMR spectroscopy. GPM and GP4M could not be measured, because unbound PEG chains can much more easily be ionized than the products so that only PEG could be observed.

1.2.2 Compatibility with acrylic monomers

To investigate the suitability of the gelatin derivatives in an acrylate-based monomer formulation a water-containing test system was established. One part of each modified GH was mixed with two parts of water. Unmodified GH was used as reference. Now a mixture of two water-miscible and biocompatible monomers was added drop-wise until precipitation of the peptide could be observed. The monomers used for that were

hydroxyethyl methacrylate (80%) and poly(ethylene glycol 400) dimethacrylate (PEGDM)(20%). The table below (Table 4) shows the obtained values.

Table 4: Monomer miscibility of gelatin derivatives

Gelatin Derivative	amount of monomer at coagulation of gelatin [%]
GH	10
GM	110
GPMM	45
GLM	90
GPM	110
GP4M	150*

* only turbidity

If only one part of the two different reactive groups on GH is modified, namely the lysine NH₂ groups in GPMM, compatibility with organic media increased by a factor of 4.5. In the case of GM, where both amino and acidic groups have been reacted with glycidylmethacrylate, 10 fold better miscibility could be observed. The difference can be explained by the free carboxylic groups in GPMM that are able to form salts and hydrogen bonds, resulting in less monomer tolerance. Further derivatization with PEG1000 didn't enhance the miscibility compared to GM. Less monomer tolerance of GLM compared to GM results from the marginal conversion with the fatty acid. Only the PEG4000 chain linked to gelatin could further improve the miscibility with organic media. In this last sample no precipitation at all was observed, only turbidity. That indicates that the usage of even higher molecular weight PEG chains might lead to completely organo-soluble gelatin derivatives.⁷³ But for these investigations a total water content of 20% can be tolerated, since stereolithography is still possible without losing the desired resolution.

1.2.3 Cytotoxicity

To determine possible cytotoxic effects of free, non-polymerized monomeric residues that might be released from the grafts after implantation, the influence of increasing doses of monomeric compounds was tested in two different cell cultures, osteoblasts and endothelial cells. Osteoblasts were cultured in conventional culture dishes and aqueous solutions of the GH derivatives in different concentrations (10^{-4} to 10^{-2} mol/L

methacrylic double bonds; 10^{-2} mol/L \approx 10-20 mg/mL) were added. After five days culture time DNA content and viability were determined (Figure 24). Some reactive diluents that will be discussed in detail in the next chapter have also been measured for comparison, namely hydroxethyl methacrylate (HEMA), trimethylolpropane triacrylate (TTA) and ethoxylated trimethylolpropane triacrylate (ETA).

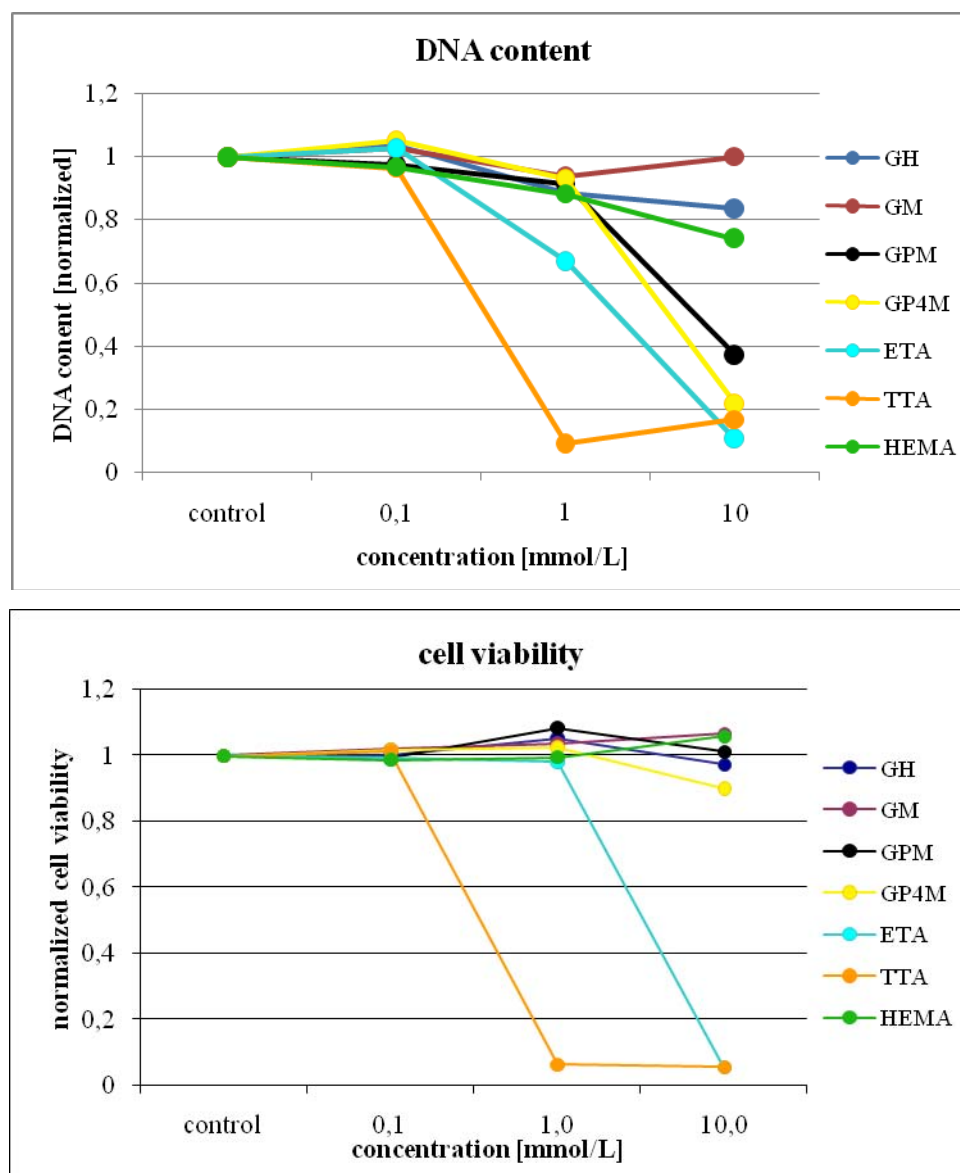


Figure 24: Cytotoxicity tests with osteoblasts

It is evident that the newly synthesized GH crosslinkers are less cytotoxic than the reactive diluents. It should be noted that a concentration of 10^{-2} mol/L is quite high and will presumably not arise *in vivo* due to diffusion of unreacted molecules. GPM and GP4M perform a bit worse than GH and GM with regard to the DNA content of the cells. That might be attributed to the insufficient purification of the products.

Additional *in vitro* LD50 measurements were done with endothelial cells. Here measurements were done with monomer concentrations of 10^{-7} - 10^{-3} mol/L methacrylic double bonds. All GH derivatives showed no toxicity up to that concentration.

2 Reactive Diluents

To be able to use SL as fabrication technique a liquid monomer formulation with certain features is required. Some of these properties can be tuned by the appropriate choice of reactive diluents. The viscosity is an important criterion, since the resolution of each SL machine is best in a certain Pas range (the Envisiontec machine used within this project worked best with formulations that had a viscosity between 0.3 and 0.5 Pas). Fast-curing materials are preferred since building speed is another important issue. Additionally the requirements from the medical application point of view must be considered, namely biocompatibility and biodegradability, as well as the mechanical properties of the cured material. Biodegradability is achieved by the use of a GH based crosslinker that leads to oligo(acrylate) fragments during degradation, which can be excreted by the body.^{67,68} Ideally the hardness and stiffness of natural bone should be achieved for an optimum healing process. Since the mechanical properties are strongly dependent on the network density of the whole system, an eye should be kept on the size of the reactive diluent and the number of reactive double bonds per molecule. The selection of several monomers on the basis of the required properties is described and discussed in this chapter.

2.1 Selection of monomers

A number of commercially available (meth)acrylic compounds having one or more reactive double bonds and other functional groups were chosen. Testing of these substances included cell adhesion experiments (biocompatibility), differential scanning photocalorimetry (Photo-DSC, photoreactivity) and the measurement of certain values describing the mechanical properties.

Firstly, specimens were prepared as homopolymers of every single substance for the biocompatibility and mechanical tests. Some of the chosen monomers were eliminated

already at that point, since photopolymerization under nitrogen sometimes didn't result in suitable test specimens due to bad reactivity (e.g. aminoethyl methacrylate, (dimethylamino)ethylacrylate). In the following figures (Figure 25, Figure 26, Figure 27) all monomers are shown that were suitable.

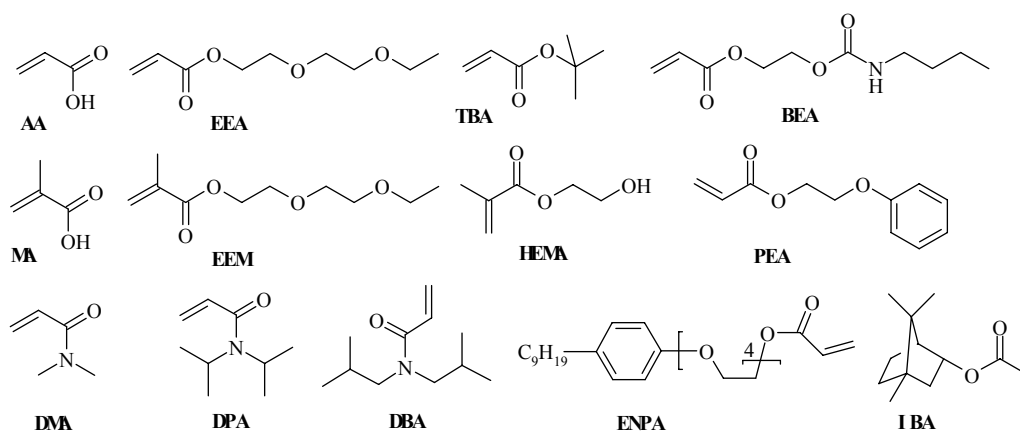


Figure 25: Monofunctional monomers

Among monofunctional reactive diluents, acrylates and methacrylates were considered as well as acrylamide derivatives. Very different properties can be expected when different functional groups such as hydroxyl, ether or urethane and also more or less bulky residues are incorporated. Hydroxyethyl methacrylate (HEMA) has often been described as a biocompatible photopolymer and is applied for contact and intraocular lenses.⁷⁶ Acrylic (AA) and methacrylic acid (MA) were selected because polymers thereof can be considered as degradation products of most esters (e.g. from acrylic acid 2-(2-ethoxy-ethoxy)-ethyl ester (EEA), methacrylic acid 2-(2-ethoxy-ethoxy)-ethyl ester (EEM), acrylic acid 2-butylcarbamoyloxy-ethyl ester (BEA), and HEMA). Generally, less is known about acrylamides and therefore N,N-diisopropyl-acrylamide (DPA), N,N-diisobutyl-acrylamide (DBA) and N,N-dimethyl-acrylamide (DMA) were investigated.

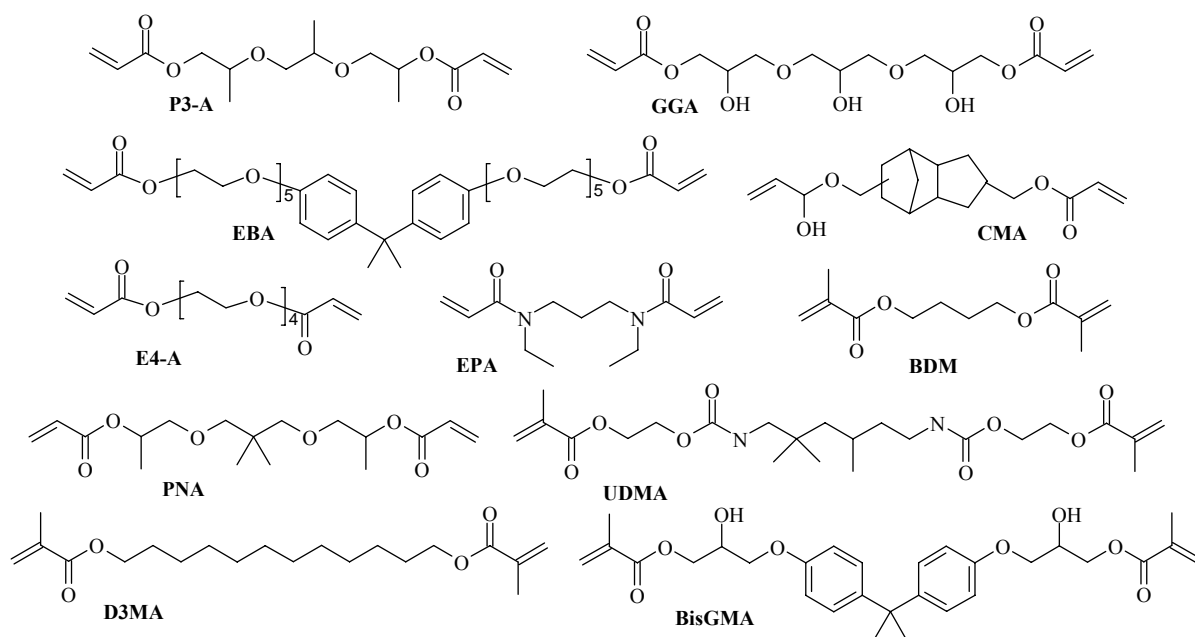


Figure 26: Difunctional monomers

Difunctional monomers N,N'-diethyl-1,3-propylenbisacrylamide (EPA), 2-methylacrylic acid 2-{2,2,4-trimethyl-6-[2-(2-methyl-acryloyloxy)-ethoxycarbonylamino]-hexylcarbamoxyloxy}-ethyl ester (UDMA), dodecyl dimethacrylate (D3MA) and bisphenol A diglycidylmethacrylate (BisGMA) are well-known from dental applications and yield polymers with outstanding mechanical properties. Because of its attribute to withstand unspecific cell attachment tetraethyleneglycol diacrylate (E4-A) is one of many PEG derivatives that have found application in biomaterials, especially in combination with peptides enhancing specific cell adhesion.

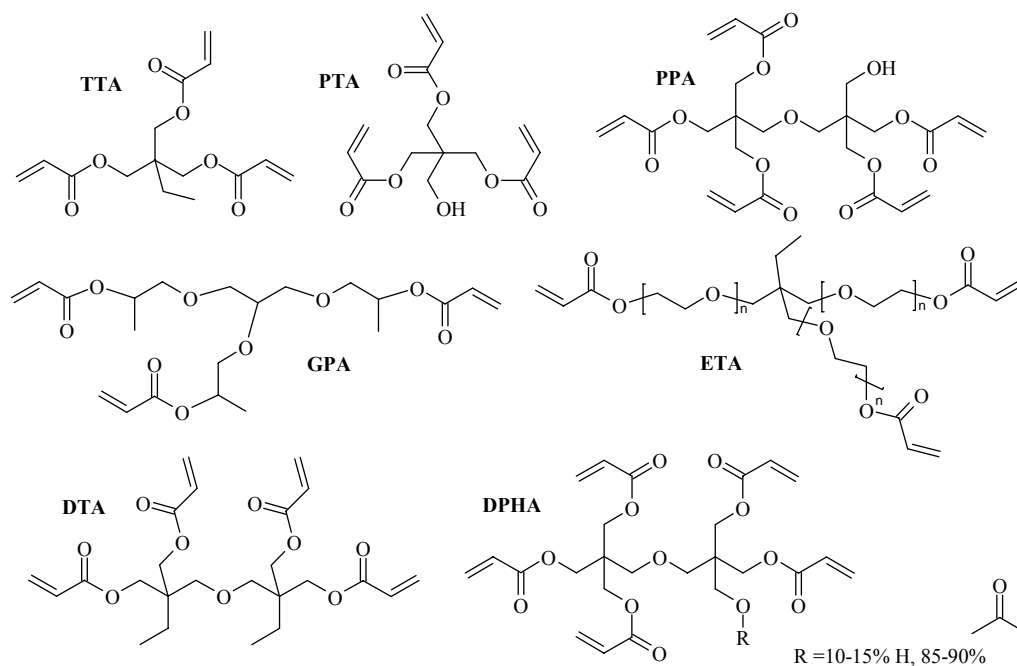


Figure 27: Multifunctional monomers

Multifunctional acrylates are better known from coatings and adhesives chemistry than biomaterials. Nevertheless they have great potential to serve as a network controlling crosslinker and reactive diluent in a monomer formulation aiming at bone replacement materials, since reactivity and mechanical stability are in general rather high.

2.2 Testing

Fabrication by SL requires high photoreactivity of the whole monomer formulation. Therefore photo-DSC measurements were performed to characterize the selected substances with regard to their curing characteristics. Since tissue engineering works best when the replacement material behaves like natural tissue, mechanical properties in the range of those of natural bone are desired. For the evaluation of the stiffness and E-moduli of the homopolymers differential mechanical analysis (DMA) and bending-strength-tests were used. Although biocompatibility seems to be the most important selection criterion, photoreactivity and mechanical properties will be discussed first, because biocompatibility is influenced by these factors. Cell adhesion tests with osteoblast-like cells served to provide information about the biocompatibility.

2.2.1 Photoreactivity

Since SL requires short building times and adequate double bond conversion, the selected monomers were analyzed with regard to their curing characteristics. Photo-DSC is a unique method for the fast and accurate evaluation of the reactivity of monomers. Various important parameters are obtained with one single measurement. The time to reach the maximum heat of polymerization (t_{\max}) is a parameter which depends on photoreactivity and inhibition period. Total double bond conversion (DBC) was calculated from the overall heat evolved (ΔH_p), where $\Delta H_{0,P}$ is the theoretical heat obtained for 100% conversion⁷⁷ (Eq. 1).

$$DBC = \frac{\Delta H_p \times M}{\Delta H_{0,P}} \quad (1)$$

Initial rates of polymerization (R_p [mol L⁻¹ s⁻¹]) were calculated from the height of the maximum of the plots h [mW/mg] and the density of the monomer ρ following Eq. 2.

$$R_p = \frac{h \times \rho}{\Delta H_{0,P}} \quad (2)$$

In the present study, the Photo-DSC measurements were carried out at room temperature with filtered light (1500 mW/cm²; 400-500 nm) applied by a light guide (Efos-Novacure) using 1 wt% of an equimolar mixture of camphorquinone (CQ) and 4-dimethylaminobenzoic acid ethyl ester (DMAB) as photoinitiator (PI). This combination is well-known from dental applications and has been described as excellently biocompatible.⁷⁸

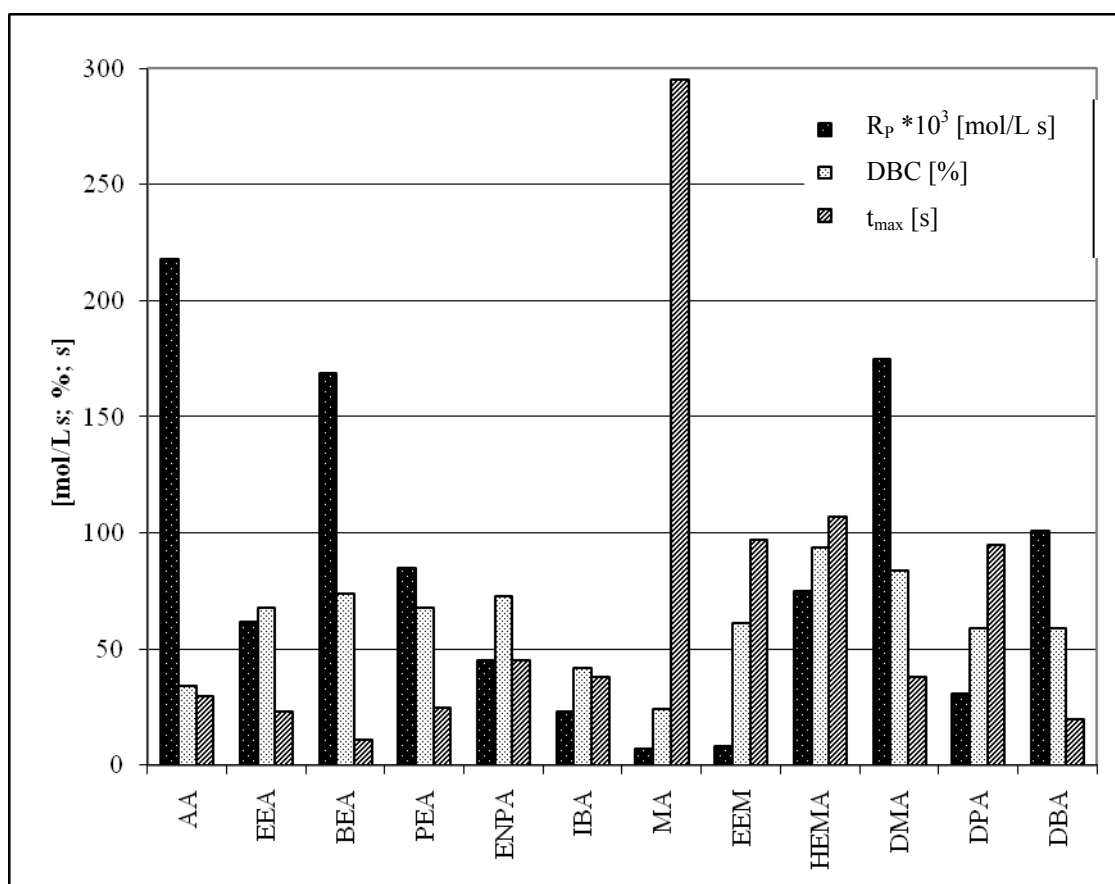


Figure 28: Photoreactivity of monofunctional monomers

Due to its high volatility, t-butyl acrylate (TBA) could not be examined. Monoacrylates (Figure 28) are known to cure slowly due to linear chain formation and the delayed gel effect compared to crosslinked systems. Because of that, higher DBC was mostly achieved. This applies especially to HEMA and DMA. As expected, acrylates and acrylamides gave significantly higher R_p and lower t_{max} than methacrylic compounds. Small monomers like AA and DMA showed higher values for the R_p than monomers with higher molecular weights. The exceptionally low reactivity of acrylamide DPA and isobornyl acrylate (IBA) can be attributed to sterically demanding substituents. Within the acrylates, sterical effects and functional groups also play an important role on the polymerization rate. High R_p and DBC of BEA and HEMA in the group of acrylates and methacrylates, respectively, might be attributed to pre-organization by hydrogen bonding.⁷⁹ The extremely low DBC of AA and MA could be explained by precipitation of the formed polymer, thus terminating propagation reaction.

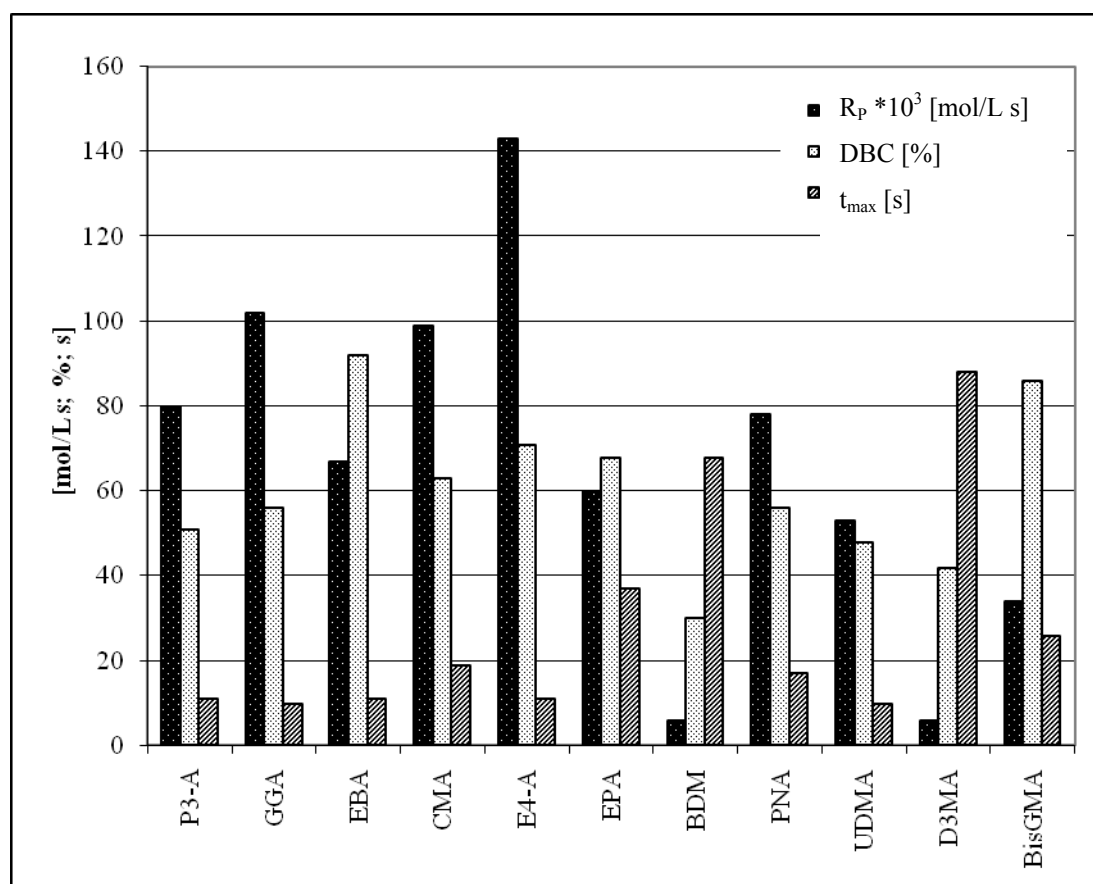


Figure 29: Photoreactivity of difunctional monomers

In Figure 29 photoreactivity data of difunctional monomers are shown. As expected, DBC is in general lower than with mono-acrylates due to network formation. In most cases sufficient R_p and good t_{max} were observed, thus making most of them suitable for SL. Only dimethacrylates with aliphatic spacers (butandiol dimethacrylate (BDM) and D3MA) showed poor performance and are therefore not qualified from the standpoint of reactivity. The presence of methacrylic groups is responsible for that fact. Other methacrylates like BisGMA, UDMA and propoxylated (2) neopentyl diacrylate (PNA) perform significantly better, which might be attributed to some kind of preorganization (of the cyclic structures for example) similar to β -hydroxyacrylates.⁷⁹ This effect is also responsible for the good performance of glycerol 1,3-diglycerolate diacrylate (GGA) among the acrylates. Due to the flexible spacers in E4-A and ethoxylated (10) bisphenol A diacrylate (EBA), excellent photopolymerization behavior and in the case of EBA a nearly complete DBC of 92% was observed. Comparably slow photoreactivity of the bisacrylamide EPA can be explained by the low molecular weight and less flexibility of the monomer, thus giving rigid and tight networks.

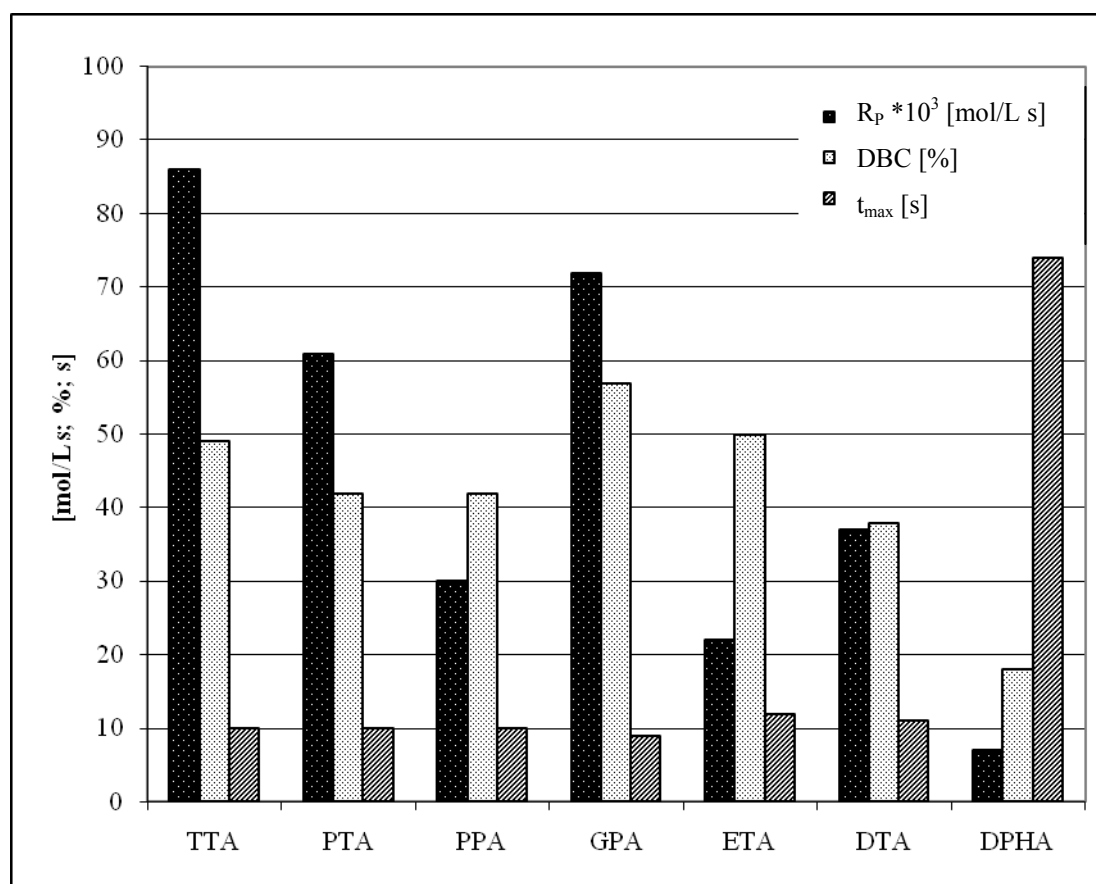


Figure 30: Reactivity of multifunctional monomers

In the case of acrylates having 3 reactive groups (Figure 30) higher DBC of propoxylated (3) glycerol diacrylate (GPA) compared to pentaerythritol triacrylate (PTA) can be explained by the flexible core of GPA. In the case of PTA tight and less flexible networks are formed. Low R_p of ethoxylated (20) trimethylpropane triacrylate (ETA) compared to trimethylpropane triacrylate (TTA) can be assigned to the high molecular weight of the monomer.

Acrylates with more than three reactive groups gave a DBC below 50%, which can be well explained by the highly cross-linked network and therefore poor mobility of the remaining unreacted double bonds. T_{max} does not depend on the number of reactive groups.

2.2.2 Mechanical Properties

To investigate the mechanical properties of the selected polymers, DMA and bending strength tests were carried out. DMA provides information about the storage modulus of the tested material in the temperature range of interest by application of a defined

force with a defined frequency. Stress amplitude and deformation amplitude are being measured and used for the calculation of the storage modulus. Measurements were done between 10°C and 50°C. Three-point bending tests were used to determine the stiffness. Test specimens were prepared as small rods (20*3*3 mm) by photopolymerization in silicon molds. Polymers from mono-acrylated monomers were tested with 20 wt% TTA or EPA as crosslinker – that was necessary to enable extraction of residual monomer and biocompatibility tests in aqueous culture medium. In comparison to traditional biopolymers some of the polymers described in this work exhibit excellent strength and stiffness values. Some materials in contrast were immeasurable due to their rubber-like texture (in spite of being crosslinked) e.g. polymers from BEA, EEA, EEM, DPA and ETA. This can be attributed to the soft and flexible side chains based on poly(ethylene glycol). Polyurethanes also belong to the class of soft and flexible polymers. MA was too brittle to be analyzed.

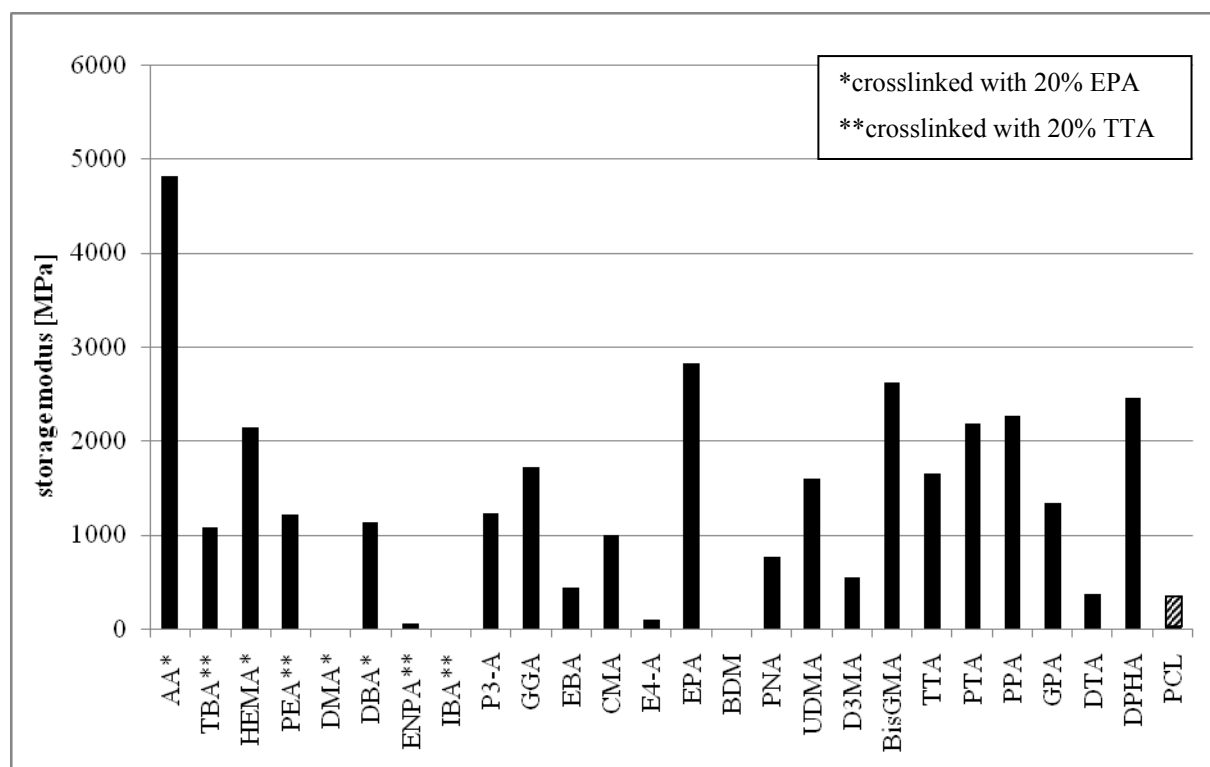


Figure 31: Storage modulus of all monomers at 37°C (MPa)

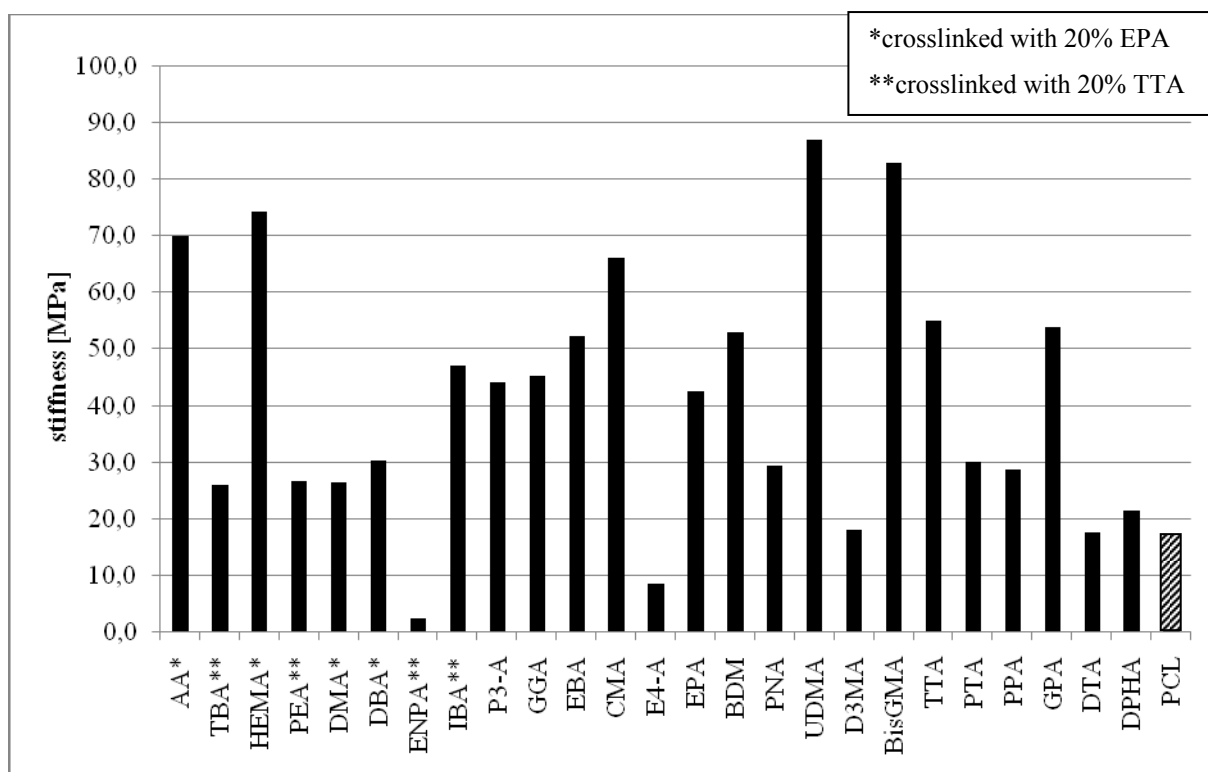


Figure 32: Stiffness at 20°C (MPa)

Several parameters that influence the mechanical properties can be derived from the summarized data in Figure 31 and Figure 32. As expected, polymers from di- or multi-acrylated monomers, which form dense networks, performed better than polymers from mono-acrylated monomers that were only slightly crosslinked with an additional crosslinker. An exception is AA, which forms hard and stiff polymers due to its small size and ability to form hydrogen bonds. Other monomers with the possibility for hydrogen bonding like HEMA, GGA, tricyclodecan dimethanol diacrylate (CMA), BisGMA, UDMA and dipentaerythritol pentaacrylate (PPA) were also among the better materials. The exceptionally low values of ethoxylated (4) nonylphenol acrylate (ENPA) regarding strength and stiffness can be explained by the long and flexible side chain. Also the monomers containing aliphatic spacers, BDM and D3MA, belong to the softer polymers under investigation. D3MA is known as a flexibilizing component in dental restorative resins, which is well-demonstrated by the values obtained in our studies. In the group of diacrylates the cyclic rings of CMA, BisGMA, and EBA are responsible for the excellent strength values. The triacrylates GPA and PTA differ in their spacer length, which is also reflected in the values for strength and storage modulus. PTA gives tight networks resulting in a more brittle material, while GPA

with its long flexible chains has a softer texture. The comparably low strength of ditrimethylolpropane tetraacrylate (DTA), PPA, and dipentaerythritol penta/hexaacrylate (DPHA, 10-15% / 85-90%) might again be assigned to the high crosslinking density and therefore brittle materials. Promising materials from a mechanical point of view include polymers from BisGMA and UDMA, well-known from dental materials, but also tripropylene glycol diacrylate (P3-A), GPA, and CMA. All these materials exhibit strength and stiffness values comparable to or beyond commonly used biopolymers (Table 5).

Table 5: Mechanical properties of common polymers and biomaterials. The values for PE, PA and POM were obtained from the Cambridge Engineering selector (Granta Design)

Material	Strength [MPa]	Storage modulus [MPa]
Polyamide (PA)	90	2800
Polyethylene (PE)	25	500
Polylactic acid (PLA) ⁸⁰	50	3500
Polycaprolactone (PCL) ⁸¹	17	318
Polyoxymethylene (POM)	90	2900
Compact bone ⁸²	50-150	11000

In order to determine the expected influence of additional fillers on the mechanical behavior, a 1:1 mixture of BEA and TTA was chosen as exemplary resin. Different contents of various fillers were added as shown in Table 6. HA and TCP have been reported to be osteoconductive fillers used in bone replacement materials.²⁰ PEG and poly(vinyl alcohol) PVA are possible fillers to tune the viscosity of the formulation in order to optimize the resolution during the SL process.

Strength and stiffness were measured by DMA and 3-point-bending as described above.

Table 6: Mechanical properties of BEA/TTA (1:1) with different fillers

filler	content [w/w %]	stiffness at 25°C [MPa]	strength at 20°C [Mpa]
-	-	1843	28
HA	25	1830	45
HA	50	1750	28
TCP	25	1490	35
TCP	50	2200	33
PEG	5	1025	24
PEG	20	590	17
PVA	5	1900	31
PVA	20	1900	17

Surprisingly only in the case of 50 w/w % TCP as filler can a significant increase in stiffness be observed. The addition of HA didn't have much influence on the storage modulus, while the mixture with 25 w/w % TCP even caused a lowered value. These findings are not only contrary to our expectations, but also in contrast to investigations done by Marc Geiss in his diploma thesis.⁸³ He found increasing stiffness values for mixtures of TTA and HEMA (4:1) up to a content of 60 wt% of HA. More than 3-fold enhancement of the storage modulus could be achieved.

The use of PEG led to a distinct decrease in stiffness as expected and is therefore not the best filler to tune the viscosity. PVA performed better in this aspect since values slightly increased.

The expected increasing effect on the mechanical properties caused by the addition of HA or TCP could only be observed for the values of the strength. Here the use of 25% seemed to be better than 50%, maybe due to increasing brittleness.

2.2.3 Biocompatibility

All monofunctional reactive diluents were copolymerized with 20 wt% of EPA to obtain crosslinked test specimens, since swelling in the aqueous test medium should be reduced. In the case of PEA, IBA, ENPA, and TBA, 20 wt% of TTA were used instead of EPA. PCL, a well-known material from medical applications (such as sutures and drug delivery devices) was used as reference polymer. To these samples, MG-63 osteosarcoma cells were seeded and cultured for three days.

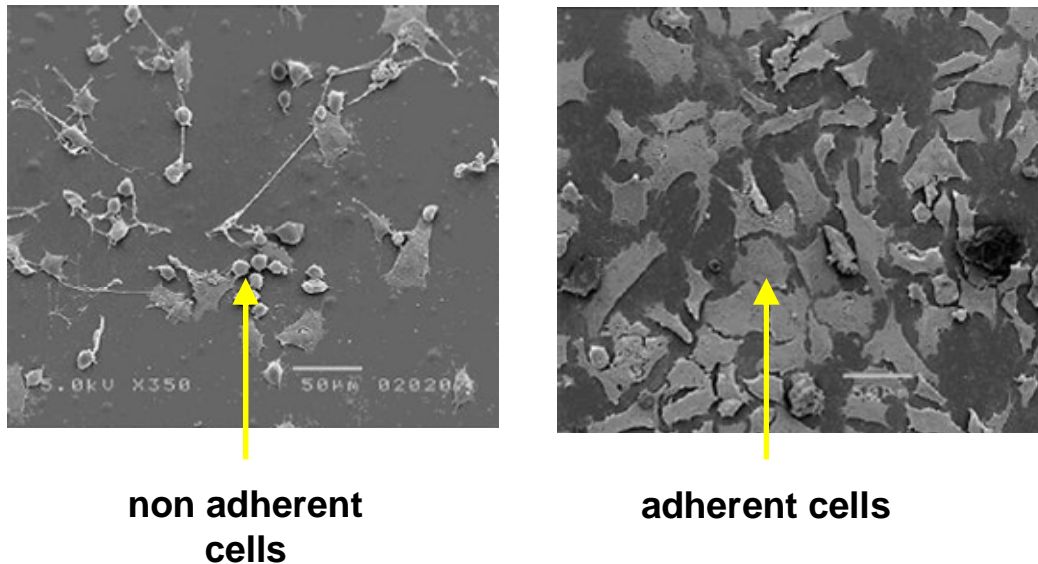


Figure 33: SEM images of adherent and non-adherent cells

These are adherent cells, meaning they must be able to adhere to a surface in order to survive. Emission of toxic substances or unsuitable surface properties (functional groups, too much or too less surface roughness, wettability, etc) lead to cell death within a few hours.

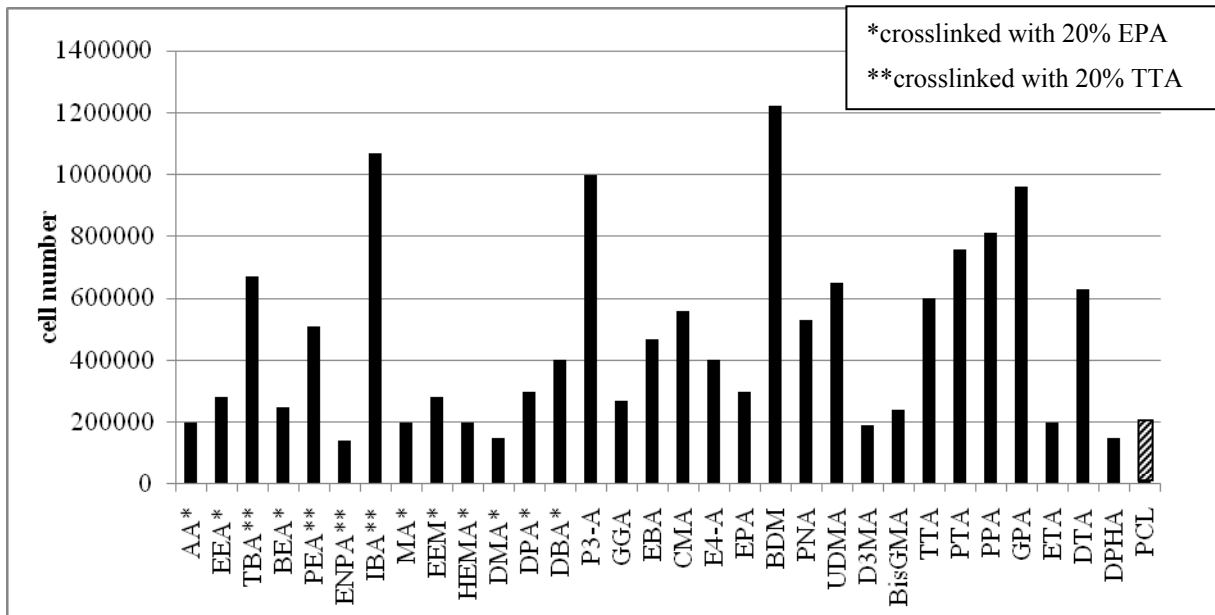


Figure 34: Cell number

Generally, all polymers investigated showed similar or better performance in cell viability compared to the reference. The comparably low values for D3MA and ENPA could be assigned to the soft and more flexible material - cell viability and proliferation are influenced by the mechanical properties of the material, as has

recently been shown^{84,85} - and to the presence of aliphatic and polyethylene glycol-like structures which is well-known to withstand cell adhesion. The lower value for strength of D3MA compared to BDM, but more reasonable the long hydrophobic spacer between the ester groups, led to a significant decrease in cell viability, although the chemical structure is very similar.

Among acrylamides DBA provides a superior support for bone cell adhesion and proliferation than DPA and DMA, which can be attributed to the better mechanical properties on the one hand and suggests better adsorption of the serum proteins of the culture medium on the other hand. This may be due to a better accessibility of the amino-group of DBA, which is known for better cell adhesion and osteoblastic differentiation.^{86,87} The low cell number found on the polymer made from HEMA was expected. Although the material is known to be compatible with cell cultures, it does not support attachment of mammalian cells and is usually used to cover culture dishes to prevent cell adhesion.⁸⁸ The hydroxyl-group of the ethylene glycol may be responsible for this behavior. The relatively poor cell adhesion of BisGMA might also be assigned to the presence of hydroxyl-groups. The good values for stiffness and strength seem to be overruled by the chemical structure. From a structural point of view, excellent results of IBA can be assigned to the camphor-like structure which is well-known for good biocompatibility.

In the case of the monomers with three or more acrylate groups, good results were observed except in the case of DPHA and ETA. Since mechanical properties could not explain this behavior, the high value of residual acrylate groups in the DPHA polymer, as can be seen from the DBC, seems to be responsible. For ETA again the oligo(ethylene glycol) chains reduce the cell adhesion.

In addition to the cell proliferation and viability studies, the morphological appearance of the cells on the two polymers, TTA and UDMA, were examined by staining the stress fibers with phalloidin and investigation by confocal microscopy. On glass, the osteoblastic MG-63 cells showed the typical cubical appearance with well-established stress fibers and distinct adhesions points to the substratum (Figure 35-A). Cells cultured on UDMA displayed a rhomboid appearance with strong stress fibers and distinct adhesion structures as well (Figure 35-B). The morphology of the cells cultured on TTA (Figure 35-C) was slightly longer compared to the cells on the other

materials, and their appearance showed a fibroblastic character. However, stress fibers and contacts to the substratum were well-established. The different morphology of the cells could indicate that during the culture period the cells did not reach the same differentiation status. This could mean that the substratum influences the development of the cells indicated by different morphological appearance.

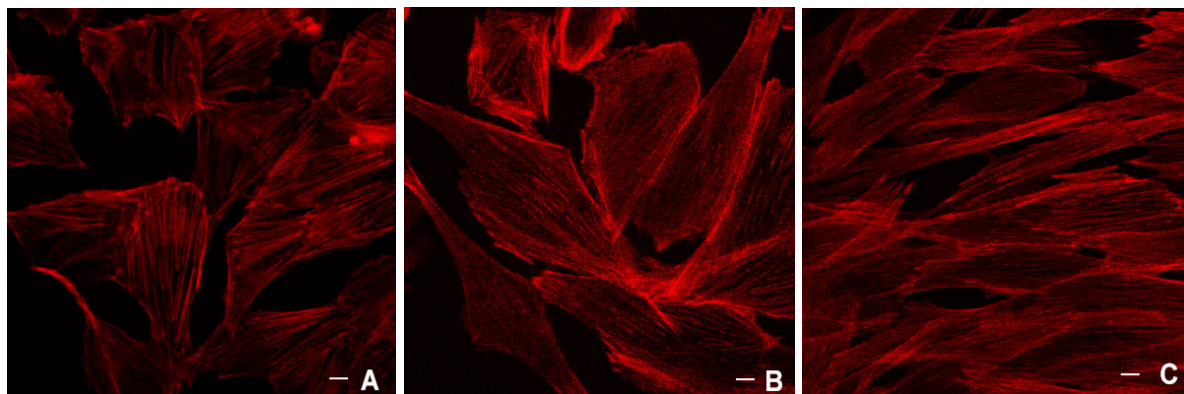


Figure 35: Morphology and stress fibers of MG-63 osteosarcoma cells cultured on glass (A) UDMA (B) and TTA (C)

From these sets of experiments it can be concluded that the presence of a single functional group does not control the cell adhesion and cell multiplication behavior, but rather the whole structure of the monomer is responsible. Nevertheless, it seemed that ether groups, as well-known from poor adhesion behavior from PEGs, but also hydroxy groups (BisGMA, HEMA) have no cell multiplication promoting influence. Carboxylic acids and ester groups, and especially amide linkage (DBA) as in proteins and urethane groups (UDMA) seemed to be preferred. Also the mechanical properties and the DBC seem to play important roles in cell adhesion.

3 Additives

Besides PIs, which are of great importance in any light curable formulation, absorbers and fillers also contribute to good performance and high resolution with SL.

3.1 Photoinitiators

It is well-recognized that the PI plays a key role in any light curable formulation. Indeed the initiator is responsible for the absorption of the incident light radiation

producing the primary radical species that initiate the conversion of monomers. Special attention should be drawn to the choice of the appropriate PI for a polymer with desired biomedical applications. Beside the biocompatibility and non-toxicity of degradation products, high performance and of course appropriate absorption characteristics are important issues due to the intended stereolithographic shaping process.

3.1.1 Low molecular weight photoinitiators

Several Type I and Type II PIs are known to be biocompatible and have found application in the medical field. The Type II system CQ and DMAB is widely used in dental formulations. These two substances were used within this work to prepare the test specimens for the investigations concerning biocompatibility and cell behavior, not least because of its photobleaching capability.⁸⁹ But due to its quite slow Type II mechanism this system is not appropriate for stereolithography. Therefore, two α -cleavable Type I photoinitiators and the new 1,5-diphenylpenta-1,4-dien-3-one (DPD)⁹⁰ (Figure 36) were tested for their applicability in a biodegradable tissue scaffold.

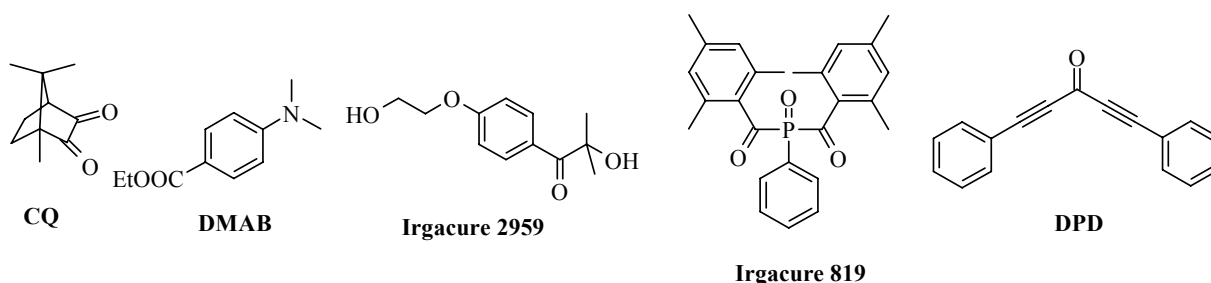


Figure 36: Structure of photoinitiators, CQ / DMAB, Irgacure 2959, Irgacure 819 and DPD

The bisacylphosphine oxide Irgacure 819 is a very promising candidate for rapid prototyping due to its high reactivity and its absorption tailing out in the visible region. This photoinitiator is ideally suitable for the rapid prototyping process using the digital light processing (DLP) principle with light emission only in the visible region. The initiator has already found widespread application in dental materials as well as biodegradable materials for tissue engineering.⁹¹ The hydroxyalkylphenone Irgacure

2959 has often been used for photocuring of biopolymers⁹² and the recently described DPD was also of interest because of the low toxicity ($LD_{50} > 1 \text{ g/kg}^{93}$). Because of the absorption below 400 nm, the application of these two initiators is limited to rapid prototyping machines with appropriate UV-lasers. Photo DSC was used to compare the efficiency of the photoinitiators. For that, 0.5 wt% of Irgacure 819 and Irgacure 2959, respectively, and 1 wt% of an equimolar mixture of CQ and DMAB were dissolved in EPA and measured with filtered light (320-500 nm, 1500 mW/cm^2). Due to the high extinction coefficient of DPD only 0.3 wt% were necessary. Results from the photo-DSC experiments are given in Table 7.

Table 7: Photoreactivity of photoinitiators in EPA

Photoinitiator	t_{max} [s]	DBC [%]	R_p * 10³ [mol L ⁻¹ s ⁻¹]
Irgacure 819	7,8	87	227
Irgacure 2959	12,6	74	141
CQ / DMAB	13,2	63	102
DPD	13,2	62	93

Using this method of analysis, the advantages of curing with Irgacure 819 as photoinitiator are evident. Exceptionally high DBC is of significant importance for low migration systems. Generally, the time for complete curing is very similar for all photoinitiators as the values for t_{max} show. Under practical conditions the available light source wavelength is responsible for the selection of the photoinitiator.

3.1.2 Development of migration stable photoinitiators

However, one important drawback of commercially available PIs is the migration of unreacted molecules to the surface of the material and eventually into the surrounding medium. Especially in medical applications, or when the material is in contact with food, negative consequences like inflammatory reactions or toxication might occur. Different approaches to overcome this problem include the incorporation of the PI into the growing polymer chain, e.g. by modification with acrylate groups and copolymerization, and raising the molecular weight. Possibilities range from dimeric

PIs to polymers with the photoreactive moiety either in the backbone or on a side chain of the polymer.^{94,95,96,97} Also the preparation of copolymers of PI and coinitiator (CoI) have been reported.⁸⁹

For this project, ring opening metathesis polymerization (ROMP) was chosen as preparation method for macromolecular photoreactive compounds, because the development of ruthenium complexes, which initiate the polymerization of strained cycloolefines and which show exceptionally high tolerance versus functional groups, made ROMP a powerful tool for the synthesis of well-defined highly functionalized materials of various architectures.^{98,99,100,101} Macromolecules can be synthesized with almost any desired molecular weight with exceptionally narrow dispersity.

In this chapter the synthesis of macroinitiators with eosin (EO) as the photoreactive moiety by ROMP will be described. Eosin has been used successfully as PI^{102,103,104,105} and photosensitizer.^{106,107,108,109} Amongst other things, the use of eosin for cell encapsulation in polyethylene glycol diacrylate gels, showing promising biocompatibility was reported.^{110,111} The photopolymerization using eosin as PI follows a Type II mechanism and involves a reductive electron transfer from a donor, usually a tertiary amine, followed by a transfer of hydrogen.^{112,113} Also here DMAB was used as CoI. In the following section the synthesis and characterization of statistic ROM-polymers with covalently immobilized eosin and/or DMAB units is presented. The performance of these macroinitiators was evaluated by photo-DSC and compared with the performance of low molecular weight PIs. Moreover, the migration stability was determined via extraction of test specimens followed by UV/Vis-absorption spectroscopy. All newly synthesized compounds were furthermore subjected to viability studies using MC3T3-E1 osteoblast-like cells to evaluate their suitability in bone replacement applications. The acrylate resin used for these experiments was trimethylolpropane triacrylate (TTA). Part of the work, especially the synthesis, was done by Martina Sandholzer at the Graz University of Technology.

3.1.2.1 General Investigations on the photoreactivity of eosin

Two forms of eosin – deprotonated as salt (eosin Y) and neutral (eosin Y spirit soluble) (Figure 37) – are reported as PIs in literature.^{103,113} Therefore, some preliminary investigations on the spectroscopic properties and photoinitiation activity

of these two species were done, using the alkyl modified EO derivative **1** (Figure 37). The alkyl-modification was aimed at providing improved solubility in an acrylate-based resin.

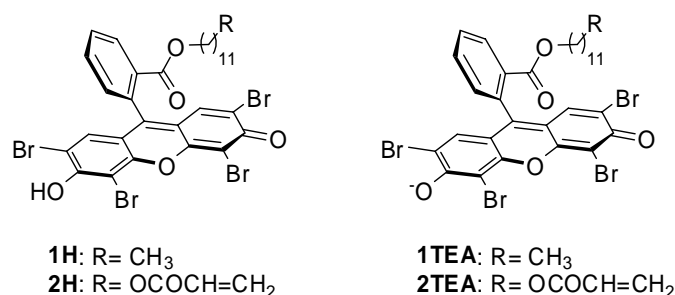


Figure 37: Low molecular weight eosin derivatives (neutral and deprotonated forms)

To convert **1** completely either to the neutral (**1H**) or deprotonated (**1TEA**) form, extraction with HCl (10%) in the first case, and addition of triethylamine (**TEA**, 1.2 mol equiv.) in the other case was used. This procedure was necessary because eosin and its derivatives are readily, at least partially, deprotonated by traces of alkaline species, e.g. amines present in the laboratory atmosphere. In Figure 38 the UV/VIS absorption and the fluorescence spectra of **1H** and **1TEA** in THF are shown. The neutral species shows an absorption maximum at 476 nm (ϵ : 21000 L mol⁻¹ cm⁻¹). Deprotonation leads to a bathochromic shift of the absorption maximum (λ_{max} : 539 nm) and an increased extinction coefficient (ϵ : 85000 L mol⁻¹ cm⁻¹). These effects are also reflected in the fluorescence spectra, where the difference in intensity is even more pronounced. Fluorescence maxima were observed at 556 nm (**1H**) and at 561 nm (**1TEA**) using an excitation wavelength of 528 nm. Due to the higher fluorescence activity of **1TEA**, one might expect a reduced photoinitiator activity.

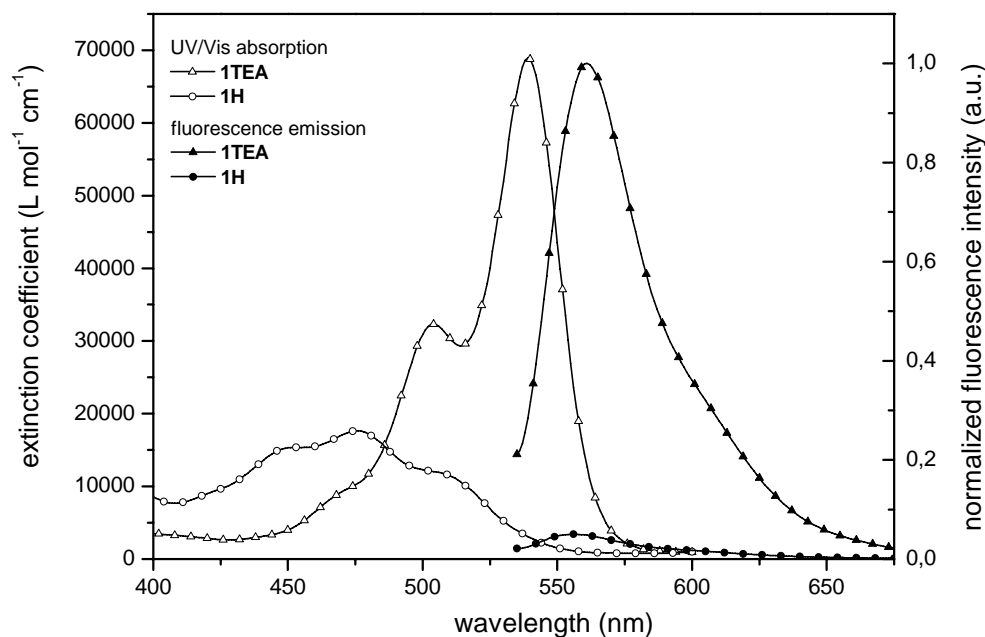


Figure 38: UV-VIS and fluorescence spectra of 1H and 1TEA in THF

Since DMAB is intended to be used as CoI for EO, it was of interest if any interaction between these two molecules occurs similar to EO/TEA. Fortunately UV-VIS measurements showed that DMAB is not able to deprotonate EO and is therefore useful as CoI.

To study the capability of EO as PI, photo DSC is a useful method. The principle and the calculation of important terms are described in chapter 2.2.1.

To investigate the influence of the irradiation, wavelength experiments were done with the common 320-500nm filter, a 250-450nm filter, and with the high pressure mercury lamp without any filter. Its emission spectrum is shown in Figure 39.

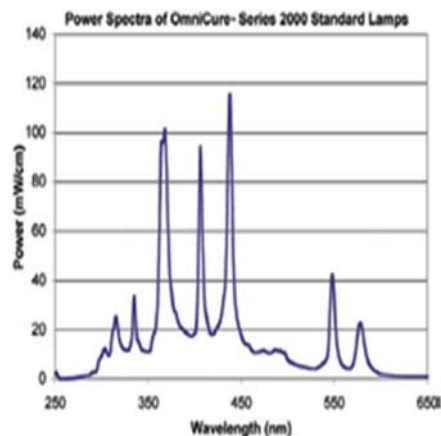


Figure 39: Emission spectrum of a high pressure mercury lamp

Figure 40 shows the photo-DSC plots of the two species of alkyl-EO (**1H** and **1TEA**, 0.3 wt%) in TTA with 1 eq of DMAB as CoI.

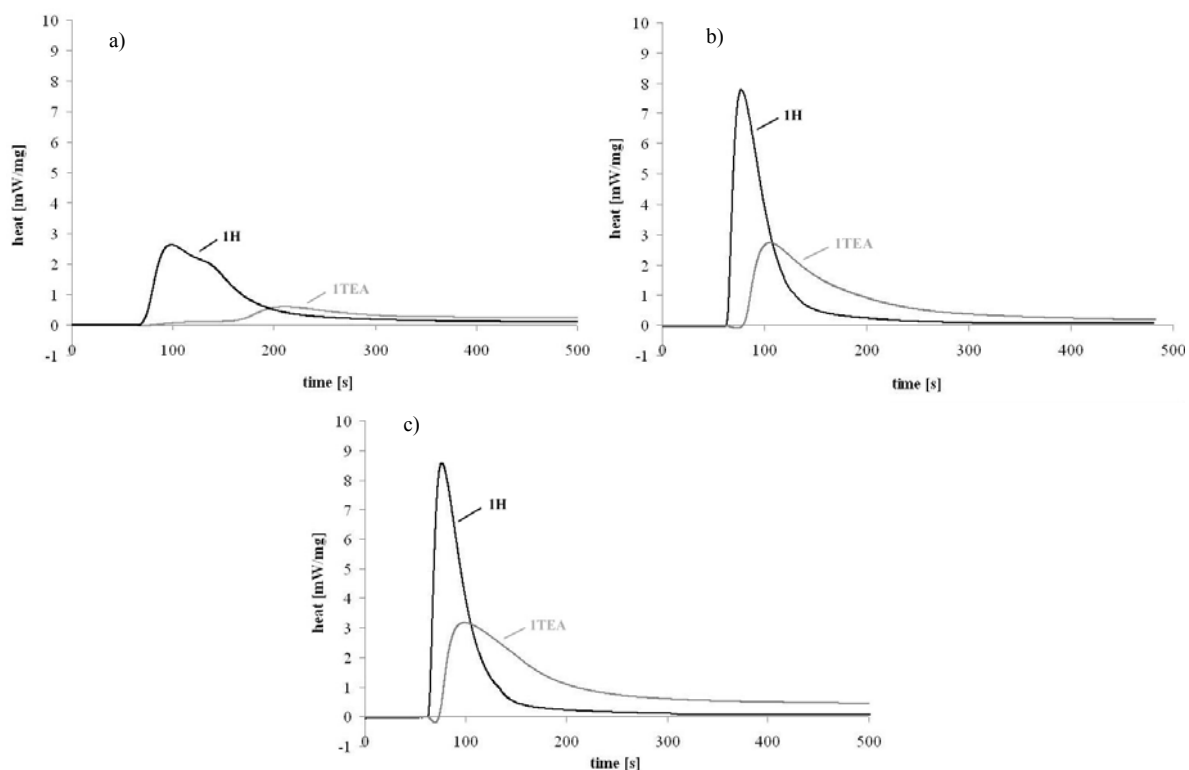


Figure 40: Photo DSC plots of **1H** and **1TEA** a) with filtered light (320-500nm) b) (250-450nm) and c) without filter

Compared to **1TEA**, the neutral form (**1H**) showed better photoreactivity in all experiments (Table 8). In the case of the 320-500 nm filter the deprotonated form **1TEA** was almost unreactive. By changing to a 250-450nm filter the photopolymerization activity significantly increased, especially for **1TEA**. Similar activity was observed without the use of any filter. These findings suggest that the absorption below 320 nm and not the strong absorption above 400 nm, as it could be expected from the UV/VIS spectra, is responsible for the initiation reaction. However, the initiation step has not yet been completely discovered and different mechanisms are described in literature.^{112,113} The comparatively low performance of **1TEA** can be attributed to an extensive radiative relaxation of the excited state.

Table 8: Photo-DSC data of 1H and 1TEA with DMAB as CoI

Filter	Initiator	t_{\max} [s]	DBC [%]	$R_p \cdot 10^3$ [mol L ⁻¹ s ⁻¹]
320-500 nm	1H	37	34	15.8
	1TEA	147	9	2.1
250-450 nm	1H	17	47	41.8
	1TEA	46	38	15.1
-	1H	16	50	50.3
	1TEA	39	43	16.3

In order to get deeper insight into the initiation mechanism and to learn more about the role of the CoI, additional experiments without DMAB were performed. In case of the system **1TEA**/TTA low photoreactivity was observed, whereas, **1H** showed no reactivity under the same conditions.

3.1.2.2 Preparation of macromolecular photoinitiators

ROMP was used to prepare different macromolecular EO based PIs. Polymers were synthesized as statistic copolymers of *endo,exo*-[2.2.1]bicyclo-2-ene-5,6-dicarboxylic acid dimethyl-ester (**6**) and the corresponding PI (**4**) or CoI monomer (**5**) (Figure 41) (that were previously synthesized according to the literature)¹¹⁴ with a modified second generation Grubbs initiator (H₂IMes)(C₅H₅N)₂(Cl)₂Ru=CHPh (**3**)¹¹⁵ in dry CH₂Cl₂ at room temperature. The polymers were isolated by repeated precipitation in n-pentane.

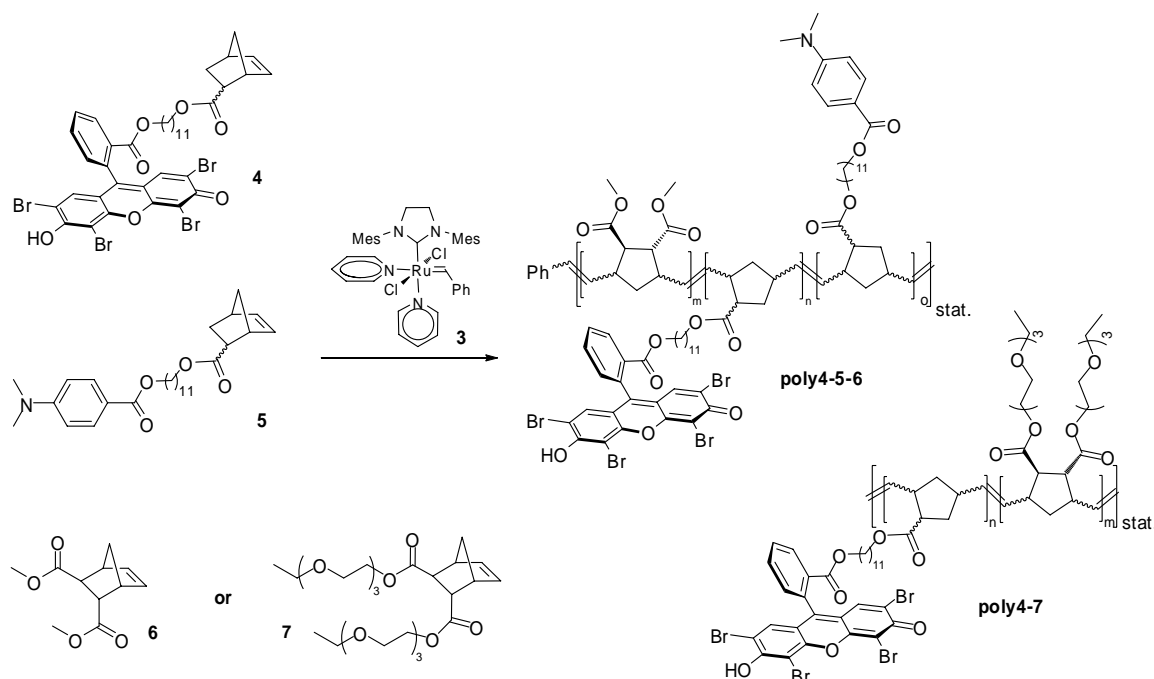


Figure 41: Synthesis of EO macroinitiators

All polymers were obtained in good yield (68%-86%) and were characterized by NMR- and IR-spectroscopy as well as gel permeation chromatography (GPC) and differential scanning calorimetry (DSC). GPC chromatograms showed monomodal size distributions with narrow polydispersity index (PDI) values ranging from 1.07 to 1.31 (Table 9).

Table 9: ROMP polymers

	polymer composition			GPC (in CHCl ₃)			DSC
	4 (parts)	5 (parts)	6 (parts)	M _n (g/M)	PDI	M _{calcd} (g/M)	T _g (°C) ^a
poly 4-6₂	2	0	88	19100	1.09	20400	68
poly 5-6₂	0	2	88	18600	1.05	19400	74
poly 4-5-6₂	2	2	88	19200	1.13	21300	51
poly 4-6₁₅	15	0	75	17300	1.16	29800	77
poly 5-6₁₅	0	15	75	23000	1.07	22600	40
poly 4-5-6₁₅	15	15	75	26800	1.31	36700	64

^adetermined from the 2nd heating run; heating rate: 10°C/min

To investigate if any aggregation effects occur, EO and DMAB were used in two different molar concentrations. In order to improve the solubility of the macromer in

the resin, the matrix monomer (**6**) was modified with oligo(ethylene glycol) moieties (**7** see Figure 41). **Poly 4-7** has the highest calculated molecular weight with M_{calc} 66500, which may lead to differences in diffusion compared to the other macroinitiators. GPC showed a M_n of 34000 and PDI of 1.25.

Another approach to get improved migration stability is to modify the initiator in a way that it gets incorporated into the growing polymer chain. That could be achieved by introduction of an acrylic moiety (**2**).

3.1.2.3 *Characterization of macromolecular photoinitiators*

The newly synthesized macroinitiators were compared to the copolymerizable EO and to the PI and CoI with low molecular weight with regard to their photoreactivity, migration stability, and toxicity.

3.1.2.3.1 **Photoreactivity**

For the following experiments EO-PIs were extracted with HCl prior to use, in order to obtain the neutral form of the dye. Although higher reactivity was observed with a 250-450 nm filter or without filter, irradiation with filtered light (320-500 nm) was chosen, since higher sensitivity of the photo DSC unit and higher sample weights allow a higher level of accuracy. The light intensity was kept constant at 20 mW/cm². Preliminary experiments indicated optimum performance, similar to camphorquinone/DMAB, with the use of 5 eq of amine. Nevertheless, all photo-DSC experiments were carried out with equimolar mixtures of eosin-dye and CoI in order to investigate the subtle interplay of these two components. The concentration of the active EO-moiety was kept constant at 3.3 $\mu\text{mol/g}$, which is the maximum amount that is soluble in the desired TTA resin.

Table 10: Photo-DSC data of EO initiators

Initiator	Coinitiator	t_{\max} [s]	DBC [%]	$R_p \cdot *10^3$ [mol L ⁻¹ s ⁻¹]
1H	DMAB	37	34	15,7
1H	poly5-6₁₅	40	35	11,7
1H	poly5-6₂	72	5	1,1
2H	DMAB	28	38	21,4
2H	poly6-7₁₇	34	33	8,5
poly4-6₁₅	DMAB	50	31	10
poly4-6₁₅	poly5-6₁₅	98	28	5,2
poly4-6₂	DMAB	37	35	13,7
poly4-6₂	poly5-6₁₅	70	31	13,1
poly4-7₁₅	DMAB	120	28	6,9
poly4-7₁₅	poly5-6₁₅	236	20	4
poly4-5-6₁₅		73	23	5,7
poly4-5-6₂		111	23	4,4

Results of the photo-DSC measurements are given in Table 10. The values for R_p and DBC are in general quite low, which can be attributed to the tri-functional monomer TTA. Even with the commercial initiator system camphorquinone/DMAB, DBC values of 50 cannot be exceeded in the polymerization of TTA. As can be seen from Table 10, low molecular weight initiators exhibited a higher reactivity compared to high molecular weight initiators. These findings can be attributed to a higher mobility of low molecular weight compounds and therefore a higher probability for the electron/proton exchange reaction necessary for a Type II mechanism.

The difference in R_p between the **2H**/DMAB mixture and the **2H**/poly **5-6₁₅** mixture is much higher than the corresponding difference between the mixtures with **1H**, which relies on the incorporation of **2H** during the polymerization. That reduces its mobility and causes fewer possibilities for the exchange of electrons and protons between the two initiating components, especially in the case of **poly 5-6₁₅** which has a quite low mobility by itself. The much lower content of the CoI in **poly 5-6₂** seems to be responsible for the very poor reactivity (almost non-reactive) of its mixture with **1H**.

Looking at the polymeric EO derivatives one can find a factor of two between the R_p of the mixtures with DMAB and the mixtures with polymeric DMAB. The slightly higher reactivity of **poly 4-6₂** compared to **poly 4-6₁₅** might be caused by aggregation of EO moieties in **poly 4-6₁₅** resulting in hindered accessibility of the reactive sites. However, the results described above give a strong indication for a bimolecular mechanism of the initiation step. Moreover, it can be concluded that the amine radical acts as the initiating species,⁹⁵ as t_{max} significantly increases when the high molecular weight amine is used.

In order to improve the solubility of the macro-PI in the TTA matrix a glycol-modified norbornene derivative (**7**) was used for the preparation of **poly4-7₁₅**. Unfortunately, **poly4-7₁₅** showed rather poor performance in the photo-DSC experiments. The use of **7** as bulk-monomer for the polymeric initiator resulted in a much higher molecular weight compared to the polymeric PIs described above. A higher molecular weight, however, presumably led to a decreased mobility of the PI.

Statistic co-polymers having both the PI and the CoI incorporated within one and the same polymer chain (**poly 4-5-6₁₅**, **poly 4-5-6₂**) showed significantly lower polymerization activity than the blend systems. Although the two reacting species are in close proximity, the mobility of the whole system is too low to enable good interactions and high reactivity. Another limiting factor might be the in-cage recombination of radicals, thus lowering the amount of initiating radicals.⁸⁹

3.1.2.3.2 Migration Stability

In order to investigate whether the newly synthesized materials show improved migration stability compared to low molecular weight systems, polymer plates were prepared and extracted. UV/Vis-absorption measurements of the extracts were performed to quantify the amount of leaked dye.



Figure 42: Extraction of polymer plates

Test specimens were made of TTA using the same amounts of initiator and CoI as already described for the photo-DSC measurements ($3.3 \mu\text{mol/g}$). The mixtures were cured in silicon molds for 5 min under nitrogen using a high pressure mercury lamp. Afterwards the specimens were extracted in an ultrasonic bath with different organic and aqueous solvents to remove any unreacted monomer, a procedure that is obligatory for a biomedical application. The test specimens were then placed in glass tubes, covered with 5 mL EtOH, sealed and extracted for 1 week at room temperature. One part of the obtained solutions was used to determine the amount of dye by UV spectroscopy. With the other part toxicological measurements were performed.

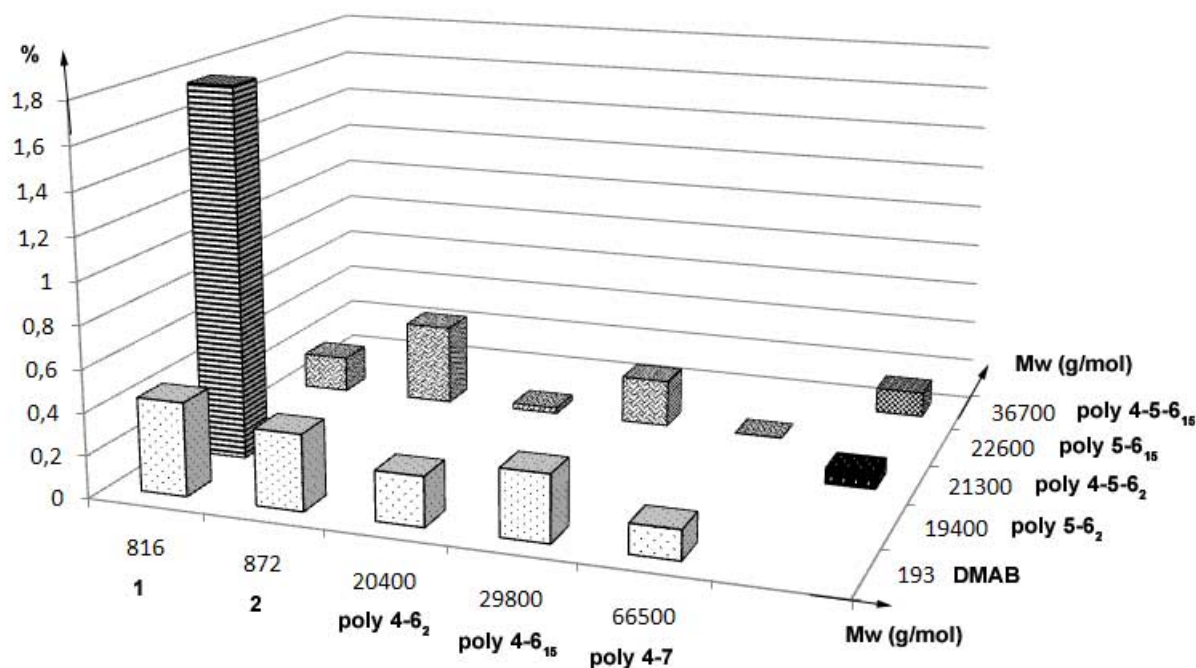


Figure 43: of extracted initiators (in %, compared to the amount used)

In Figure 43 the amount of extracted initiator (% of the amount used in the formulation), obtained from the EtOH extraction step is shown. The amount of initiator leaked during the extraction ranged from 0.08 % to 1.77 %, which can be seen as good migration stability since absolute values range from 0.9 μg to 55 μg . A factor of 10 could be observed between the leaking of high molecular initiators (**poly4-7** with **poly5-6₁₅**, 0.03%) and monomolecular initiators (**1H**, 0.44%).

The relatively high value of leaked initiator of the system **1H/poly 5-6₂** corresponds to the poor results of the photo DSC measurements. Low conversion and therefore low network density results in a high amount of unreacted substances prone to migrate out of the material.

As expected, the migration stability could be improved by using high molecular weight EO as PI. The amount of leaked initiator ranged from 0.23 % for **poly4-6₂** to 0.31 % for **poly4-6₁₅** both used with low molecular weight DMAB as CoI. When **poly5-6₁₅** was used instead of DMAB as CoI the amount of initiator determined in the EtOH extracts was even reduced to 0.23 %-0.03 %. The improved migration stability of EO-polymers in combination with **poly5-6₁₅** compared to the mixtures of EO-polymers with low molecular weight DMAB can presumably be attributed to an interaction between the polymer chains. Addition of the reactive DMAB radical to the

double bonds of the ROM-polymer can lead to the formation of networks if both, PI and CoI are used in their polymeric forms.¹¹⁶

Although relatively poor reactivity in the photo-DSC measurements was observed for **poly4-5-6₂** and **poly4-5-6₁₅** these compounds show fairly high migration stability. The amount of leaked initiator was 0.08 % for **poly4-5-6₂** and 0.12 % for **poly4-5-6₁₅**. These results can be attributed to the high molecular weight of these macro-initiators resulting in a reduced mobility. The same trend was observed in case of **poly4-7** (leakage: 0.09-0.14 %) which has the highest molecular weight of all substances under investigation.

3.1.2.3.3 **In vitro LD50**

Since the substances presented herein have a potential application in the synthesis of bone replacement materials, all newly synthesized compounds were examined with regard to toxicology. For the viability study and the determination of the in-vitro LD50, MC3T3-E1 osteoblast-like cells were used. The cells were continuously exposed to increasing concentrations (10^{-9} - 10^{-3} mol/L) of monomers and polymers and to the ethanol extracts gained from the migration study. Monomers as well as ROM-polymers proved to be non-toxic up to a concentration of 10^{-5} M. Above this concentration the substances precipitated in the aqueous test medium. The EtOH extracts did not show a toxic reaction either.

3.2 **Further Additives**

3.2.1 *Fillers*

Soluble organic fillers are necessary to adjust the viscosity of the monomer formulation to achieve the highest possible resolution of the SL machines. Between 0.3 and 0.5 Pas fabrication is easiest. Poly(vinyl pyrrolidone) (PVP), PVA and cellulose-acetate-butyrate (CAB) have previously been tested regarding biocompatibility¹¹⁷ and found to be acceptable in a bone replacement material.

Insoluble inorganic fillers such as HA and TCP are osteoconductive²⁰ and serve to enhance the mechanical stability of the material.

3.2.2 Absorbers

Depending on the RP machine and the corresponding light source two different absorbers were used.

The Prefactory DLP machine from Envisiontec, described in the next chapter, works with visible light and therefore a colored absorber was necessary. A substance containing chrome was kindly provided by Envisiontec. The exact structure of the molecule could not be determined. Tests with endothelial cells showed no cytotoxicity up to 10^{-3} mol/L in spite of the containing chrome (no measurements were performed above this concentration). For optimum layer thickness, an amount of 0.1 wt% was added to each formulation. The obtained objects were orange, which might be disadvantageous for certain applications.

The laser of the μ -SL machine demanded a substance with an absorption maximum around 350 nm. 2,2'-Dihydroxy-4,4'-dimethoxybenzophenone (HMBP) was found to be a cheap and good possibility to control the penetration depth.

The third RP method used within this project was the two photon polymerization. Because of its principle, which will be explained in the next section, no absorber is needed in this case.

4 3D-Structuring

When it comes to the fabrication of a bone implant for a specific patient, with interconnected pores of defined size, RP techniques offer great possibilities because of their layer-by-layer processing. Compared to classic melt- and solution-techniques such as Injection molding and Electrospinning, or SFF techniques such as FDM or SLS, RP methods based on light-induced curing of a photosensitive resin have exceptional potentialities since higher resolutions are achievable and processing at room temperature enables the incorporation of temperature sensitive materials, e.g. growth factors.

During this project three different kinds of SL were applied, which differ in the light source and the achievable resolutions. They will be discussed in detail in the following section. Since monomer formulations had to be adjusted individually for each

technique, their composition and design is described in the corresponding sub-chapters.

4.1 Digital light processing

DLP is the RP method with the lowest resolution used in the framework of this study, but it is by far good enough to replicate human bone with its inner structure. The utilized Perfactory Mini DLP machine from Envisiontec GmbH allows shaping parts with a xy-resolution of 45 μm and a minimum layer thickness of 25 μm . This computerized fabrication technique works like all SL methods with layer-by-layer photopolymerization. A CAD model of the designed object is sliced, and the image of the first slice projected into the bottom of a resin tank, where photopolymerization takes place according to this image. The polymer adheres to the z-stage which is then moved upwards (30 μm). Since each individual layer is exposed in one shot, the build speed (approximately 5-15 vertical mm/hr) is fairly high.

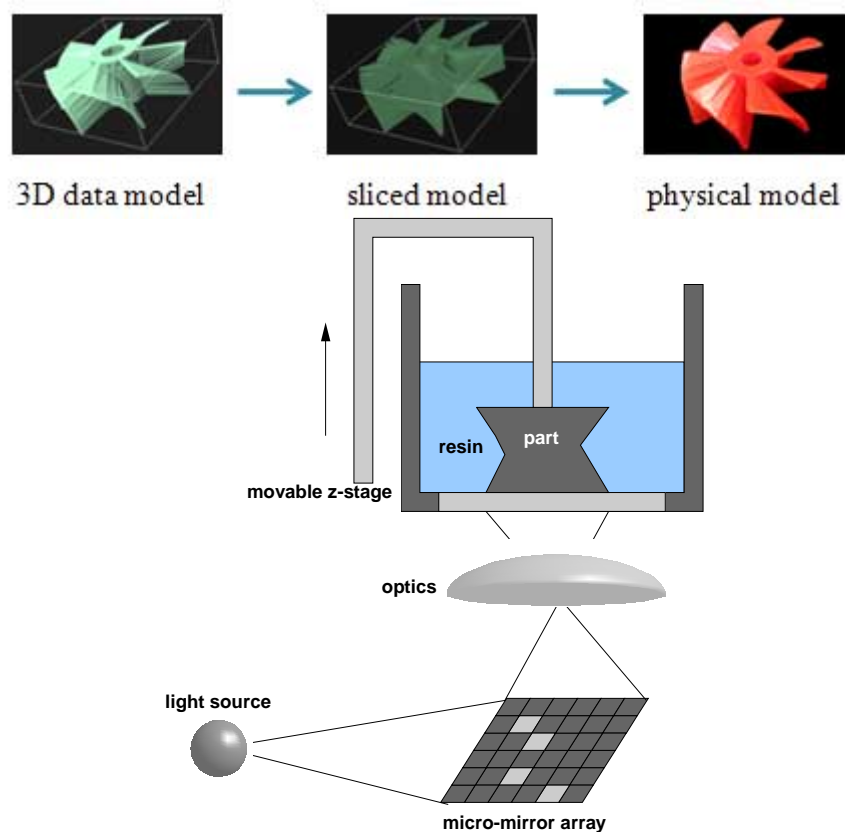


Figure 44: Digital light processing

The vat is only coated with a thin layer of resin, thus the required amount of initial resin is quite low (50-100 mL). Drawbacks of the method are mostly related to the attachment of the polymerized resin to the transparent silicone layer. Especially monomers with low molecular weight tend to migrate into the silicone. In this case the silicone layer can be destroyed after a couple of exposures, requiring a replacement of the vat.

Four different monomer formulations have been designed especially for this machine. Two of them are biocompatible, and the other two are both biocompatible and biodegradable. Table 11 shows the detailed composition of the four resins.

Table 11: Composition of resins for DLP

component	resin 1	resin 2	resin 3	resin 4
biodegradable basis monomer	-	-	11.4% GM	8.0% GP4M
reactive diluent 1	72% DBA	48.8% DBA	11.4% PEGDM	11.9% PEGDM
reactive diluent 2	11% MSA	7.4% MSA	45.7% HEMA	10.0% E4-A
reactive diluent 3	9.9% UDMA	6.7% UDMA	-	47.8% HEMA
photoinitiator	3% Irg 819	3% Irg 819	3% Irg 819	2.4% Irg 819
solvent	-	-	22.9% H ₂ O	15.9% H ₂ O
soluble filler	4% CAB	4% CAB	5.5% PVP	3.9% PVP
insoluble filler	-	30% HA	-	-
absorber	0.1% OR1	0.1% OR1	0.1% OR1	0.1% OR1

Resins 1 and 2 are biocompatible but non-degradable polymers that differ only in the addition of HA as osteoconductive filler, which additionally enhances the mechanical properties of the polymer. These resins were mainly developed as model resins to adjust the settings of the DLP machine such as time (12 s) and intensity (66 mW) of exposure, to find the optimal dynamic viscosity (0.3 Pa s) for highest resolution and also the optimum concentrations of photoinitiator (3%) and light absorber (OR1; 0.1%). The successful fabrication of a spongiosa like structure (Figure 45c) with resin 2 showed that building is also possible with finely powdered solid particles. Although light scattering occurred, feature resolution did not decrease due to the addition of 30 wt% of HA. Beside their function as model systems for the following biodegradable resins, they could possibly also find application in the medical field, where hard and stiff materials are required that do not degrade.

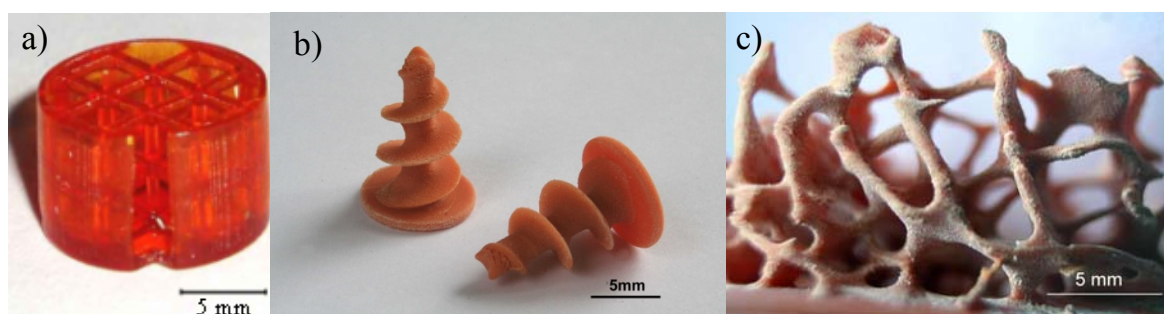


Figure 45: Structures prepared by DLP with resin 1 (a) and 2 (b and c)

After the preliminary results from resin 1 and 2 it was quite easy and resin-saving to find the optimum settings of the DLP machine for the two biodegradable resins 3 and 4. Nevertheless some shrinkage of the objects could be observed a few days after fabrication due to evaporation of the water. This factor has to be considered when implants of exact size should be built. Storage in humid atmosphere might be helpful. Figure 46 shows the obtained cellular structures.

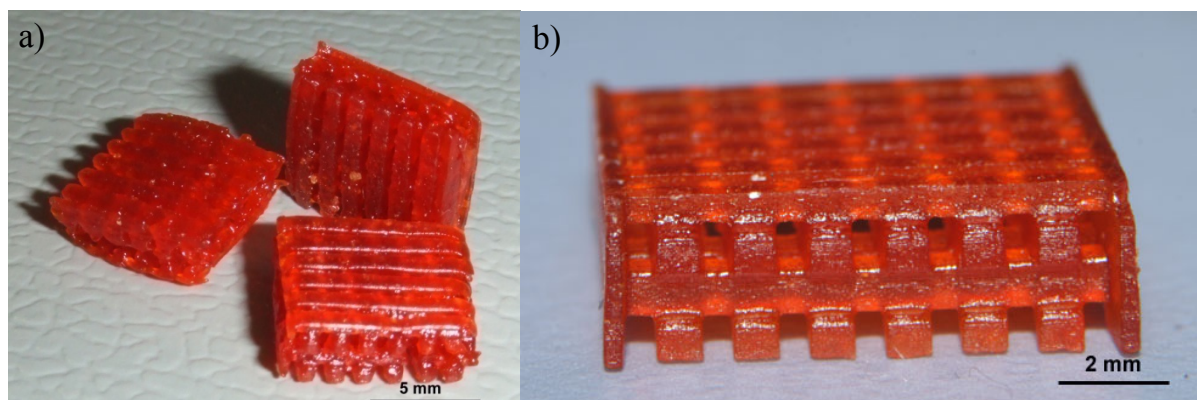


Figure 46: Objects prepared by DLP using resin 3 (a) and 4 (b)

Figure 46(a) shows that the use of water diminishes the resolution and geometry because of shrinkage. Further optimization of the formulation in resin 4 led to clearer structures without artifacts.

Resin 4 was characterized exemplarily regarding its photoreactivity. FT-IR spectroscopy was used for the determination of the DBC, because for a resin, which is a complex mixture of monomers the calculation via Photo-DSC is not possible. So, first a photo-DSC measurement was done, from which t_{\max} was obtained. Then the cured polymer specimen and a drop of the uncured monomer formulation were analyzed using an ATR-IR unit. The comparison of the peak areas for the C=C bonds

in the polymer and the monomer spectra using peak deconvolution gave the DBC. The C=O bond at 1725 cm^{-1} served as the reference bond.

Table 12: Photoreactivity data of resin 4

t_{\max} [s]	DBC [%]
20	74

The obtained values were surprisingly good, since only 10% of the mixture was made up by an acrylate, E4-A. The other components were methacrylates, which are known to react slower. Resin 4 exhibited a t_{\max} quite close to the value of E4-A, which was 11 s. The influence of HEMA, which represents 48% of the mixture, seemed to be rather small. Its initial t_{\max} was 107 s.

4.2 Micro-Stereolithography

Alternatively, a micro-SL system based on a UV-laser was utilized. Here a laser is traced over the surface of the resin. After lowering of the object and coating, the next layer is cured. The details of the setup are described by Neumeister et al.¹¹⁸

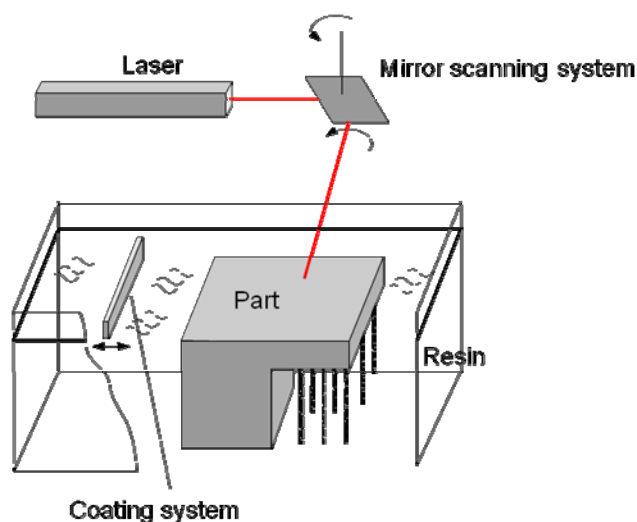


Figure 47: Micro-Stereolithography

The xy-resolution for this system is around $5\ \mu\text{m}$ and the minimum layer thickness is $10\ \mu\text{m}$. In contrast to the DLP-systems there are no issues with swelling of the silicone vat since the micro-SL uses a traditional approach where the resin is solidified at its

upper surface. Care has to be taken to use resins with low viscosity, otherwise consistently thin layers are hard to achieve. Since the resin surface is in contact with air, oxygen inhibition might play a role with some monomers.

The use of water is not possible with this kind of SL because curing happens on the surface and the layer thickness is only 10 μ m. Evaporation would occur and drastically reduce the resolution. Therefore no resins containing water could be used and only biocompatible but no biodegradable polymers were fabricated. Table 13 shows the composition of the used monomer formulations.

Table 13: Composition of resins for μ -SL

component	resin 5	resin 6
reactive diluent 1	49.1% ETA	78.7% UDMA
reactive diluent 2	49.1% TTA	19.6% PEG700DA
photoinitiator	1.5% Irg 2959	1.5% Irg 819
absorber	0.3% HMBP	0.2% HMBP

HMBP with its absorption maximum at 350nm was used as absorber. Due to the different irradiation wavelength and the use of highly reactive monomers, lower contents of initiator could be used compared to DLP. Hard and stiff polymers as shown in Figure 48 and Figure 49 were obtained.

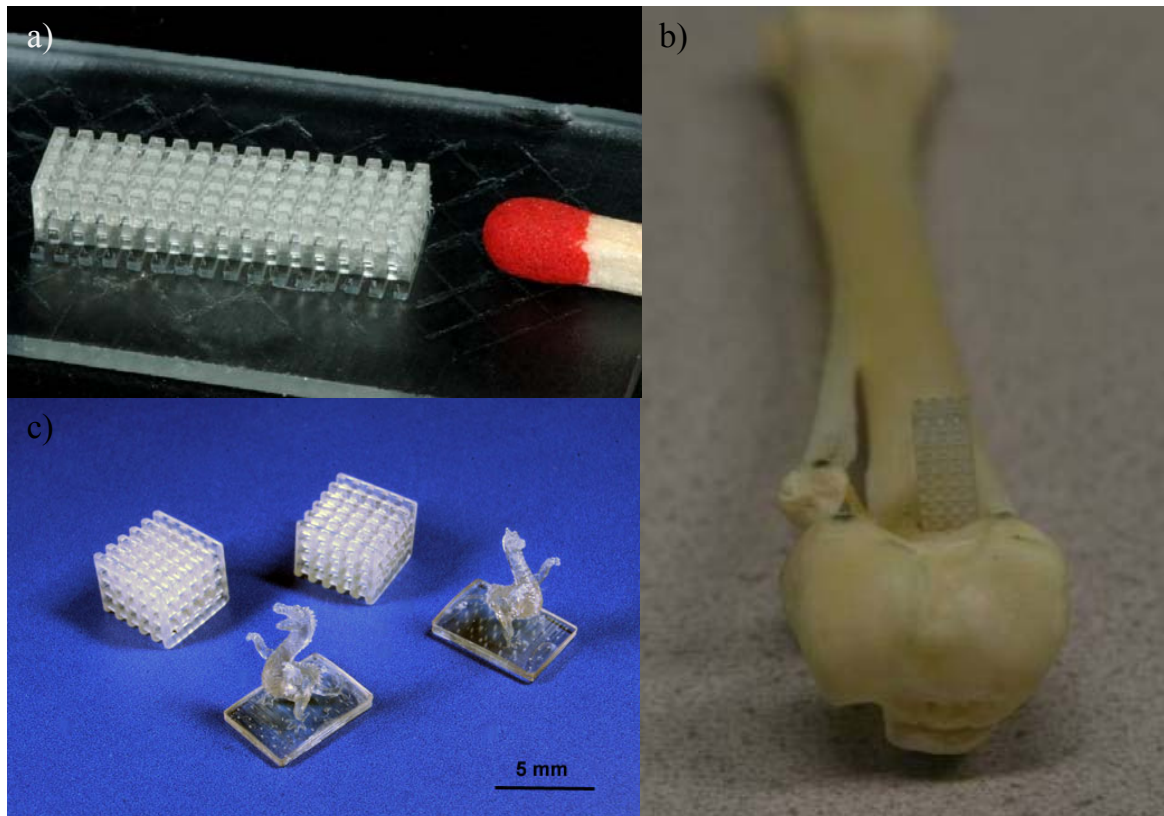


Figure 48: Objects prepared by μ -SL using resin 5 (a and b) and resin 6 (c)

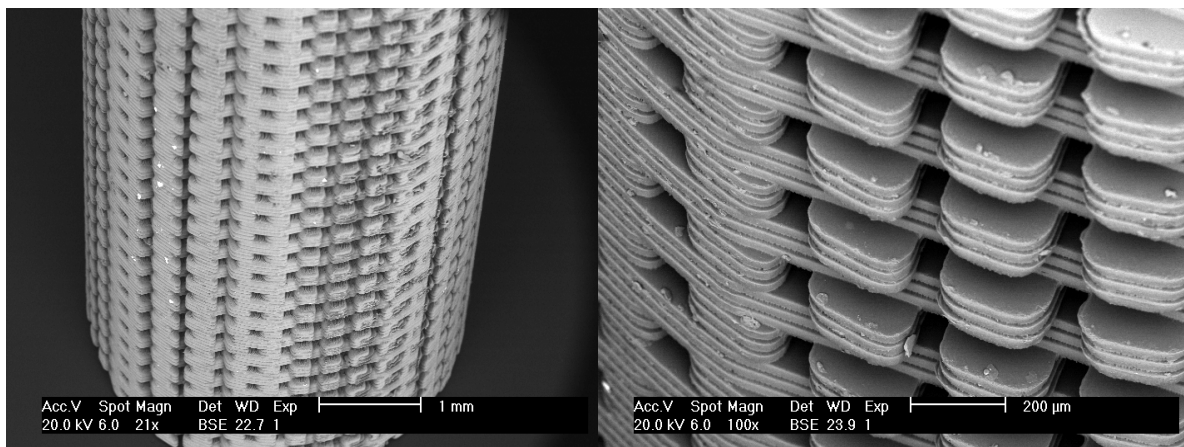


Figure 49: SEM images of cellular structures prepared with resin 5

Clear structures with high resolution and without artifacts could be obtained.

4.3 Two Photon Absorption Polymerization

A third method is the fabrication with two photon polymerization that enables a theoretical spatial fabrication resolution down to 120 nm¹¹⁹ and surface roughness well below 50 nm. Although such a high resolution is not necessary for the preparation of a

cellular bone implant, this method might be useful for other medical applications and the fabrication of a biocompatible structure was therefore tested. The Two Photon Polymerization process employs femtosecond laser pulses (Ti:Sapphire laser, 130 fs, 1kHz, 750–850 nm) which are focused into the volume of a photopolymer, being transparent at the laser wavelength.

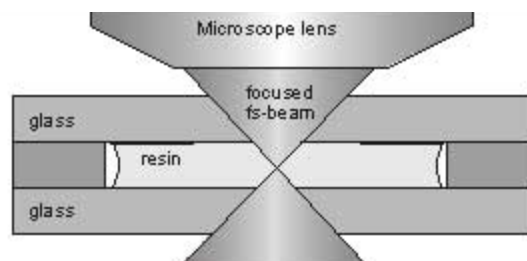


Figure 50: Principle of a two photon absorption machine

Solidification is performed in a highly localized volume due to the quadratic dependence of the two-photon absorption rate on the laser intensity. When two photons of 800 nm are absorbed simultaneously by a suitable photoinitiator⁹⁰ they act as one 400 nm photon and start the polymerization. By this method feature resolutions below the diffraction limit of the used light are possible (Figure 51).⁹⁰

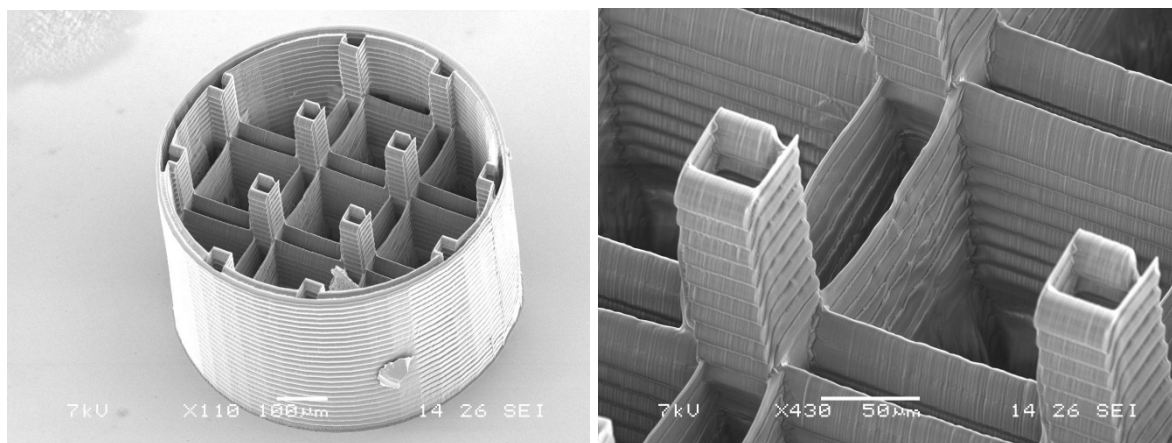


Figure 51: Structures prepared by two photon polymerization

The resin used for these experiments was a 1:1 mixture of ETA and TTA with 0.08% of NDPD⁹⁰ as photoinitiator.

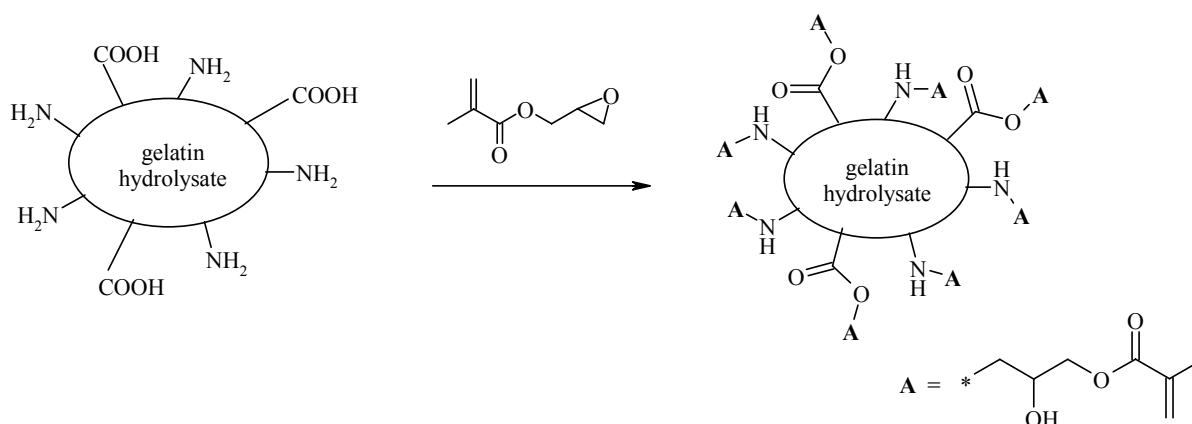
Experimental

1 Basis Monomer

1.1 Synthesis of gelatin derivatives

Preliminaries: The enzymatic gelatin hydrolysate (GH, obtained by Aldrich G0262) with a molecular weight of up to 6000 g/mol was dialyzed prior to use, using a membrane with a MWCO (molecular weight cut off) of 3500 g/mol. A 20% solution of GH in distilled water was dialyzed against a 20 fold excess of distilled water for 24 h with several changes of water. Approximately 75% of the used material was cut off.

1.1.1 Gelatin hydrolysate – methacrylate (GM)



Reagents	MW (g/mol)	density (g/mL)	mmol	g	mL	eq
dialyzed gelatin hydrolysate (GH)	-	-	1.65 ^{*)}	1.0	-	1
glycidylmethacrylate	142	1.075	8.25	1.2	1.1	5
hydroquinone monomethylester	124	-	0.02	0.002	-	0.01
diluted NaOH (pH 8.5)					50	

^{*)}total amount of free amino and acidic groups of gelatin according to literature

Procedure:

GH was dissolved in distilled water and adjusted to pH 8.5 with diluted NaOH. The mixture was heated up to 40°C, then 5 eq of glycidylmethacrylate were added together with the inhibitor, and stirred overnight. The solution was then extracted with EE and

dialyzed against distilled water for 24 h with several changes of water. Afterwards the remaining water was evaporated and the product dried in vacuum.

Yield: 0.77g yellow solid (63% of theory)

Analysis:

For the determination of the conversion of amino groups titration with 0.01M HCl was performed against methyl red. Acidic groups were titrated with 0.01M NaOH against phenolphthalein. GH before modification showed following values:

<i>amino groups</i>	<i>0.105 mmol/g</i>
<i>acidic groups</i>	<i>0.360 mmol/g</i>

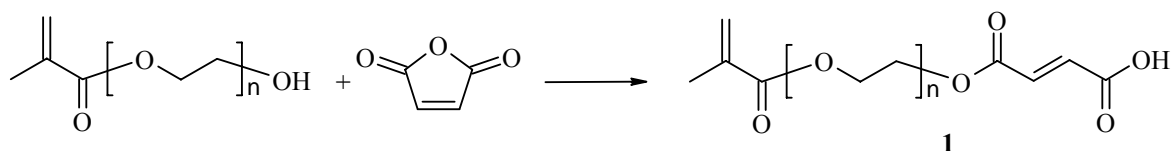
<i>Titration of GM</i>	<i>modified amino groups</i>	<i>0.105 mmol/g</i>
	<i>modified acidic groups</i>	<i>0.136 mmol/g</i>
	<i>corresponding to 0.241 mmol/g methacrylic groups</i>	

¹H-NMR of GH with phenol as internal standard showed that peak at 0.9 ppm correspond to 0.288 mmol/g CH₃ groups.

<i>¹H-NMR (D₂O) δ(ppm):</i>	<i>6.2 (H<u>C</u>H=C)</i>	<i>Int = 0.287</i>
	<i>5.7 (<u>H</u>CH=C)</i>	<i>Int = 0.283</i>
	<i>0.9 (CH₃)</i>	<i>Int = 1</i>
	<i>corresponding to 0.245 mmol/g methacrylic groups</i>	

1.1.2 Gelatine hydrolysate – PEG-methacrylate (GPMM)

1.1.2.1 Preparation of monomethacrylate-PEG-acid¹²⁰



Reagents	MW (g/mol)	mmol	g	mL	eq
PEG monomethacrylate	360	2.8	1.0	-	1
maleic anhydride	98	4.2	0.41	-	1.5
4-dimethylamino pyridine	122	0.08	0.01	-	0.03
hydroquinone	110	0.02	0.002	-	0.01
CHCl ₃				25	

Procedure:

PEG-monomethacrylate was preliminarily dried over CaCl₂ over night. Maleic anhydride and 4-dimethylaminopyridine were dissolved in chloroform (5 mL) at 60°C and the solution obtained was added to a solution of PEG monomethacrylate and hydroquinone in chloroform (20 mL) at 60°C. The solution was stirred at 60°C for 24 h, cooled to room temperature and washed with water (5 × 10 mL). The CHCl₃ phase was dried over Na₂SO₄, filtered and the solvent evaporated in vacuum. The product was dried in vacuum.

Yield: 0.85g slightly yellow oil (67% of theory)

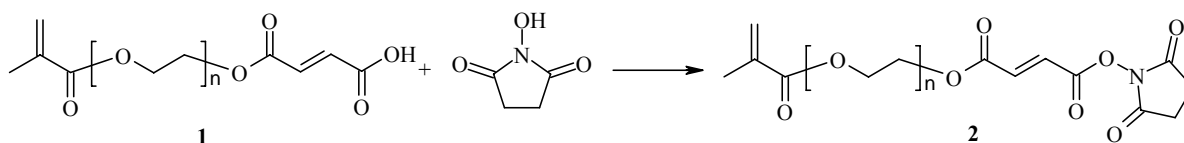
Analysis:

DC (CHCl₃/MeOH 5:1, +AcOH): $R_f = 0.34$

¹H-NMR (CDCl₃) δ (ppm):

- 9.29 (s, 1H, COOH)
- 6.28 (dd, 2H, CH=CH)
- 6.09 (s, 1H, HCH=C)
- 5.54 (s, 1H, HCH=C)
- 4.26-4.39 (m, 4H, CH₂-O-CO)
- 3.64 (d, 16.7H, CH₂-O)
- 1.91 (s, 3H, CH₃)

1.1.2.2 Preparation of monomethacrylate-PEG-NHS¹²¹



Reagents	MW (g/mol)	density (g/mL)	mmol	g	mL	eq
monomethacrylate - PEG – acid (1)	458	-	7.7	3.54	-	1
NaHCO ₃	84	-	39.6	3.33	-	5
N-Hydroxysuccinimid (NHS)	117	-	10.8	1.26	-	1.4
diphenylchlorophosphate (DPCP)	269	1.296	11.8	3.17	2.4	1.5
CHCl ₃ abs.	-	-	-	-	250	-

Procedure:

The synthesis was done according to literature. To a solution of the acid (1) in water-free CHCl₃, 5 eq of NaHCO₃, 1.4 eq of NHS and finally 1.5 eq of diphenyl chlorophosphate were added. The mixture was heated to 40°C and stirred under nitrogen for 24 h. Afterwards it was extracted with a saturated solution of NaHCO₃ and brine. The organic phase was dried over Na₂SO₄, filtered, the solvent evaporated and the product dried in a vacuum oven at 40°C.

Yield: 3.24g colorless oil (72% of theory)

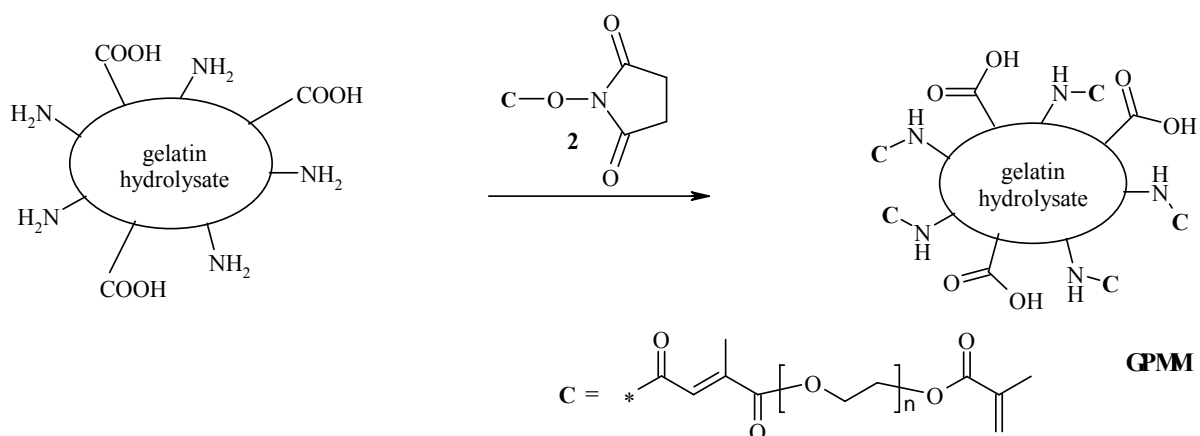
Analysis:

DC (CHCl₃/MeOH 5:1, +AcOH): $R_f = 0.74$

¹H-NMR (CDCl₃) δ (ppm):

- 6.48 (dd, 2H, CH=CH)
- 6.09 (s, 1H, HCH=C)
- 5.54 (s, 1H, HCH=C)
- 4.29 (d, 4H, CH₂-O-CO)
- 3.65 (d, 15.5H, CH₂-O)
- 2.82 (s, 4H, CO-CH₂-CH₂-CO)
- 1.91 (s, 3H, CH₃)

1.1.2.3 Preparation of GPMM¹²²



Reagents	MW (g/mol)	mmol	g	mL	eq
GH		0.92	2.42	-	1
monomethacrylate - PEG – NHS (2)	557	1.63	0.91		1.8
phosphate buffered saline (PBS)				50	
DMF				5	

Procedure:

GH was dissolved in PBS. The PEG reagent (2) in DMF was added dropwise within 30 min. The mixture was stirred at room temperature for 24 h. The product was isolated by dialysis against distilled water for 24 h with several changes of water. Finally the solvent was evaporated in vacuum and the solid product dried in vacuum.

Yield: 1.51 g yellow solid (52% of theory)

Analysis:

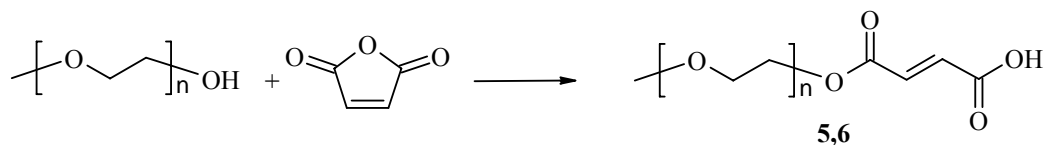
Titration data are not available in this case.

¹ H-NMR (D ₂ O) δ(ppm):	6.2 (HCH=C)	Int = 0.032
	5.7 (HCH=C)	Int = 0.033
	0.9 (CH ₃)	Int = 1

corresponding to 0.028 mmol/g methacrylic groups

1.1.3 Gelatin hydrolysate – PEG, methacrylate (GPM and GP4M)

1.1.3.1 Preparation of monomethyl-PEG-acid



Reagents	MW (g/mol)	mmol	g	mL	eq
monomethyl-PEG	1000/4000	10/2.5	10	-	1
maleic anhydride	98	50/12.5	4.90/1.22	-	5
4-dimethylamino pyridine	122	0.8/0.2	0.098/0.025	-	0.08
CHCl ₃ abs				150	

Procedure:

The synthesis was done as described above (*chapter 1.1.2.1*).

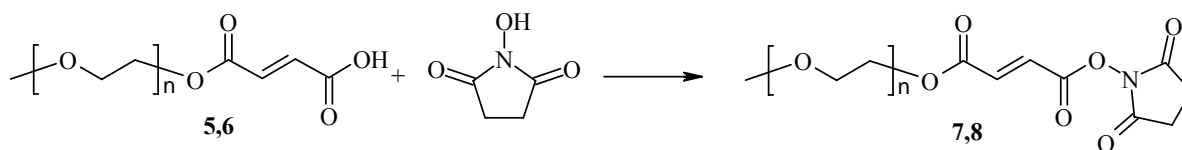
Yield: PEG1000 (**5**): 7.8 g colorless waxlike solid (71% of theory)

PEG4000 (**6**): 9.5 g yellow waxlike solid (87% of theory)

Analysis:

¹ H-NMR (CDCl ₃) δ(ppm):	6.24 (q, 2H, CH=CH)
	4.29 (t, 2H, CH ₂ -COOR)
	3.42-3.65 (m, 90H, [360H] CH ₂)
	3.31 (s, 3H, CH ₃)

1.1.3.2 Preparation of monomethyl-PEG-NHS¹²³



Reagents	MW (g/mol)	mmol	g	mL	eq
monomethyl-PEG-acid (5,6)	1098/4098	9.1/2.4	10	-	1
NHS	117	10.1/2.6	1.17/0.31	-	1.1
dicyclohexyl carbodiimide	206	10.9/2.9	2.25/0.59	-	1.2
4-dimethylamino pyridine	122	0.18/0.05	0.022/0.006	-	0.02
EE abs.				250	

Procedure:

The reagents were dissolved in dry EE and stirred for 24 h at room temperature under nitrogen atmosphere. Afterwards, solid byproducts were filtered off and the solvent was evaporated in vacuum. For further purification the product was redissolved in dry EE and once again filtered. After evaporation of the solvent the product was dried in vacuum.

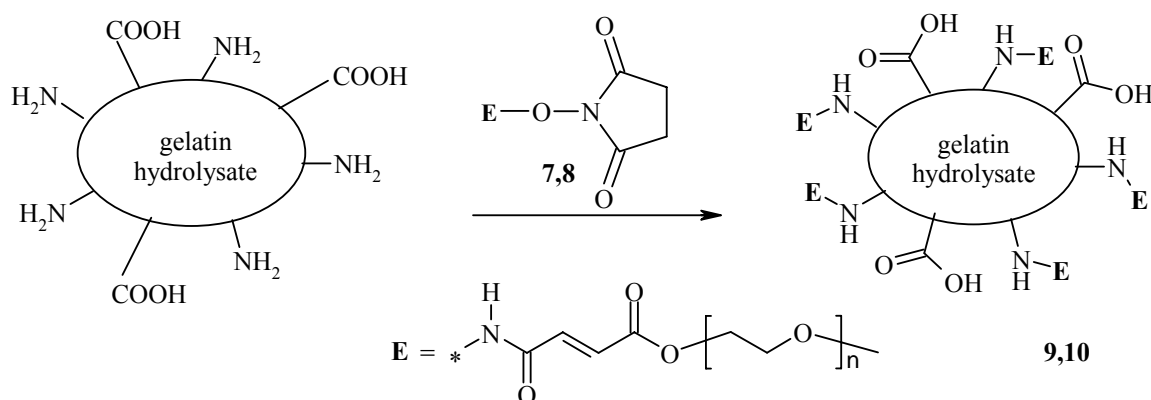
Yield: PEG1000 (7): 9.9 g brown waxlike solid (98% of theory)

PEG4000 (8): 8.2 g brown waxlike solid (82% of theory)

Analysis:

¹ H-NMR (CDCl ₃) δ (ppm):	7.06 (dd, 2H, CH=CH)
	4.37 (t, 2H, CH ₂ -COOR)
	3.50-3.75 (m, 90H, [360H] CH ₂)
	3.51 (s, 3H, CH ₃)
	2.86 (s, 4H, CO-CH ₂ -CH ₂ -CO)

1.1.3.3 Modification of GH with monomethyl-PEG-NHS¹²⁴



Reagents	MW (g/mol)	mmol	g	mL	eq
GH		0.38	1	-	1
monomethyl-PEG-NHS (7,8)	1197/4197	0.57	0.68/2.39		1.5
DMSO abs.				15	

Procedure:

The reagents were dissolved in dry DMSO under nitrogen atmosphere and stirred at room temperature for 24 h. The aqueous solution was then washed with EE and the remaining reaction mixture was dialyzed for 24 h against distilled water. The solvent was finally evaporated in vacuum and the product dried in vacuum.

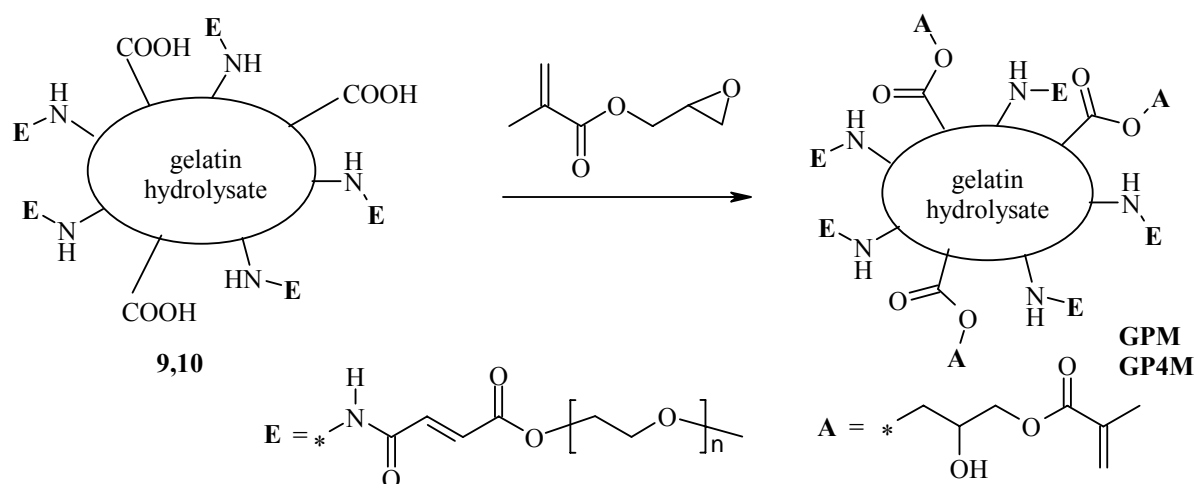
Yield: PEG1000 (**9**): 0.89 g yellow solid (63% of theory)

PEG4000 (**10**): 1.84 g yellow solid (72% of theory)

Analysis:

<i>PEG 1000 (9) Titration</i>	<i>modified amino groups</i>	<i>0.105 mmol/g</i>
<i>¹H-NMR (D₂O) δ(ppm):</i>	<i>3.7 (CH₂-O)</i>	<i>Int = 21.455</i>
	<i>0.9 (CH₃)</i>	<i>Int = 1</i>
	<i>modified amino groups</i>	<i>0.230 mmol/g</i>
<i>PEG 4000 (10) Titration</i>	<i>modified amino groups</i>	<i>0.105mmol/g</i>
<i>¹H-NMR (D₂O) δ(ppm):</i>	<i>3.7 (CH₂-O)</i>	<i>Int = 54.93</i>
	<i>0.9 (CH₃)</i>	<i>Int = 1</i>
	<i>modified amino groups</i>	<i>0.167 mmol/g</i>

1.1.3.4 Preparation of GPM and GP4M



Reagents	MW (g/mol)	density (g/mL)	mmol	g	mL	eq
9,10	-		1.27	1.0	-	1
glycidylmethacrylate	142	1.075	2.54	0.36	0.3	2
hydroquinone monomethylester				0.02		
diluted NaOH (pH 8.5)					20	

Procedure:

The modification with glycidylmethacrylate was done as described above (*chapter 1.1.1*).

Yield: PEG1000 (GPM): 0.63 g yellow solid (53% of theory)

PEG4000 (GP4M): 0.67 g yellow solid (57% of theory)

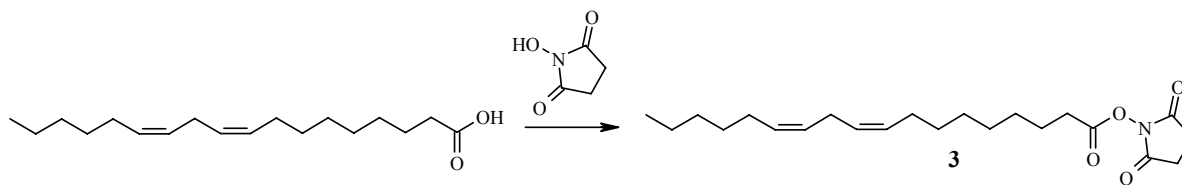
Analysis:

<i>PEG 1000 (GPM)</i>	<i>Titration</i>	<i>modified amino groups</i>	<i>0.105 mmol/g</i>
		<i>modified acidic groups</i>	<i>0.212 mmol/g</i>
	<i>¹H-NMR (D₂O) δ(ppm):</i>	<i>6.2 (HCH=C)</i>	<i>Int = 0.011</i>
		<i>5.7 (HCH=C)</i>	<i>Int = 0.010</i>
		<i>3.7(CH₂-O)</i>	<i>Int = 21.455</i>
		<i>0.9 (CH₃)</i>	<i>Int = 1</i>
		<i>modified amino groups</i>	<i>0.206 mmol/g</i>
		<i>modified acidic groups</i>	<i>0.009 mmol/g</i>
		<i>PEG 4000 (GP4M)</i>	<i>Titration</i>
		<i>modified acidic groups</i>	<i>0.328 mmol/g</i>

$^1\text{H-NMR}$ (D_2O) δ (ppm):	6.2 ($\text{H}\underline{\text{C}}\text{H}=\text{C}$)	$\text{Int} = 0.081$
	5.7 ($\underline{\text{H}}\text{CH}=\text{C}$)	$\text{Int} = 0.069$
	3.7 ($\text{CH}_2\text{-O}$)	$\text{Int} = 54.93$
	0.9 (CH_3)	$\text{Int} = 1$
	modified amino groups	0.132 mmol/g
	modified acidic groups	0.068 mmol/g

1.1.4 Gelatin hydrolysate – linolic amide, methacrylate (GLM)

1.1.4.1 Preparation of linolic acid NHS ester



Reagents	MW (g/mol)	density (g/mL)	mmol	g	mL	eq
linolic acid	280		18	5	-	1
NaHCO ₃	84	-	72	6	-	4
NHS	117	-	2.3	19.8	-	1.1
DPCP	269	1.296	21.6	5.8	4.5	1.2
CHCl ₃ abs.					200	

Procedure:

The synthesis was done as described above (*chapter 1.1.2.2*).

Yield: 6.30g yellow oil (87% of theory)

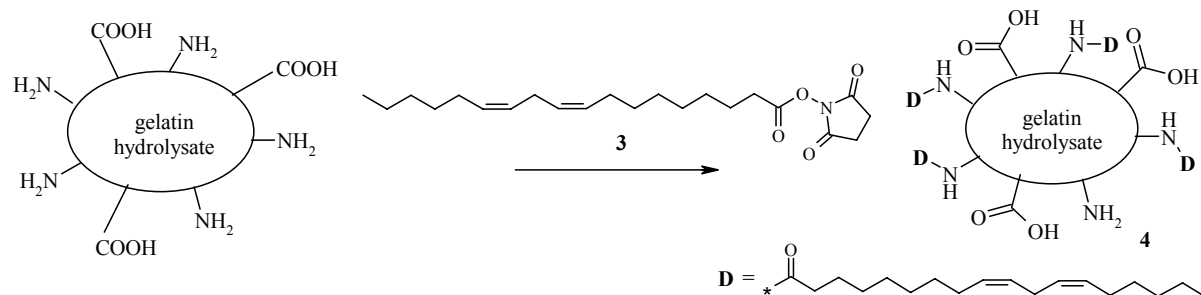
Analysis:

DC (CHCl₃/MeOH 5:1, +AcOH): $R_f = 0.91$

¹H-NMR (CDCl₃) δ (ppm):

- 5.26-5.47 (m, 4H, CH=CH)
- 2.82 (s, 4H, CO-CH₂-CH₂-CO)
- 2.79 (t, 2H, =CH-CH₂-CH=)
- 2.60 (t, 2H, CH₂-COOR)
- 2.04 (t, 4H, CH₂-CH=CH)
- 1.75 (t, 2H, CH₂-CH₂-COOR)
- 1.22-1.45 (m, 14H, CH₂)
- 0.89 (t, 3H, CH₃)

1.1.4.2 Modification of GH with linolic acid¹²⁵



Reagents	MW (g/mol)	mmol	g	mL	eq
GH	-	0.38	1.0	-	1
linolic acid NHS ester (3)	380	0.76	0.3		2
DMSO abs			0.02	15	

Procedure:

Two eq of the linolic acid NHS ester (3) was reacted with GH in water-free DMSO at room temperature for 24 h. The product was obtained by precipitation in cold EtOH. After washing with warm EE the white solid product was dried in vacuum.

Yield: 0.84g yellow-white solid (77% of theory)

Analysis:

Titration of GM *modified amino groups* *0.105 mmol/g*

NMR could not be used to determine the conversion in this case, because signals resulting from linolic acid were overlapping with those of GH.

1.2 Testing

1.2.1 GPC and MALDI-TOF

GPC measurements were performed on a Viscotek GPCmax VE 2001, equipped with Waters Ultrahydrogel 120, 250 columns and a Viscotek RI Detector VE3580. Samples were dissolved in H₂O (10 mg in 1 mL) and filtered with a syringe filter (Millipore Millex-FG Hydrophobic PTFE 0.2 μm). The injection volume was 100 μl, the flow rate was set to 1 mL/min and the temperature was 40°C. Poly(ethylene oxide) was used for calibration.

MALDI-TOF Mass Spectrometry was performed on a Micromass ToFSpec 2E Time-of-Flight Mass Spectrometer. The instrument is equipped with a nitrogen laser (337 nm wavelength, operated at a frequency of 5 Hz), and a time lag focusing unit. Ions were generated by irradiation just above the threshold laser power. Positive ion spectra were recorded in reflectron mode applying an accelerating voltage of 20 kV and externally calibrated with a suitable mixture of poly(ethyleneglycol)s (PEG). The spectra of 100-150 shots were averaged. Analysis of data was done with MassLynx-Software V3.5 (Micromass/Waters, Manchester, UK).

Samples were dissolved in 1% TFA (c = 0.1 and 0.01 mg/mL, respectively), 2,5-dihydroxybenzoic acid (2,5-DHB) and α-cyano-4-hydroxycinnamic acid (CHCA) were used as matrix (c = 10 mg/mL in acetonitrile : 1% TFA = 70 : 30 (v / v)). Generally, solutions were mixed in the cap of a microtube in the ratio of 1 μL : 10 μL. 0.5 μL of the resulting mixture were spotted onto the target and allowed to air dry.

1.2.2 Compatibility with acrylic monomers

For the determination of the miscibility of the gelatin derivatives with organic media, all the synthesized substances were diluted in the 2-fold excess of distilled water. A 4:1 mixture of HEMA and PEGDM was added dropwise to the aqueous solutions until turbidity and precipitation was observed.

1.2.3 Cytotoxicity

For the viability study and the determination of the *in-vitro* LD50 MC3T3-E1 osteoblast-like cells were used. As culture medium Dulbecco's Modified Eagle's Medium (α -MEM) supplemented with 10% fetal calf serum (FCS), glucose (5 g/L), gentamicin (30 μ g/L), L-glutamin and ascorbic acid was used. Cells were kept in a humidified air under 5 % CO₂ at 37 °C for 5 days. The cells were continuously exposed to increasing concentrations (10^{-4} - 10^{-2} mol/L) of the monomers and GH derivatives. Then, the cells were washed with phosphate buffered saline. The DNA, was coloured using the Hoechst 22855 dye and the fluorescence was measured at 460 nm (λ_{ex} : 360 nm). From these results the *in-vitro* LD50 was determined via interpolation of a calibration function.

Additionally experiments were done with endothelial cell cultures. Human umbilical vein endothelial cells (HUVEC) were seeded into cell culture plates at a density of 40000 cells/cm² and incubated for 24 h with increasing concentrations (10^{-7} - 10^{-3} mol/L) of the substances at 37°C. Cells grown in M199 medium containing 10% fetal calf serum alone served as proliferation control. Inhibition of cell proliferation was assessed using the EZ4U assay.

2 Reactive Diluents

2.1 Selection of monomers

All reagents, unless otherwise noted, were purchased from Sigma-Aldrich and were used without further purification. The monomers MA, EEA, EEM, BEA, HEMA, IBA, TBA, PTA and GGA were also obtained from Sigma Aldrich. DMA and AA were received from Fluka, BDM and MA were received from Merck. EPA, D3MA, BisGMA and UDMA were obtained from Ivoclar Vivadent as a gift. Further monomers – obtained as a gifts - are: P3-A (Miramer M220, Rahn AG), GPA (Miramer M320, Rahn AG), PPA (Sartomer 399, Cray Valley), PNA (Sartomer 9003, Cray Valley), DTA (Sartomer 355, Cray Valley), PEA (Sartomer 339C, Cray Valley), ENPA (Sartomer 504, Cray Valley), CMA (Sartomer 833S, Cray Valley), EBA (Ebecryl 150, Cytec), DPHA (85-90% hexa-acrylate, Cytec), E4-A (Sartomer), ETA

(Cray Valley, Sartomer 415, with 20 mol ethoxylated, MW 1176g/mol), TTA (Rahn, Genomer 1330) and DPA (Chemie Linz). DBA was prepared as described.¹²⁶ Photoinitiators Irgacure 819 and Irgacure 2959 were received from Ciba SC as a gift.

2.2 Testing

2.2.1 Photoreactivity

Differential scanning photocalorimetry (Photo-DSC) was conducted with a modified Shimadzu DSC 50 equipped with a home-made aluminum cylinder (height 6.8 cm). Filtered light (320-500 nm) was applied by a light guide (EXFO Omnicure 2000) attached to the top of the aluminum cylinder. The light intensity at the level of the surface of the cured samples was measured by an EIT Uvicure[®] high energy UV integrating radiometer. Irradiation was carried out for at least 5 min. A light intensity of 20 mW/cm² which corresponded to 1000 mW/cm² at the tip of the light guide, was used. The measurements were carried out with 1 wt% of an equimolar mixture of camphorquinone (CQ) and N,N-dimethylaminobenzoic acid ethyl ester (DMAB) as initiator in an isothermal mode at room temperature under air atmosphere. The mass of the samples was 5-10 mg. The time to reach the maximum polymerization heat (t_{\max}), the double bond conversion (DBC) and the maximum rate of polymerization (R_p) were determined.

The DBC was calculated from the overall heat evolved (ΔH_p), where $\Delta H_{0,p}$ is the theoretical heat obtained for 100% conversion (Eq. 1).

$$DBC = \frac{\Delta H_p M}{\Delta H_{0,p}} \quad (1)$$

Initial rates of polymerization R_p (mol L⁻¹ s⁻¹) were calculated from the height of the maximum of the plots h (mW/mg) and the density of the monomer ρ following Eq. 2.

$$R_p = \frac{h\rho}{\Delta H_{0,p}} \quad (2)$$

In Table 14 the values used for the calculations are listed. The values for the density were obtained from the company that provided the monomers. The theoretical heat was calculated based on experimental data for similar substances.⁷⁷

Table 14: Values necessary for the photo-DSC calculations

<i>abbreviation</i>	<i>MW [g/mol]</i>	ρ [g/l]	$\Delta H_{0,P}$ [J/mol]
AA	72.06	1051	67000
EEA	188.23	1016	81000
BEA	215.25	1064	80500
PEA	192.21	1100	78000
ENPA	506.00	1030	78000
IBA	208.30	1000	78000
MA	86.09	1015	42500
EEM	202.25	1018	50000
HEMA	130.14	1070	50000
DMA	99.13	962	80600
DPA	155.24	887	111000
DBA	183.30	888	80500
P3-A	300.35	1040	156000
GGA	348.45	1076	156000
EBA	776	1140	156000
CMA	332.00	1080	156000
E4-A	310.11	1115	156000
EPA	238.33	1025	120600
BDM	226.27	1010	120000
PNA	328.4	1187	156000
UDMA	470.57	1087	120000
D3MA	338.48	950	120000
BisGMA	512.59	1160	120000
TTA	296.32	1103	234000
PTA	298.29	1180	234000
PPA	525	1190	390000
GPA	428.20	1090	234000
ETA	1176	1115	234000
DTA	466.52	1100	312000
DPHA	571.55 ^{*)}	1170	507000

^{*)} determined for 87% hexa-acrylate

2.2.2 Mechanical properties

To investigate the mechanical properties of the selected polymers, dynamical mechanical analysis and bending strength tests were carried out. Therefore, test specimens (rods, 20 mm length, 3 mm width, 3 mm height) were made from the monomers with 1 wt% of an equimolar mixture of CQ and DMAB as initiator. Photocuring was performed with a high pressure mercury lamp (1000 W, distance 15

cm) under nitrogen atmosphere within 3 -10 min depending on the type of monomer. Afterwards, the test specimens were extracted with different organic solvents (CHCl_3 , MeOH, EtOH), phosphate buffered saline (PBS), and H_2O in an ultrasonic bath to remove residual monomer similar to the tests of biocompatibility. Polymers from mono-acrylates were prepared as copolymers with 20 wt% of a crosslinker, either EPA or TTA, because the linear homopolymers would be destroyed in the extraction step. These copolymers were also used for biocompatibility tests to avoid swelling and dissolution in the cell culture.

To determine the stiffness, the beams were placed in a dynamic mechanical analysis machine (TA Instruments DMA 2980) with a span-width of 20 mm. An extra initial load was applied in order to assure the direct contact between the sample and the clamp. The beams were tested with a frequency of 1.0 Hz and an amplitude of 40 μm in the temperature range between 10°C and 50°C. Typical curves obtained by this method are displayed in Figure 52.

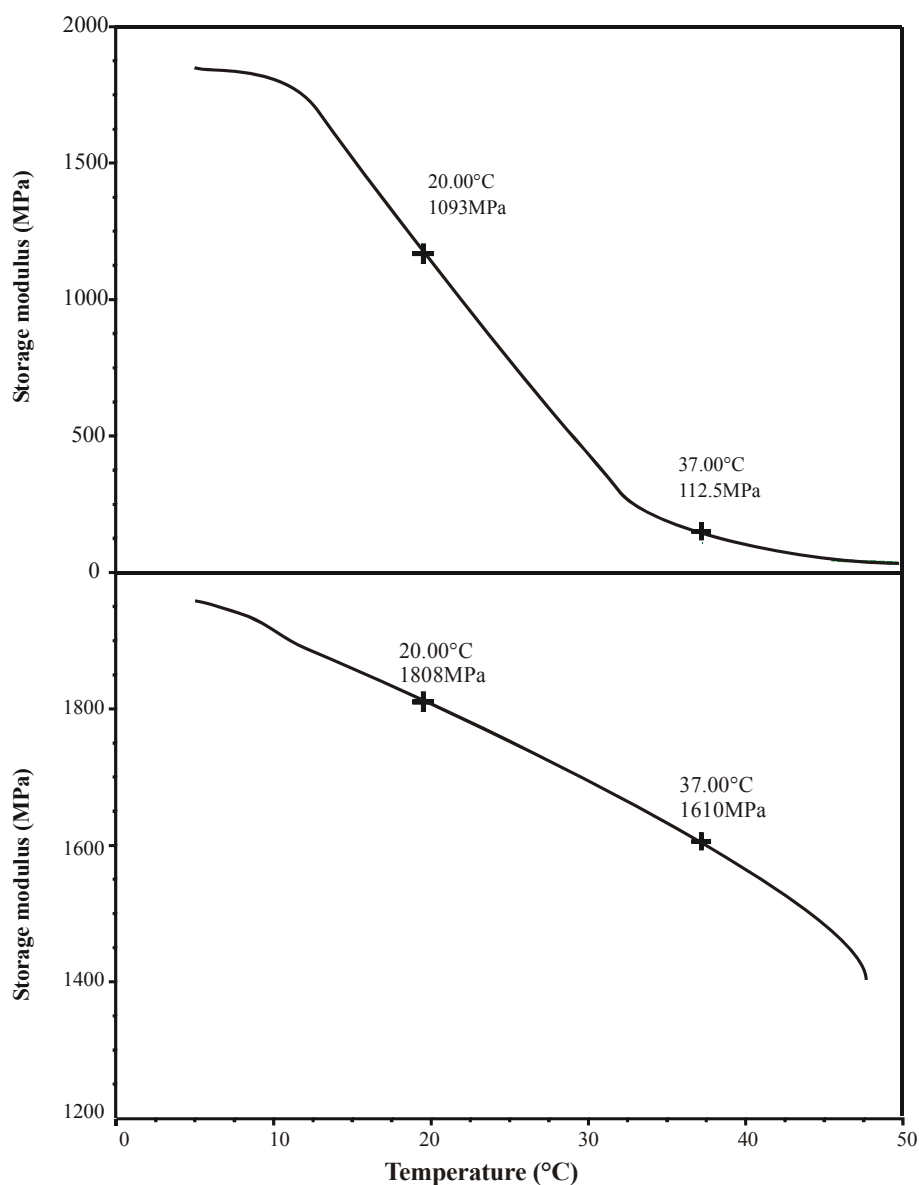


Figure 52: Dynamic mechanical analysis of BEA (top) and DBA (bottom) crosslinked with 20 wt% EPA

The bending strength and the failure strain were measured with a universal tensile testing machine (Zwick Z050, Zwick/Roell). The maximal strain applicable in the middle of the beam was determined. A preload of 0.5 N was used and the velocity of the crosshead was 5 mm/min and 10 mm/min after 0.25% strain, respectively.

2.2.3 Biocompatibility

Test specimens were made from all monomers to verify their biocompatibility. In the case of monofunctional components 20 wt% crosslinker, EPA or TTA, was added. In

all cases 1 wt% of an equimolar mixture of CQ and DMAB was used as initiating system. The mixture was filled into a silicon mold (0.9 cm diameter, 0.15 cm height) and photocured with a high-pressure mercury lamp (1000 W, distance 15 cm) under nitrogen atmosphere. Depending on the type of monomer, the curing time was between 3 and 10 min. Afterwards the test specimens were extracted with different organic solvents (CHCl₃, MeOH, EtOH), phosphate buffered saline (PBS) and water in an ultrasonic bath to remove residual monomer.

To estimate whether osteoblasts accept the new polymers as growth support (biocompatibility) measurements of cell viability and multiplication of cells of the osteosarcoma cell line MG63 with the cell proliferation assay EZ4U (Biomedica, Austria) were used. This assay is based on the conversion of an uncoloured tetrazolium salt into a formazan dye by the mitochondria of living cells.

Cells were kept in a humidified air under 5% CO₂ at 37°C. Culture medium was α MEM (minimum essential medium) supplemented with 5% FBS (fetal bovine serum), 4.5 g/l glucose and 30 μ g/mL gentamicin. For propagation cells were sub-cultured twice a week using 0.001% pronase E (Roche) and 0.02% EDTA in Ca²⁺ and Mg²⁺ free phosphate-buffered saline (PBS) before reaching confluence.

The test specimens were placed into a multiwell plate and sterilized for 30 min in a distance of 14 cm with a 15 W UV lamp (Sylvania) on both sides. Thereafter, the space between the test specimen and the wall of the well were closed with agarose, cells were seeded at a density of 50000 cells/cm² and cultured for three days. Then, a change to fresh culture medium was performed and after one hour the assay mixture was added. After a further 3 hours culture period the colour of the medium was measured in a microplate reader at 492 nm against 620 nm. The measured extinction was converted to cell number by a calibration curve performed in separate experiments. Statistical analyzes were performed by ANOVA with Scheffe's post hoc test using StatView 4.5 (Abacus Concepts, Inc. CA) and $P \leq 0.05$ was considered to be significant.

3 Additives

3.1 Photoinitiators

3.1.1 *Low molecular weight photoinitiators*

Photo-DSC measurements were again used to compare the photoreactivity of different photoinitiators. The setup was used as described above. Irgacure 819 and Irgacure 2959 were measured at a concentration of 0.5 wt% and DPD at 0.3 wt%. For the Type II system 1 wt% of an equimolar mixture of CQ and DMAB was used. EPA was used as resin for the experiments.

3.1.2 *Development of migration stable photoinitiators*

3.1.2.1 *General Investigations on the photoreactivity of eosin*

The neutral form of eosin **1H** was obtained by extraction with diluted HCl, and the deprotonated form **1TEA** was achieved by addition of an excess of triethylamine and subsequent evaporation.

UV-Visible absorption spectra were recorded on a Cary 50 Bio UV-Visible Spectrophotometer, fluorescence spectra on a Hitachi F-7000 Fluorescence Spectrophotometer. For UV/Vis absorption and fluorescence measurements a cell made of quartz glass (Hellma, d: 1cm, spectral range: 200 nm-2500 nm) was used.

Photo-DSC measurements were performed as described above. An amount of 0.3 wt% of 1H and 1TEA, respectively, was dissolved in TTA and mixed with 1 eq of DMAB. Beside the usual setup having a 320-500 nm filter additional experiments were done with a 250-450 nm filter and without any filter.

3.1.2.2 *Preparation of macromolecular photoinitiators*

The synthesis of the macromolecular PIs was done by Martina Sandholzer at the Graz University of Technology and is published elsewhere.^{127,128}

3.1.2.3 Characterization of macromolecular photoinitiators

3.1.2.3.1 Photoreactivity

Photo-DSC measurements were performed as described previously. All PIs were used at a concentration of the dye of 3.3 $\mu\text{mol/g}$ in TTA. Again filtered light (320-500 nm) with an intensity of 20 mW/cm^2 was applied.

In this case $\Delta H_{0,p}$ was not taken from the literature, but calculated using equation (1).

$$DBC = \frac{\Delta H_p M}{\Delta H_{0,p}} \quad (1)$$

ΔH_p was taken from a photo-DSC measurement, while DBC was obtained by ATR-IR spectroscopy of the cured and the uncured sample using peak deconvolution software (PeakFit V4.12, SSI). $\Delta H_{0,p}$ was determined to be 185000 J/mol.

3.1.2.3.2 Migration stability

For the determination of the migration stability, test specimens (round platelets, 1.3 cm diameter, 0.2 cm height) were prepared by photopolymerization in silicon molds under nitrogen for at least 5 min. The polymers were extracted with CHCl_3 , MeOH, EtOH and water in an ultrasonic bath for 2 h to remove any unreacted monomer. The specimens were then placed in glass tubes, covered with 5 mL ethanol and extracted for one week. The solutions were used to determine the amount of leaked dye by UV spectroscopy. In order to guarantee complete deprotonation of the eosin, dye samples were spiked with excess triethylamine. The concentration of leaked eosin was determined according to the Lambert-Beer law (Eq. 3):

$$A = \varepsilon \cdot c \cdot d \quad (3)$$

According to literature, ε in alkaline EtOH was set as 112000 $\text{L mol}^{-1} \text{cm}^{-1}$.^{129,130} All measurements were carried out in a cell made of quartz glass (d: 1 cm, spectral range: 200 nm-2500 nm).

3.1.2.3.3 In vitro LD 50

For the viability study and the determination of the *in-vitro* LD50 MC3T3-E1 osteoblast-like cells were used. As culture medium Dulbecco's Modified Eagle's Medium (α -MEM) supplemented with 10% fetal calf serum (FCS), glucose (5 g/L),

gentamicin (30 $\mu\text{g/L}$), L-glutamin and ascorbic acid was used. Cells were kept in a humidified air under 5 % CO_2 at 37 °C for 5 days. The cells were continuously exposed to increasing concentrations (10^{-9} - 10^{-3} mol/L) of monomers and polymers as well as the extraction medium. Then, the cells were washed with phosphate buffered saline. The DNA, was coloured using the Hoechst 22855 dye and the fluorescence was measured at 460 nm (λ_{ex} : 360 nm). From these results the *in-vitro* LD50 was determined via interpolation of a calibration function. A typical curve is shown in Figure 53. Above a concentration of 10^{-5} mol/L most of the substances precipitated, so that no values could be obtained for higher concentrations.

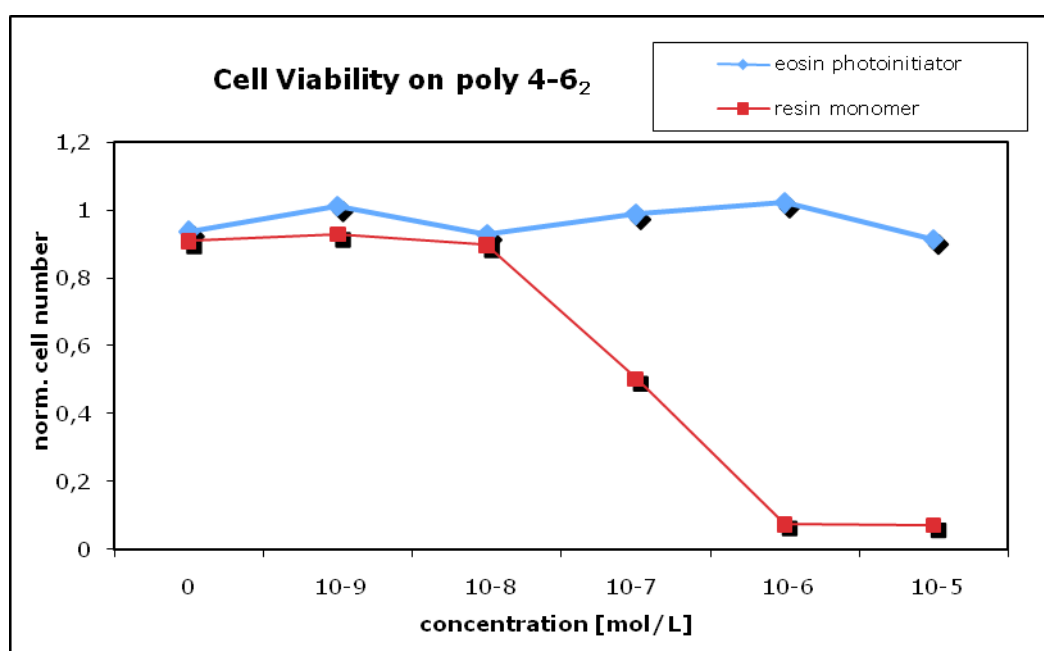


Figure 53: Cell viability on eosin macroinitiator and TTA

4 3D-Structuring

4.1 Digital light processing

Fabrication according to the DLP principle was conducted with a commercial unit based on digital light processing (Prefactory Mini, Envisiontec GmbH). Scaffolds were built with a layer thickness of 50 μm , at a lamp power of 650 mW/dm², and 15 sec of irradiation time per layer.

4.2 Micro-Stereolithography

The μ -SL works with a neodymium doped yttrium aluminum garnet ($Y_3Al_5O_{12}$) laser (Nd:YAG). Monochromatic light of 355nm is generated. Structures were built on glass plates using a layer thickness of 50 μ m. The scanning velocity was usually 20 mm/s and the laser power set to 2.5 mW.

4.3 Two Photon Absorption Polymerization

The equipment comprised an amplified ultrafast Ti:S laser system (Spectra Physics Maitai and Spitfire combination; 130 fs, 1 kHz) working in the wavelength range 750–850 nm. Good structures were obtained with 12,5 μ W at a feedrate of 1 mm/min.

Materials and Methods

Reagents and solvents were – unless otherwise noted – all applied in a quality that is common for organic synthesis and – if necessary – purified as Perrin *et al.* described. All solvents were distilled before use. Anhydrous solvents were dried with common procedures.

For **thin layer chromatography (TLC)** aluminum foils, coated with silicagel 60 F254 from the company Merck were applied.

FTIR spectra were measured with an ATR-arrangement using a Biorad FTS-135 IR-device.

Photo-DSC measurements were performed with a DSC-50 device from the company Shimadzu. The filtered UV radiation (320 - 500 nm, EXFO Omnicure 2000) was applied to the measurement by the aid of a light guide and a self-made aluminum block.

¹H- NMR- and **¹³C-NMR-**spektra were measured with a BRUKER AC-E-200 FT-NMR- spectrometer. The chemical shift is displayed in ppm (s = sigulett, d = duplet, t = tripllett, q4 = quartett, q5 = quintet, m = multipllett). Deutero-chloroform (CDCl₃), deuterated water (D₂O) and deuterated dimethyl sulfoxid (d₆-DMSO) were used as solvents.

For the dialysis of the products a **dialysis membrane** (Spectrum Laboratories Inc.) with a MWCO of 3500 g/mol was used.

The preparation and analysis of photosensitive compounds or mixtures took place at a **red light lab**. Therefore adhesive filter foils from the company Aslan (C 118 – Art. Nr. 11816) were used to cover the windows and the fluorescent lamps.

The curing of the photo resins was performed with a **UV plant** from the company UV-Technik Meyer with a special dysprosium UV lamp (UVH 2022 DY-0, 380V, 2.2kW, irradiation power 1kW)

The extraction of residual monomer was performed in an **ultrasonic bath** from Fungilab.

Stereolithography was performed on three different machines: the Prefactory from Envisiontec works with the DLP principle. The μ -Stereolithography unit consists of a laser (Lightwave Electronics 355nm Quasi-CW Laser System XCYTE) and a scanner (SCANLAB hurrySCAN 14). TPA was performed with an amplified ultrafast Ti:S laser system (Spectra Physics Maitai and Spitfire combination; 130 fs, 1 kHz) working in the wavelength range 750–850 nm at Joanneum Research Weiz.

For the measurements of the viscosity a Modular Compact **Rheometer** (Physica, Anton Paar) equipped with a cone plate CP25-1 was used. Shear rates were modulated from 0.1 s^{-1} to 100 s^{-1} .

Mechanical properties were determined using a dynamic mechanical analysis machine (TA Instruments DMA 2980) for the stiffness tests and a universal tensile testing machine (Zwick Z050, Zwick/Roell) for the bending strength tests.

GPC measurements were performed on a system consisting of a Viscotek GPCmax VE 2001, Waters Ultrahydrogel 120, 250 columns and a Viscotek RI Detector VE3580.

MALDI-TOF Mass Spectrometry was performed on a Micromass TofSpec 2E Time-of-Flight Mass Spectrometer. Analysis of data was done with MassLynx-Software V3.5 (Micromass/Waters, Manchester, UK).

Conclusion



The manifold disadvantages of existing bone replacement materials explain the intensive research and numerous investigations in the field of bone tissue engineering. Many different approaches are continuously reported in literature. Recently Solid Freeform Fabrication (SFF) techniques have gained interest for their possibility to design scaffolds with well-defined pore structures. Among these techniques Stereolithography (SL) – working with layer-by-layer photopolymerization - enables very high feature resolutions while processing takes place at ambient temperature, offering the possibility to incorporate temperature-sensitive materials like growth factors. Compared to other SFF techniques relatively few materials have been developed so far that can be used with SL. Therefore the objective of the present study was the development of a biocompatible monomer formulation that can be used with SL delivering a biodegradable scaffold for bone tissue engineering.

The designed monomer formulation consists of several components: a biodegradable basis monomer that acts as a crosslinker, reactive diluents to control the viscosity of the monomer formulation as well as the mechanical properties of the resulting polymer, an appropriate photoinitiator, and several additives.

One part of the present study comprehended the synthesis and development of a new biodegradable acrylate-based crosslinker. As basis material an enzymatic gelatin hydrolysate (GH) was chosen, because of its natural origin, enzymatic degradability,

and its positive effect on bone cell adhesion. Modifications of this GH had to be done to obtain the desired properties, namely the ability to be photopolymerized and compatibility with organic materials that should make up the rest of the monomer formulation. Photopolymerizable groups could be introduced fairly easy by reaction with glycidylmethacrylate, which reacts with both free amino and acidic groups. Different approaches were followed to enhance miscibility with organic compounds, but the most successful was the modification with poly(ethylene glycol) (PEG) 4000 chains by reaction of GH amino groups with an activated ester of PEG. Thereby formulations containing up to 70% reactive diluents beside the GH-crosslinker and water could be achieved.

Furthermore a set of commercially available reactive diluents of different chemical structure, hydrophobicity, and molecular weight have been tested concerning reactivity, biocompatibility, and mechanical properties. Best results were obtained for multi-acrylated monomers resulting in stiff materials like UDMA, TTA and GGA. For the final monomer formulation containing GH it was necessary to use water-miscible monomers like HEMA and E4-A.

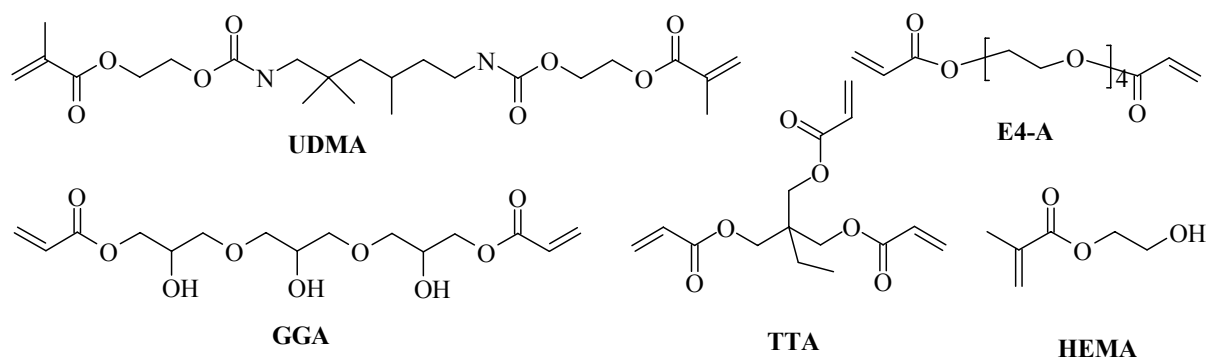


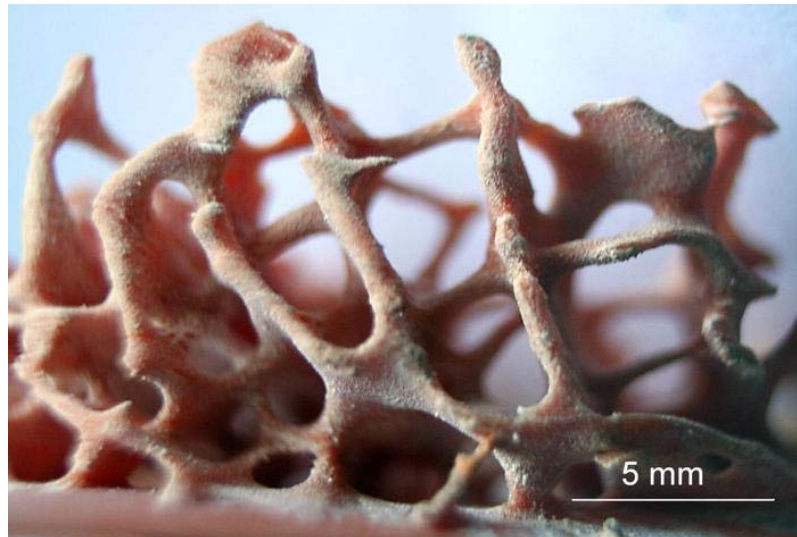
Figure 54: Best reactive diluents

In addition to testing low molecular weight photoinitiators for their applicability, photoinitiating macromers were also synthesized and tested. These were based on eosin as light-sensitive moiety and DMAB as co-initiator. Investigations into reactivity and migration stability revealed a high potential of these macromers for medical applications where migration stability and toxicity are of concern.

By applying several additives such as organic and inorganic fillers and light absorbers, the monomer formulation was completed. In fact, more than one monomer formulation

was developed, because three different SL machines were available for the fabrication of tissue scaffolds, and each machine needed a special optimization with regard to photoinitiator, light absorber, and viscosity. Finally it was possible to construct scaffolds with all three methods.

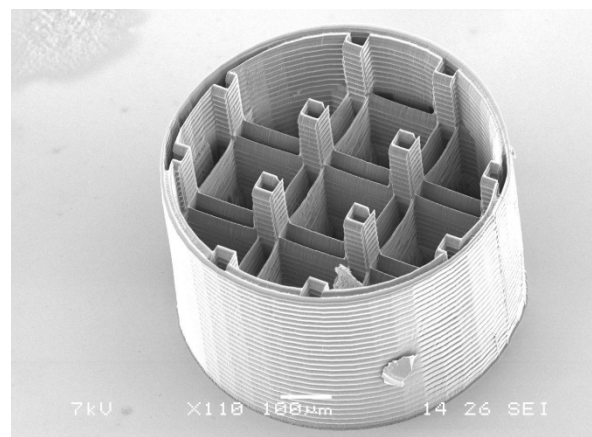
Digital light processing



μ -Stereolithography



Two Photon Absorption Polymerization



Abbreviations

3DP	three-dimensional printing
AA	acrylic acid
BDM	butandiol dimethacrylate
BEA	acrylic acid 2-butylcarbamoxyloxy-ethyl ester
BisGMA	bisphenol A diglycidylmethacrylate
CAB	cellulose-acetate-butyrate
CAD	computer-aided design
CoI	coinitiator
CQ	camphorquinone
D3MA	dodecy dimethacrylate
DBA	N,N-Diisobutyl-acrylamide
DBC	double bond conversion
$\Delta H_{0,P}$	theoretical heat of polymerization
ΔH_p	heat of polymerization
DMA	N,N-dimethyl-acrylamide
DMA	differential mechanical analysis
DMAB	4-dimethylaminobenzoic acid ethyl ester
DPA	N,N-diisopropyl-acrylamide
DPD	1,5-diphenylpenta-1,4-dien-3-one
DPHA	dipentaerythritol penta/hexa-acrylate
DTA	ditrimethylolpropane tetraacrylate
E4-A	tetraethyleneglycol diacrylate
EBA	ethoxylated (10) bisphenol A diacrylate
EEA	acrylic acid 2-(2-ethoxy-ethoxy)-ethyl ester
EEM	methacrylic acid 2-(2-ethoxy-ethoxy)-ethyl ester
ENPA	ethoxylated (4) nonylphenol acrylate
EO	eosin
EPA	N,N'-diethyl-1,3-propylenbisacrylamide
ETA	ethoxylated (20) trimethylolpropane triacrylate
FDA	United States Food and Drug Administration
FDM	fused deposition modeling
GGA	glycerol 1,3-diglycerolate diacrylate
GH	(enzymatic) gelatin hydrolysate
GPA	propoxylated (3) glycerol diacrylate
HA	hydroxy apatite
HEMA	hydroxyethyl methacrylate
HMBP	2,2'-Dihydroxy-4,4'-dimethoxybenzophenone
IBA	isobornyl acrylate
LDM	low-temperature deposition manufacturing

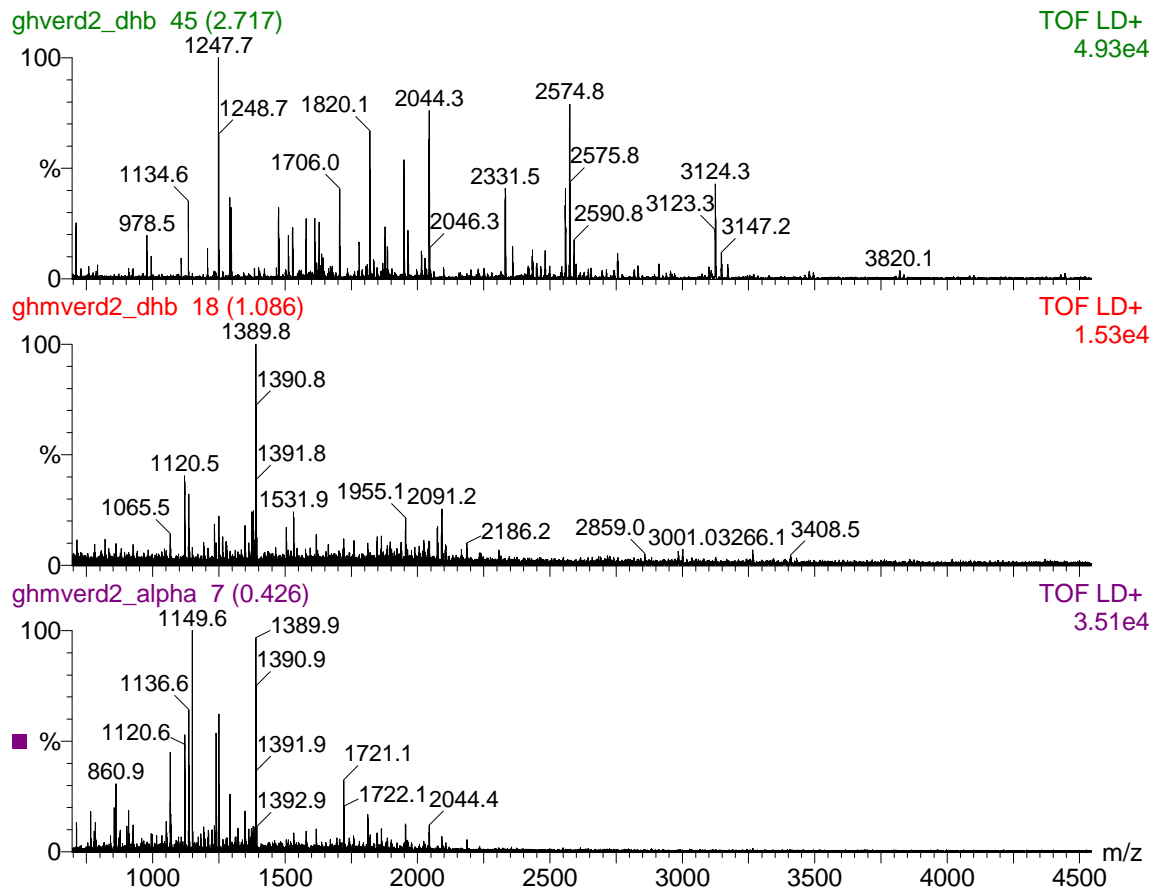
MA	methacrylic acid
MDM	multinozzle deposition manufacturing
MSA	methacrylic anhydride
OR1	absorber orange 1
P3-A	tripropylene glycol diacrylate
PA	polyamide
PAM	pressure-assisted microsyringes
PCL	poly(ϵ -caprolactone)
PDI	polydispersity index
PE	polyethylene
PED	precision extruding deposition
PEG	poly(ethylene glycol)
PEGDA	poly(ethylene glycol) diacrylate
PEM	precise extrusion manufacturing
PGA	poly(glycolic acid)
PI	photoinitiator
PLA	poly(lactic acid)
PNA	propoxylated (2) neopentyl diacrylate
POM	polyoxymethylene
PPA	dipentaerythritol pentaacrylate
PPF	poly(propylene fumarate)
PTA	pentaerythritol triacrylate
PVA	poly(vinyl alcohol)
PVP	poly(vinyl pyrrolidone)
RGD	arginine – glycine - asparaginic acid
ROMP	ring opening metathesis polymerization
R_p	rate of polymerization
RP	rapid prototyping
SFF	Solid Free-Form Fabrication
SGC	solid ground curing
SL	Stereolithography
SLS	selective laser sintering
TBA	t-butyl acrylate
TCP	β -tricalciumphosphate
t_{max}	time to reach the maximum polymerization heat
TTA	trimethylolpropane triacrylate
UDMA	2-methyl-acrylic acid 2-{2,2,4-trimethyl-6-[2-(2-methyl-acryloyloxy)-ethoxycarbonylamino]-hexylcarbamoxy}-ethyl ester

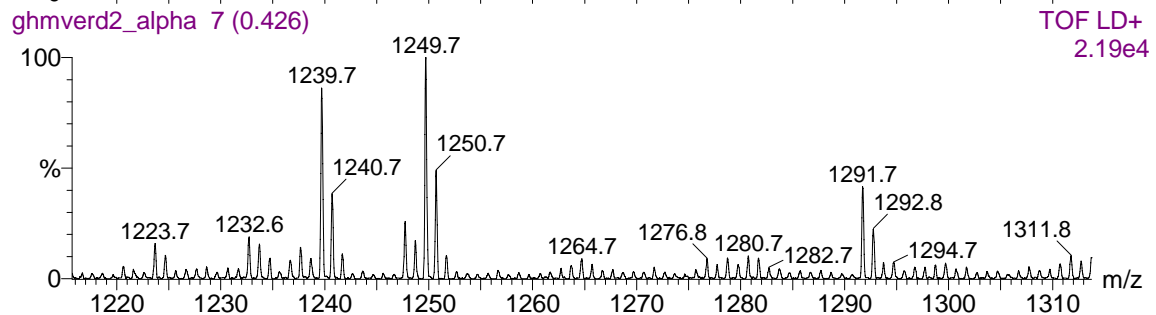
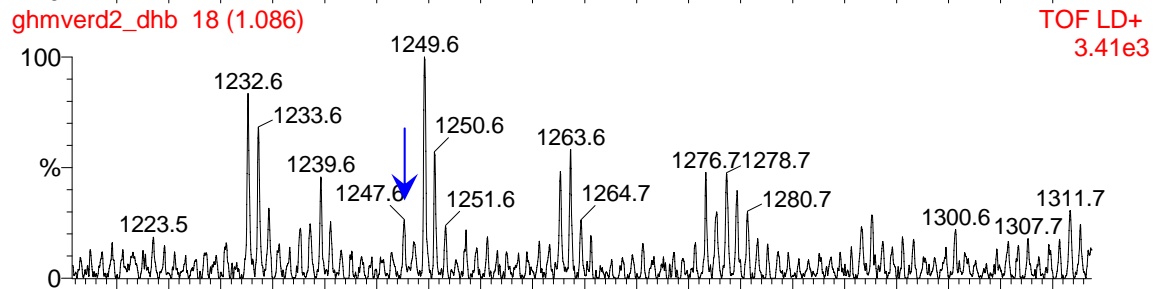
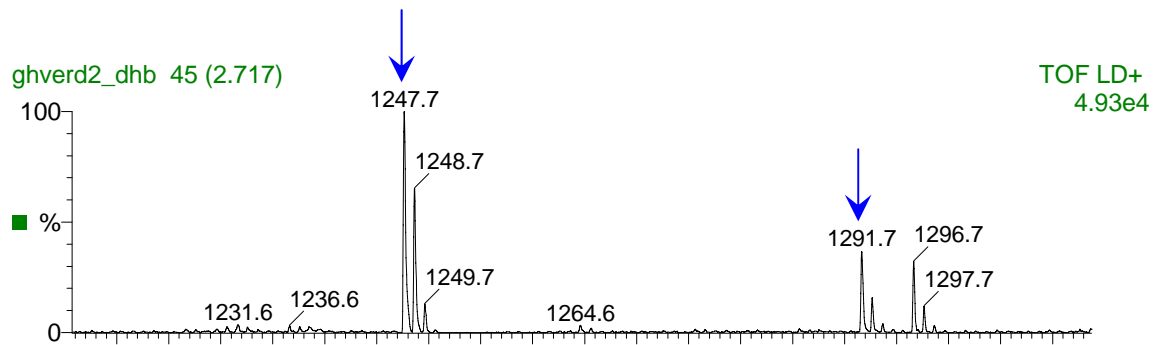
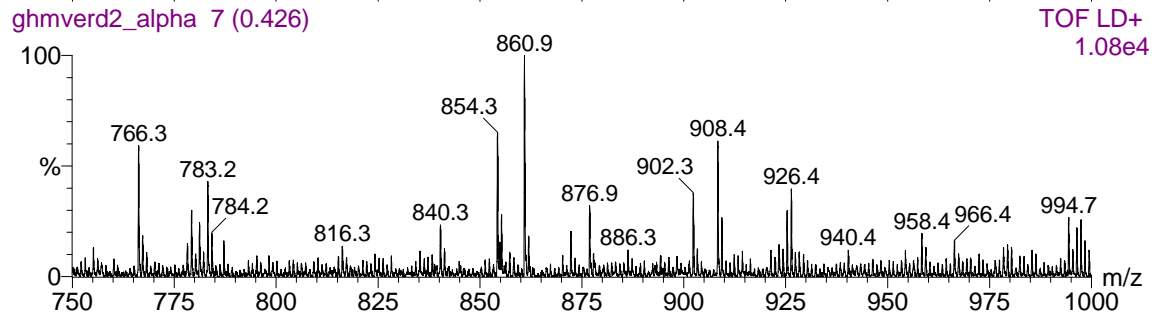
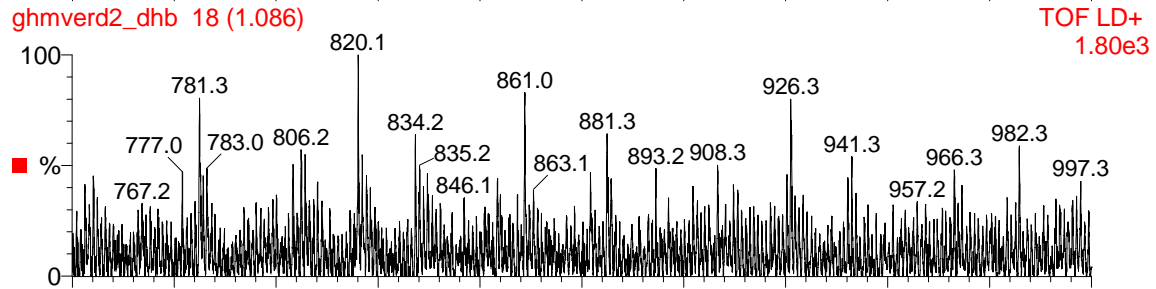
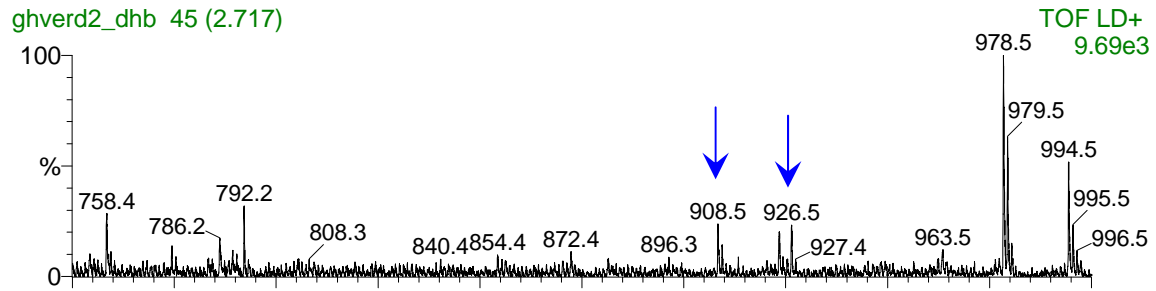
MALDI-TOF Spectra (ad chapter 1.2.1)

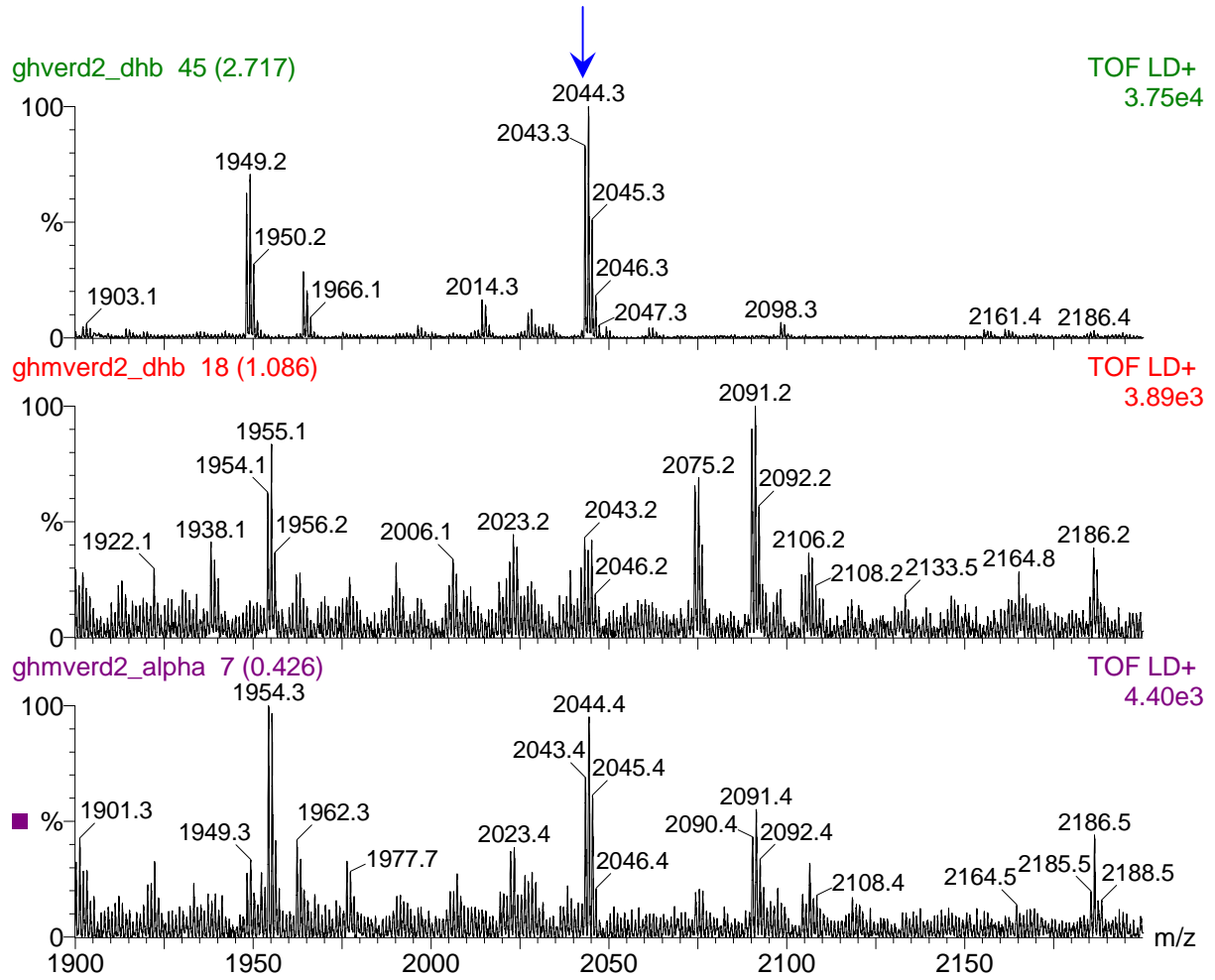
spectra at the top: GH spectra shifted +142.06Da (corresponding to addition of a single glycidylmethacrylate per peptide molecule)

spectra in the middle: GM in DHB

spectra at the bottom: GM in α -cyanocinnamic acid



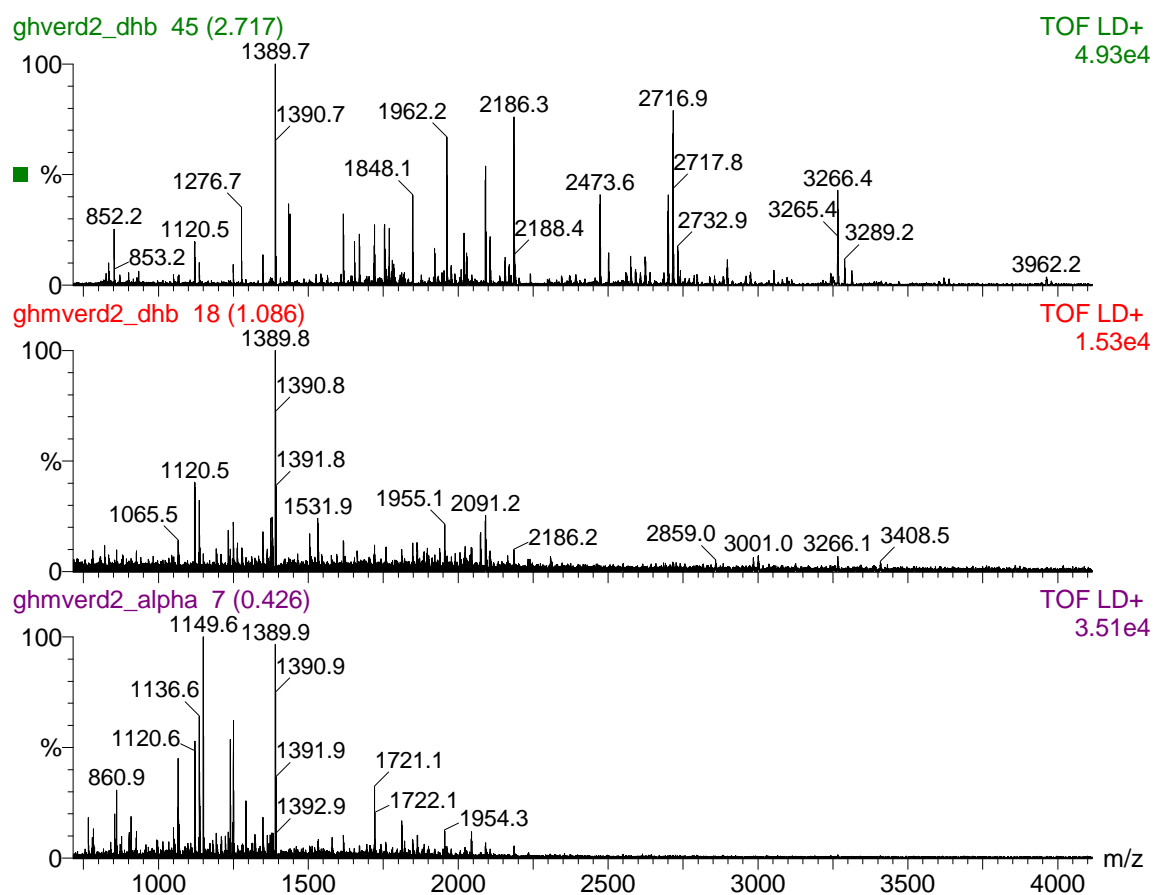


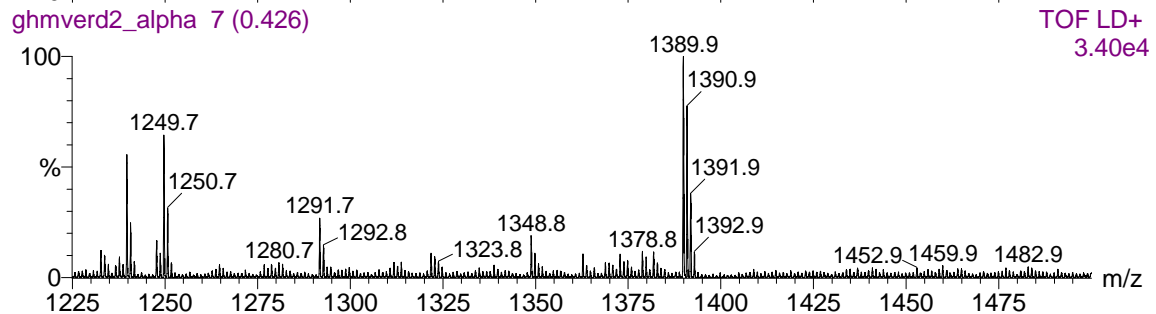
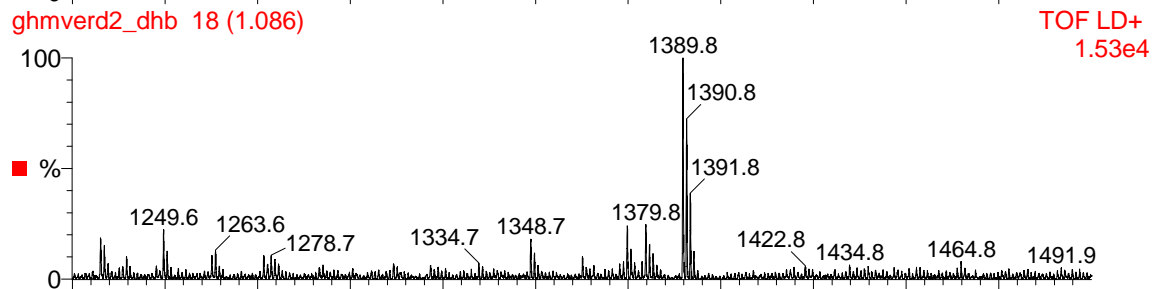
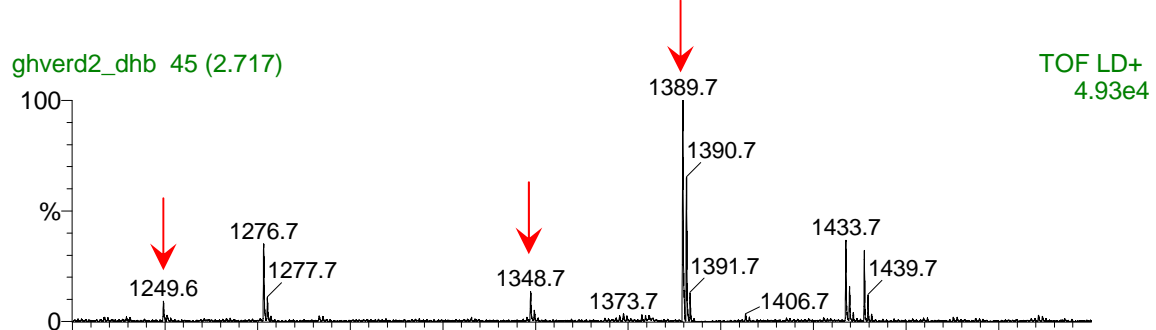
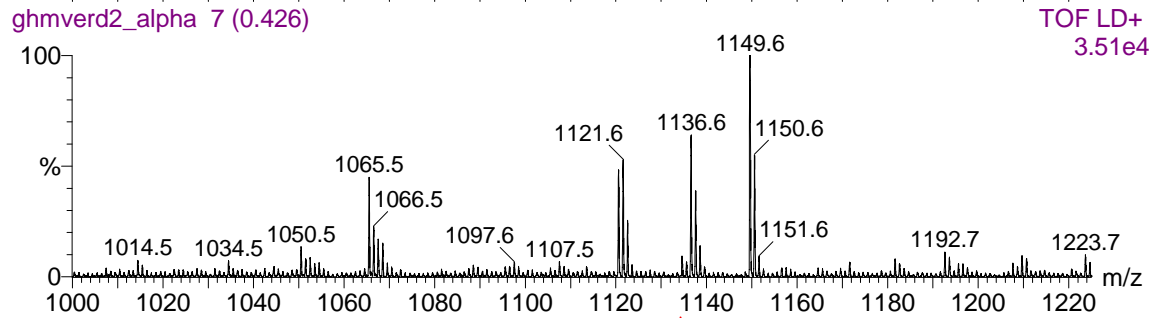
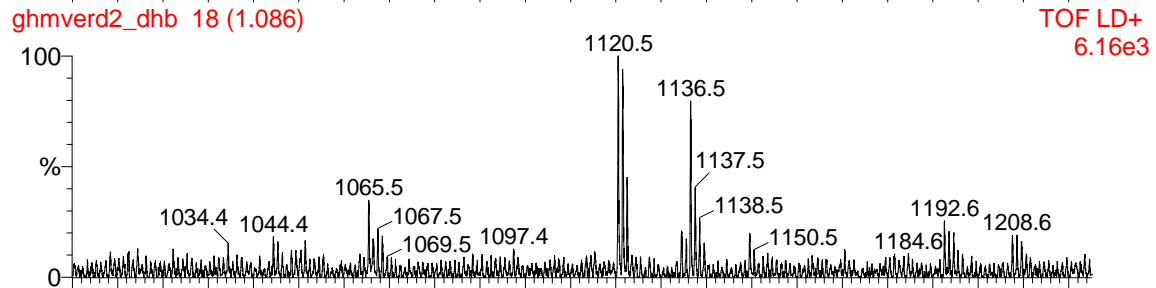
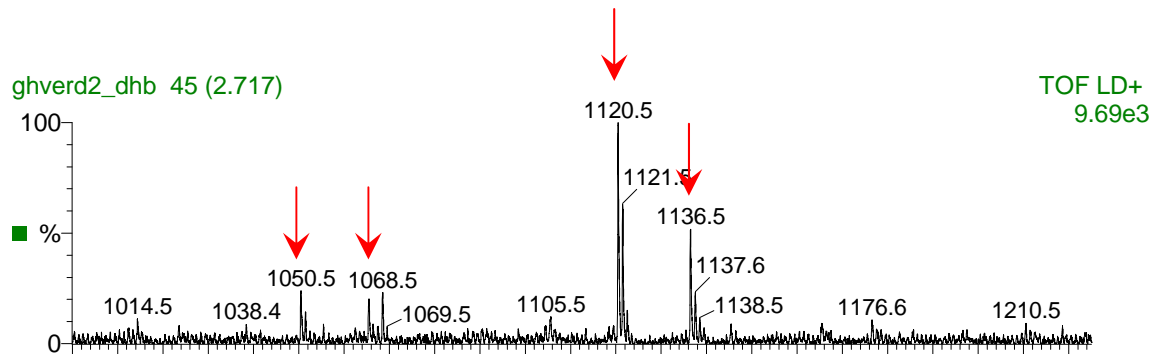


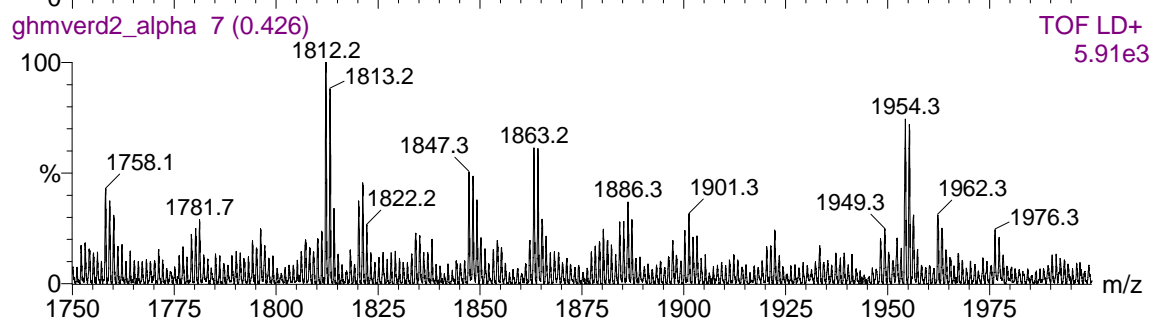
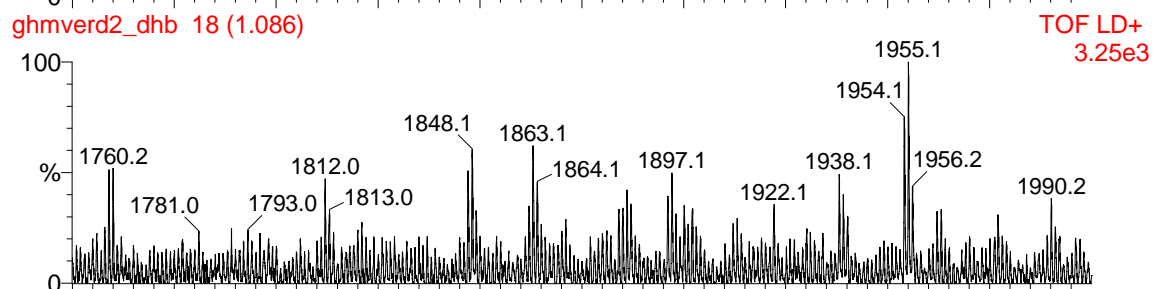
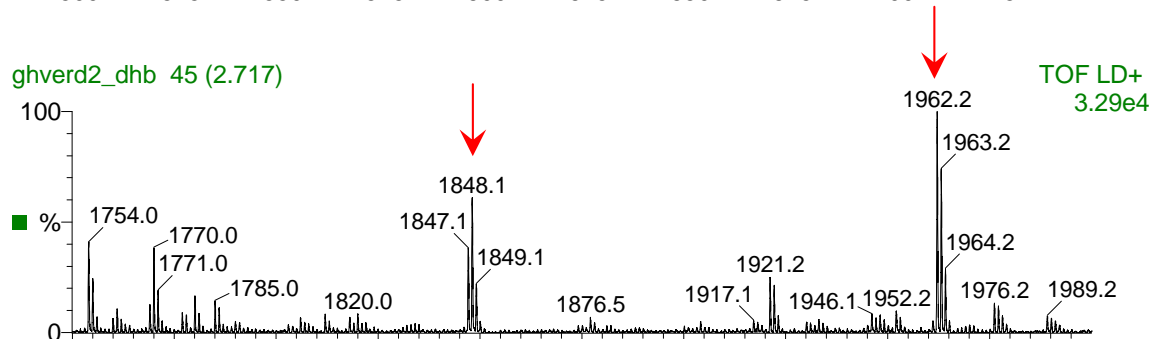
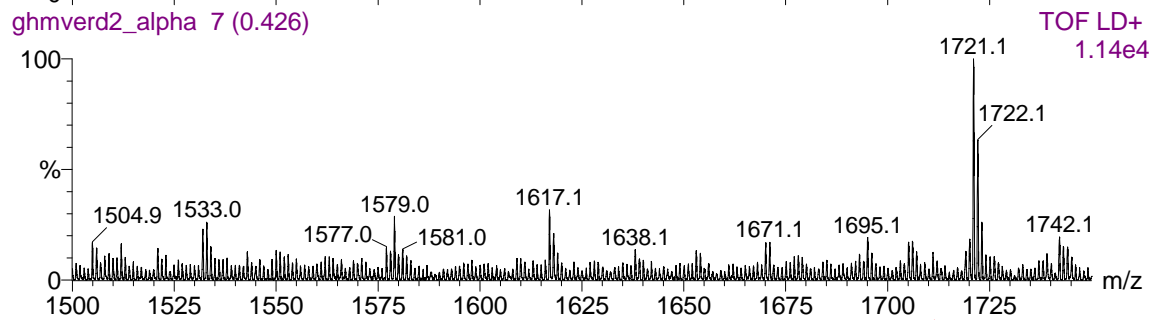
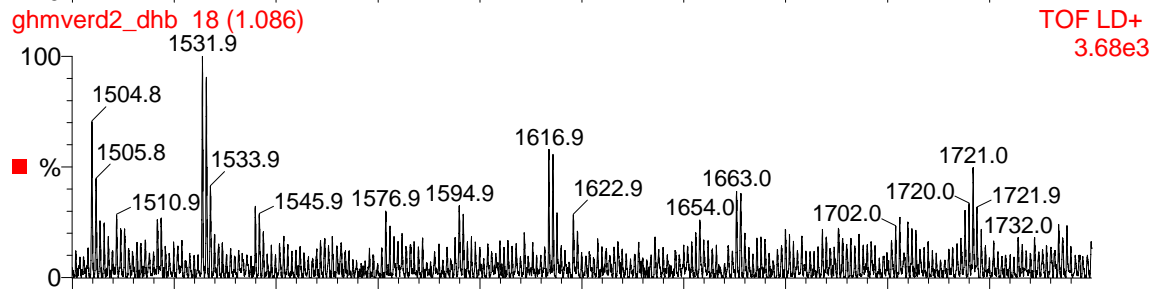
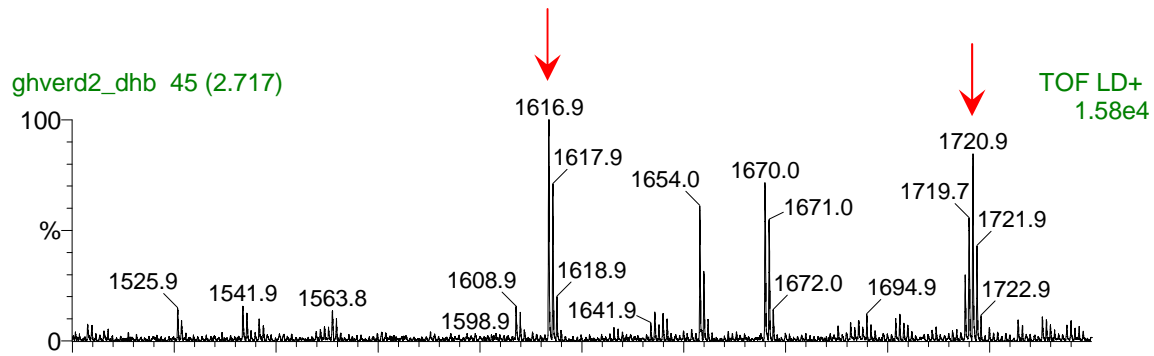
spectra at the top: GH spectra shifted +284,13Da (corresponding to two-fold addition of glycidylmethacrylate)

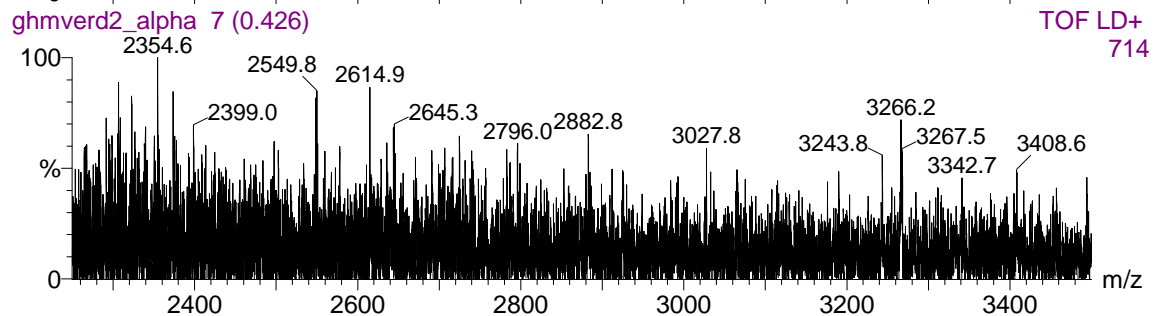
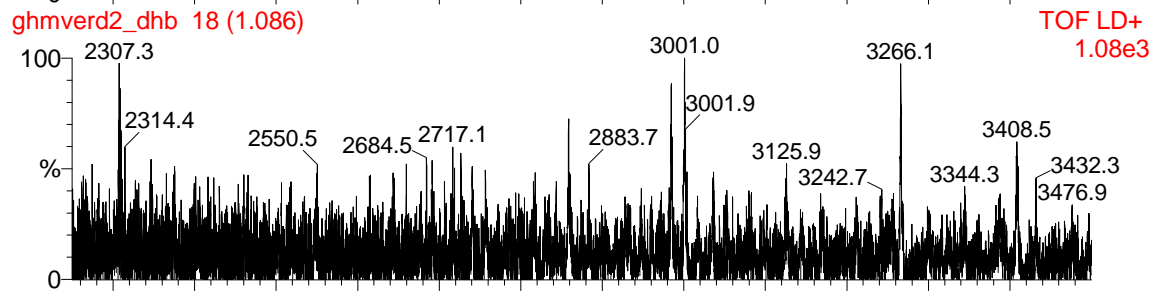
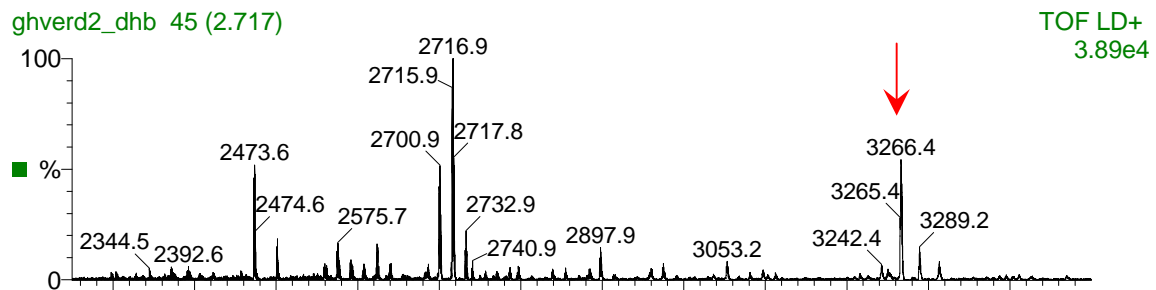
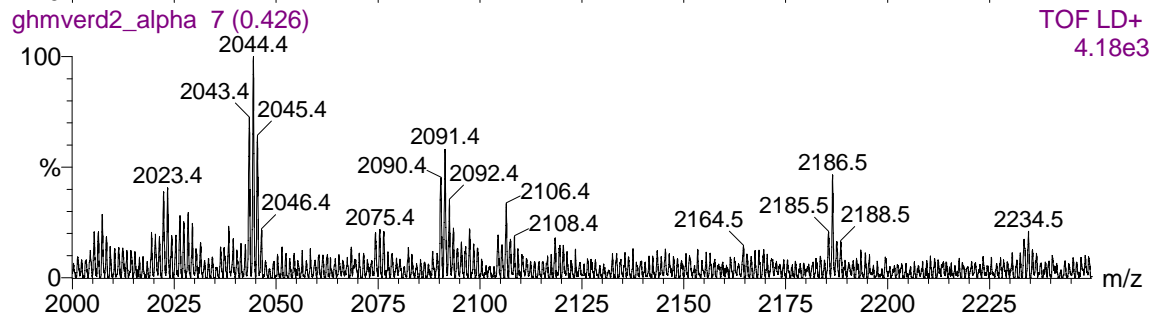
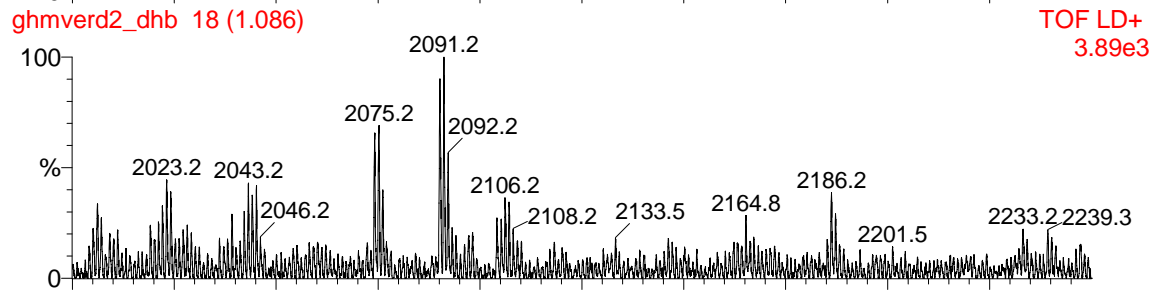
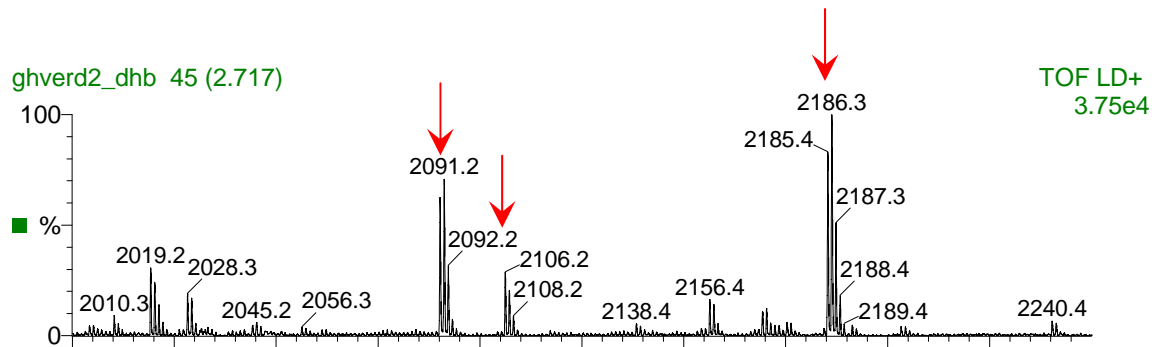
spectra in the middle: GM in DHB

spectra at the bottom: GM in α -cyanocinnamic acid





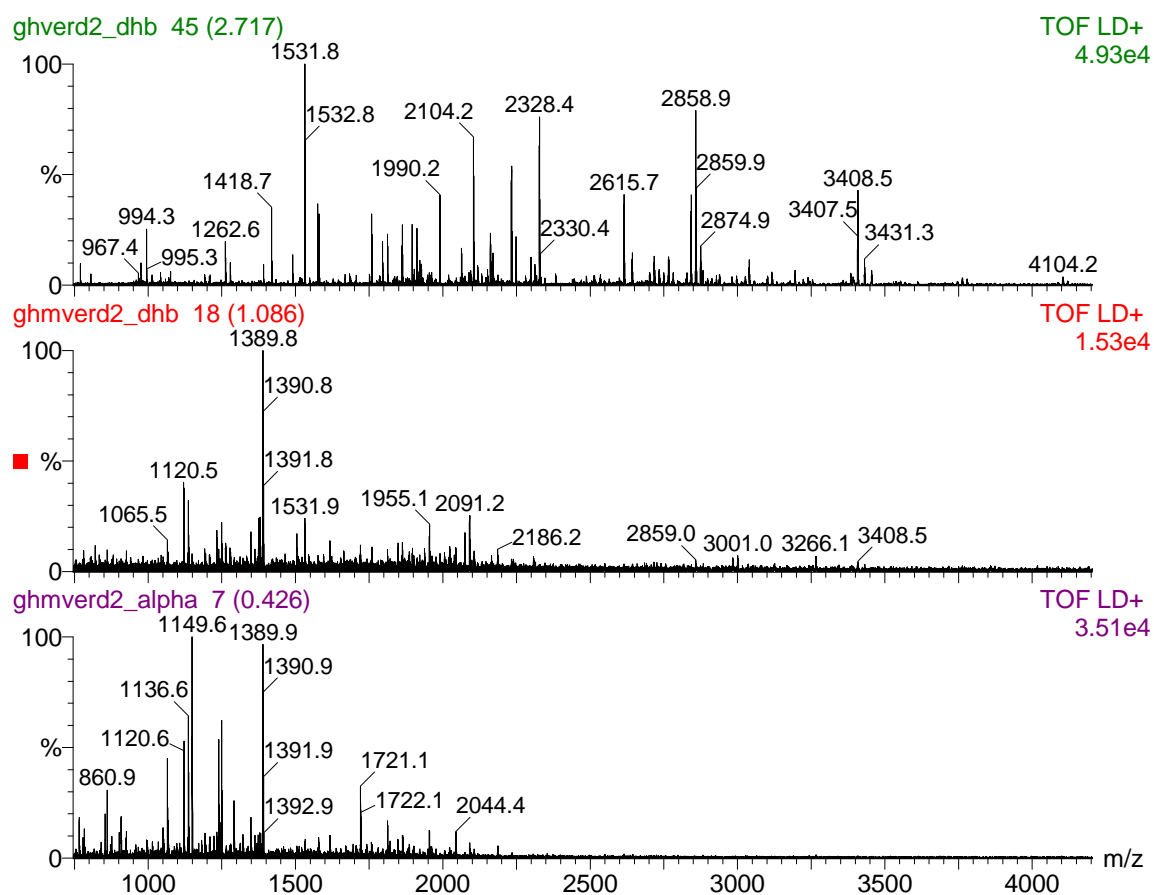


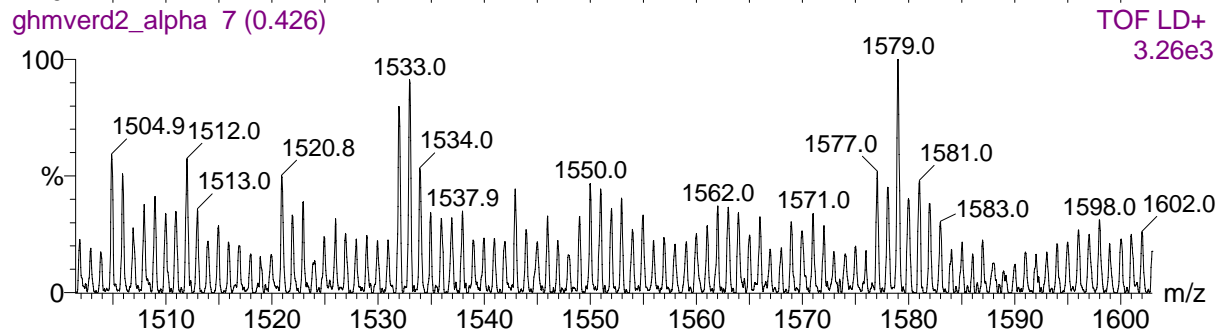
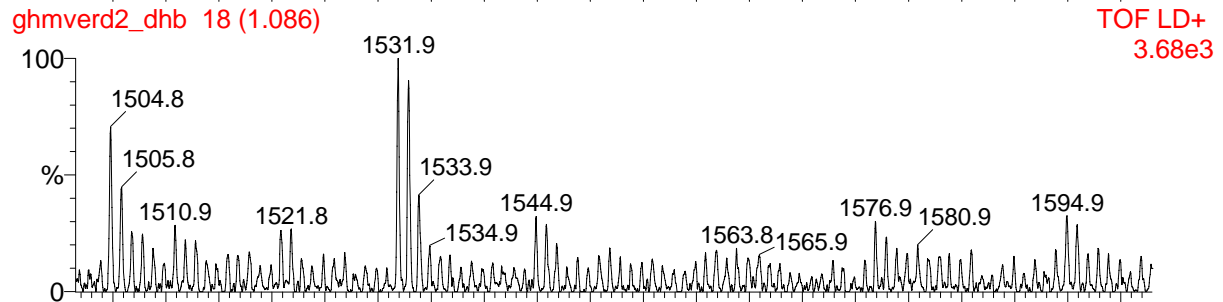
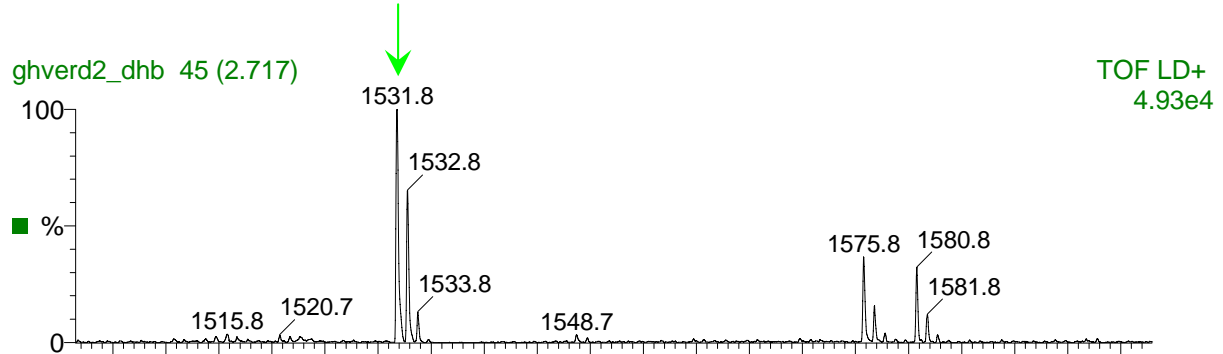
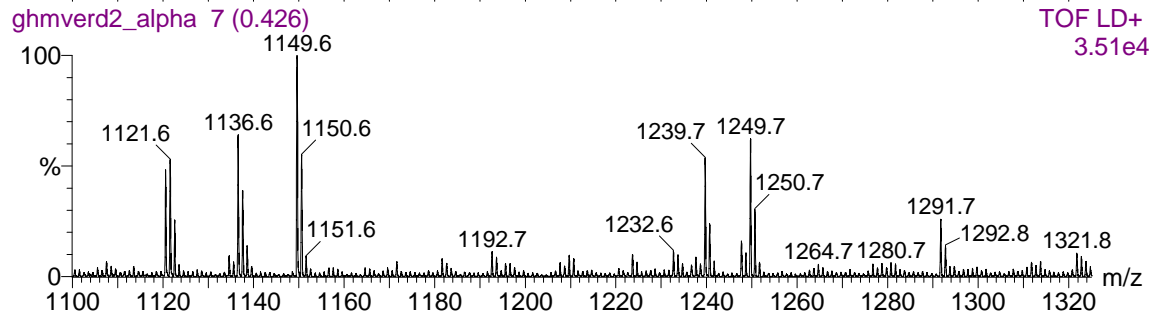
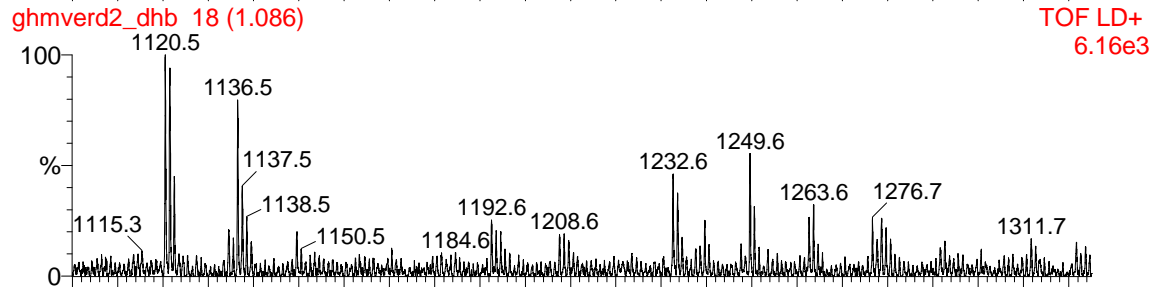
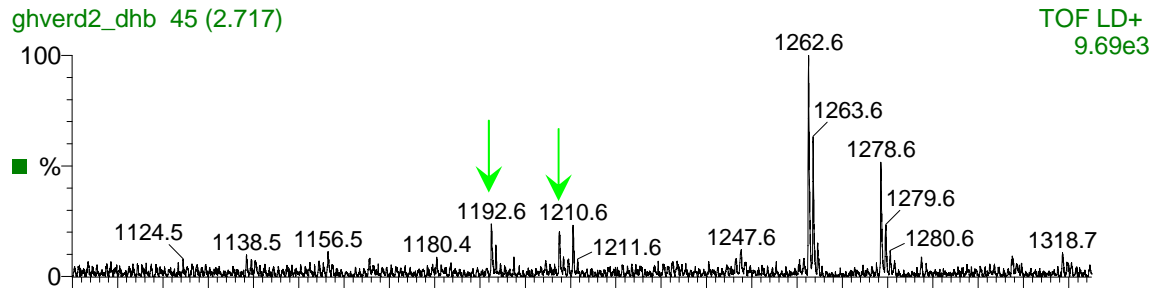


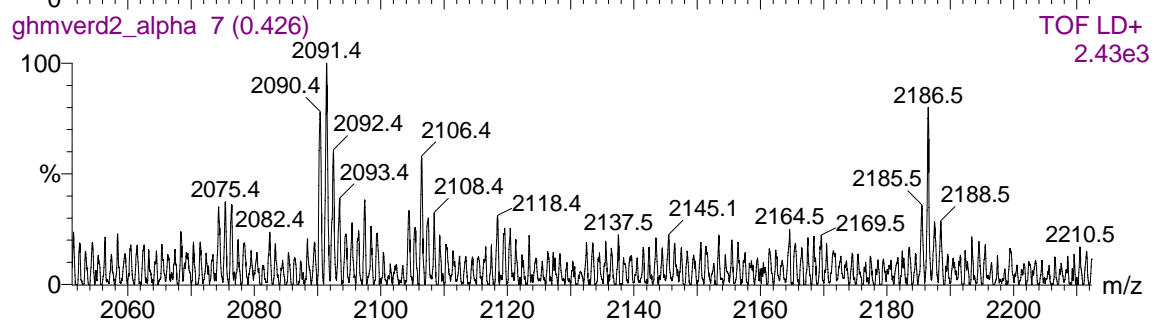
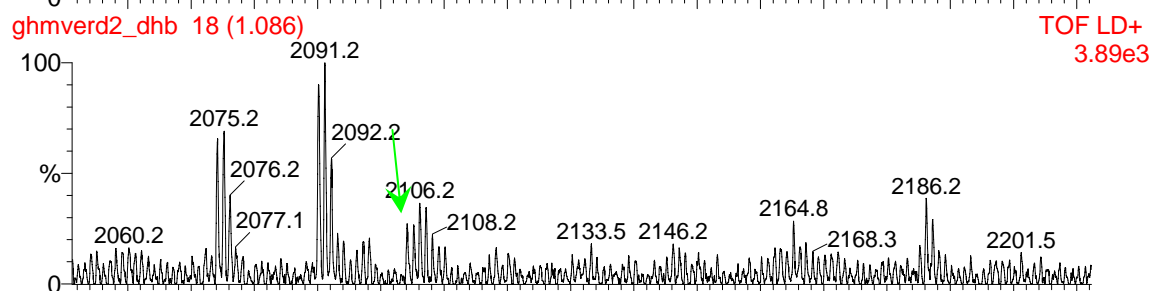
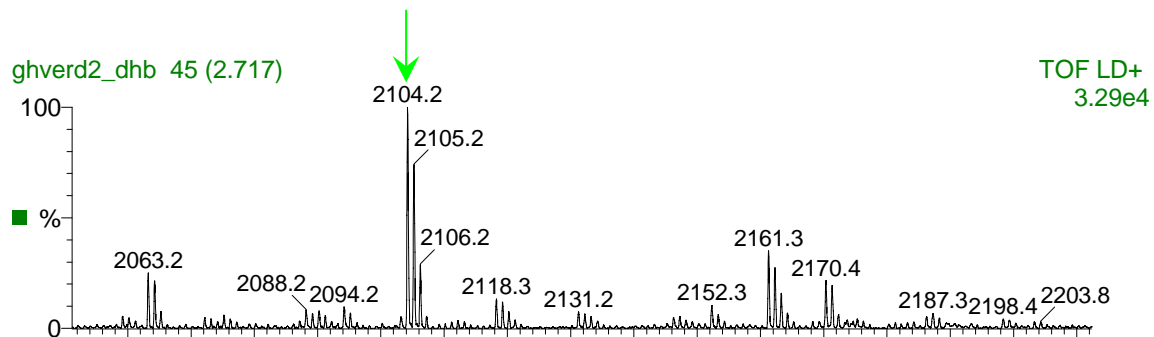
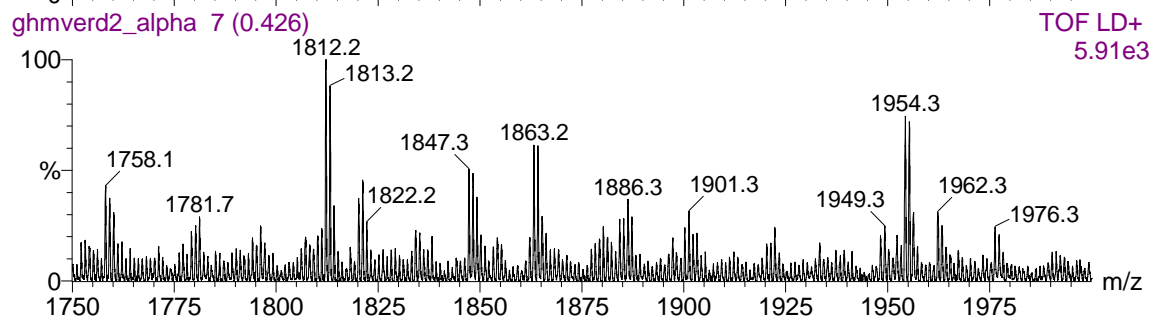
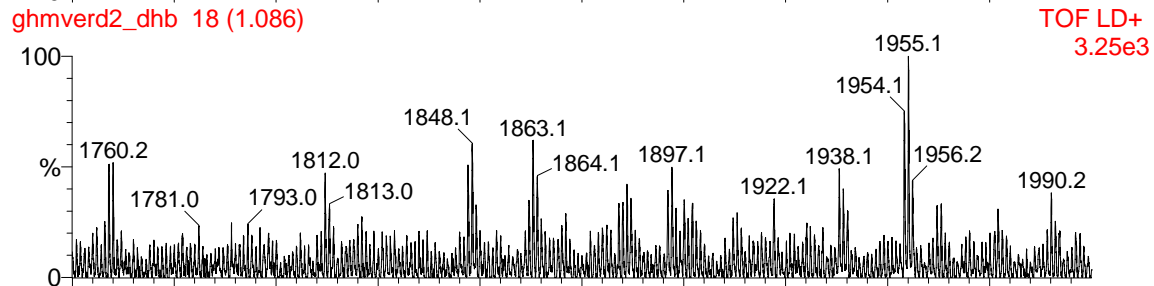
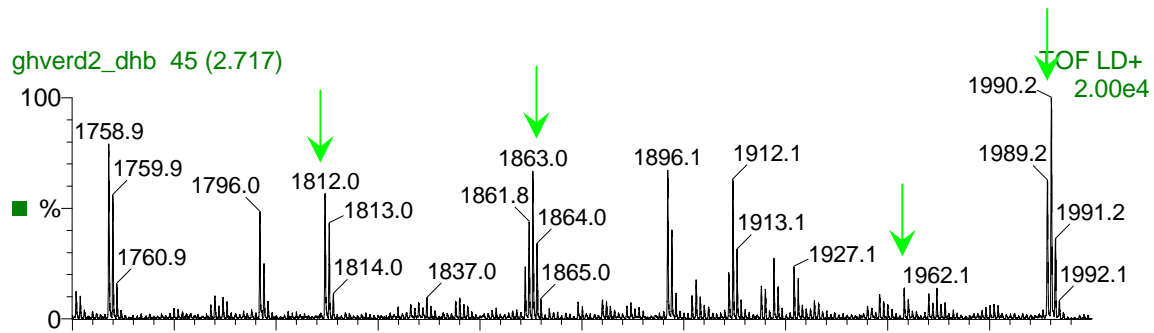
spectra at the top: GH spectra shifted +426,18Da (corresponding to three-fold addition of glycidylmethacrylate)

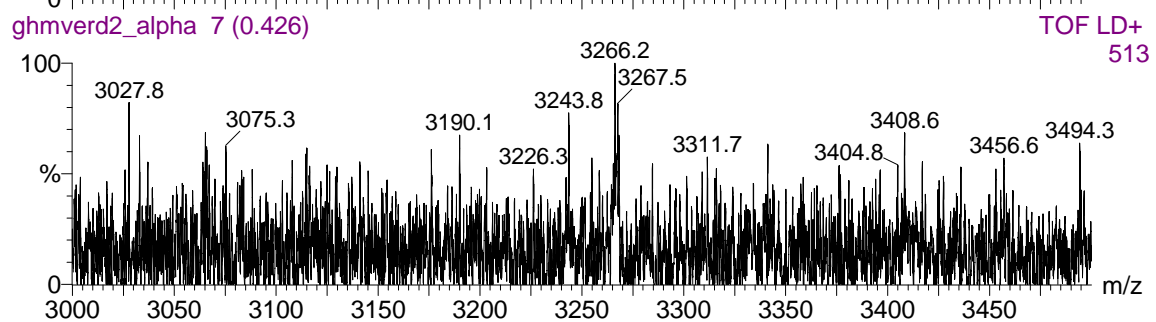
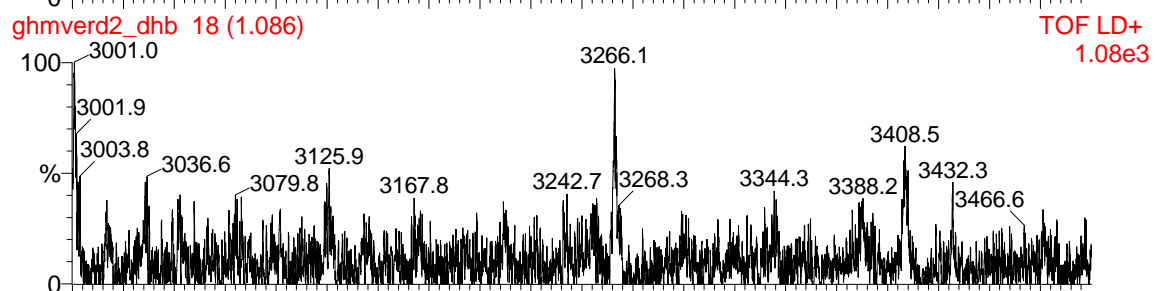
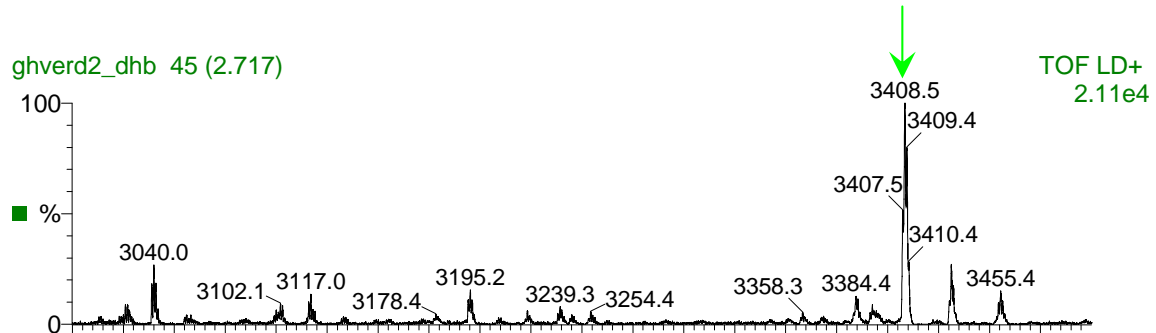
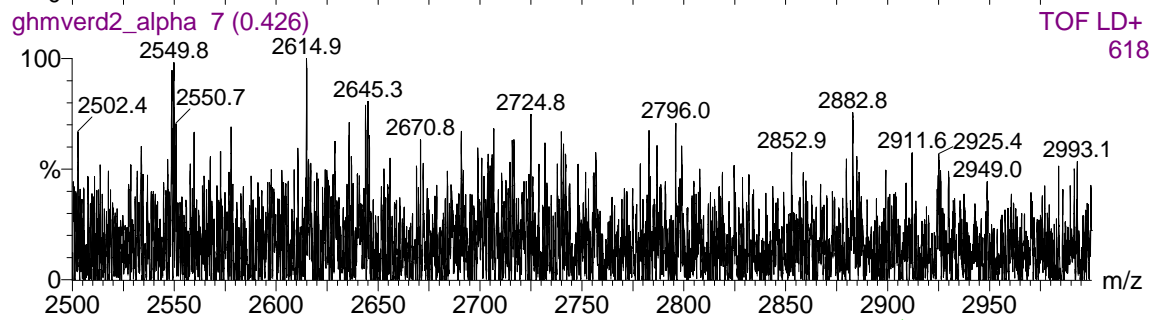
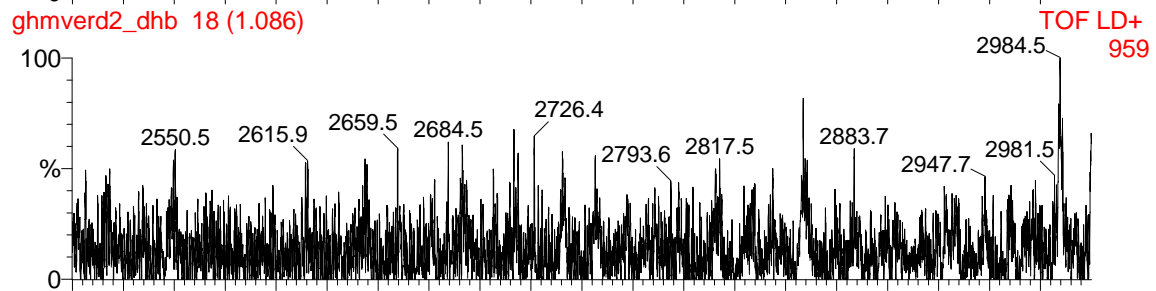
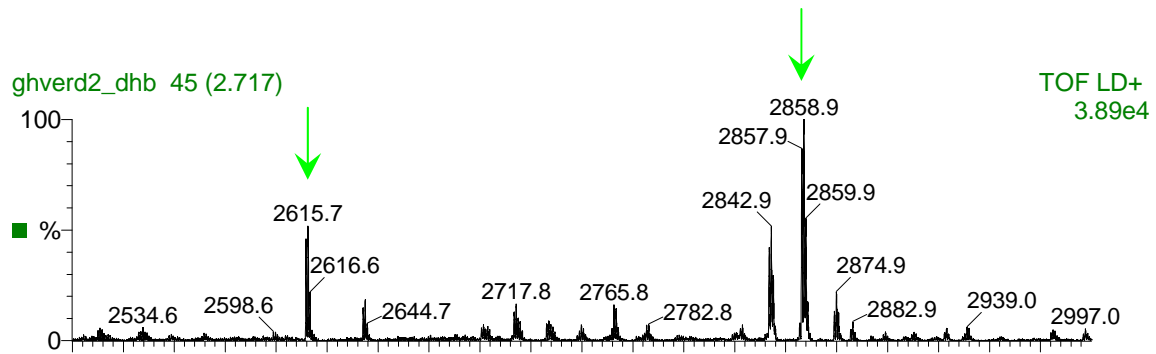
spectra in the middle: GM in DHB

spectra at the bottom: GM in α -cyanocinnamic acid









Experimental data of reactive diluents (ad chapter 2.2.1)

<i>abbreviation</i>	<i>cell number</i>	$R_P * 10^3$ [<i>mol l⁻¹ s⁻¹</i>]	<i>DBC</i> [%]	t_{max} [s]	<i>storage modulus</i> 37°C [MPa]	<i>stiffness</i> [MPa]
AA	200000	218	34	30	4813	70,0
EEA	280000	62	68	23	-	-
TBA	670000	-	-	-	1080	26,1
BEA	250000	169	74	11	-	-
PEA	510000	85	68	25	1220	26,6
ENPA	140000	45	73	45	55	2,4
IBA	1070000	23	42	38	-	47,1
MA	200000	7	24	295	-	-
EEM	280000	8	61	97	-	-
HEMA	200000	75	94	107	2139	74,1
DMA	150000	175	84	38	-	26,4
DPA	300000	31	59	95	-	-
DBA	400000	101	59	20	1125	30,3
P3-A	1000000	80	51	11	1230	44,2
GGA	270000	102	56	10	1713	45,3
EBA	470000	67	92	11	430	52,3
CMA	560000	99	63	19	1000	66,1
E4-A	400000	143	71	11	94	8,7
EPA	300000	60	68	37	2827	42,5
BDM	1220000	6	30	68	-	52,9
PNA	530000	78	56	17	760	29,4
UDMA	650000	53	48	10	1592	86,9
D3MA	190000	6	42	88	550	18,0
BisGMA	240000	34	86	26	2625	82,9
TTA	600000	86	49	10	1655	55,0
PTA	760000	61	42	10	2180	30,0
PPA	810000	30	42	10	2260	28,7
GPA	960000	72	57	9	1340	53,9
ETA	200000	22	50	12	-	-
DTA	630000	37	38	11	375	17,7
DPHA	150000	7	19	74	2450	21,4
PCL	200000	-	-	-	318	17

References

- ¹ Oyen, M.L. „The Materials Science of Bone: Lessons from Nature for Biomimetic Materials Synthesis“; MRS Bulletin; 2008; **33**; 49-55.
- ² Sikavitsas, V.I.; Temenoff, J.S.; Mikos, A.G. “Biomaterials and bone mechanotransduction”; Biomaterials; 2001; **22**; 2581-2593.
- ³ Salgado, A.J.; Coutinho, O.P.; Reis, R.L. „Bone Tissue Engineering: State of the Art and Future Trends“; Macromolecular Bioscience; 2004; **4**; 743-765.
- ⁴ Kretlow, J.D.; Mikos, A.G. “Review: Mineralization of Synthetic Polymer Scaffolds for Bone Tissue Engineering”; Tissue Engineering; 2007; **13**; 927-938.
- ⁵ Lee, J.; Cuddihy, M.J.; Kotov, N.A. “Three-Dimensional Cell Culture Matrices: State of the Art”; Tissue Engineering; 2008; **14**; 61-86.
- ⁶ Eisenbarth, E. „Biomaterials for Tissue Engineering“; Advanced Engineering Materials; 2007; **9**; 1051-1060.
- ⁷ Rezwani, K.; Chen, Q.Z.; Blaker, J.J.; Boccaccini, A.R. “Biodegradable and bioactive porous polymer/inorganic composite scaffolds for bone tissue engineering”; Biomaterials; 2006; **27**; 3413-3431.
- ⁸ Lu, H.H.; Tang, A.; Oh, S.C.; Spalazzi J.P.; Dionisio K. “Compositional effects on the formation of a calcium phosphate layer and the response of osteoblast-like cells on polymer-bioactive glass composites”; Biomaterials; 2005; **26**; 6323-6334.
- ⁹ Ohgushi, H.; Dohi, Y.; Yoshikawa, T.; Tamai, S.; Tabata, S.; Okunaga, K., Shibuya, T. “Osteogenic differentiation of cultured marrow stromal stem cells on the surface of bioactive glass ceramics”; Journal of Biomedical Materials Research A; 1996; **32**; 341-348.
- ¹⁰ Purna, S.K.; Babu, M. “Collagen based dressings - a review”; Burns; 2000; **26**; 54-62.
- ¹¹ Wahl, D.A.; Czernuszka, J.T. “Collagen-Hydroxyapatite Composites for Hard Tissue Repair”; European Cells and Materials; 2006; **11**; 43-56.
- ¹² Nair, L.S.; Laurencin, C.T. „Biodegradable polymers as biomaterials“; Prog. Polym. Sci.; 2007; **32**; 762-798.
- ¹³ Yan, C.; Li, X.; Chen, X.; Wang, D.; Zhong, D.; Tan, T.; Kitano, H. “Anticancer gelatin microspheres with multiple functions”; Biomaterials; 1991; **12**; 640-644.
- ¹⁴ Sutter, M.; Siepmann, J.; Hennink, W.E.; Jiskoot, W. “Recombinant gelatin hydrogels for the sustained release of proteins”; Journal of Controlled Release; 2007; **119**; 301–312.
- ¹⁵ Hori, K.; Sotozono, C.; Hamuro, J.; Yamasaki, K.; Kimura, Y.; Ozeki, M.; Tabata, Y.; Kinoshita, S. “Controlled-release of epidermal growth factor from cationized gelatin hydrogel enhances corneal epithelial wound healing”; Journal of Controlled Release; 2007; **118**; 169–176.
- ¹⁶ Chuang, V.T.G.; Kragh-Hansen, U.; Otagiri, M. “Pharmaceutical Strategies Utilizing Recombinant Human Serum Albumin”; Pharmaceutical Research; 2002; **19**; 569-577.
- ¹⁷ Allison, D.D.; Grande-Allen, K.J. “Review: Hyaluronan: A Powerful Tissue Engineering Tool”; Tissue Engineering; 2006; **12**; 2131-2140.

- ¹⁸ Bencherif, S.A.; Srinivasan, A.; Horkay, F.; Hollinger, J.O.; Matyjaszewski, K.; Washburn, N.R. "Influence of the degree of methacrylation on hyaluronic acid hydrogel properties"; *Biomaterials*; 2008; **29**; 1739-1749.
- ¹⁹ George, M.; Abraham, T.E. "Polyionic hydrocolloids for the intestinal delivery of protein drugs: Alginate and chitosan — a review"; *Journal of Controlled Release*; 2006; **114**; 1–14
- ²⁰ Temenoff, J.S.; Mikos, A.G.; "Injectable biodegradable materials for orthopedic tissue engineering"; *Biomaterials*; 2000; **21**; 2405-2412.
- ²¹ Hutmacher, D.W. "Scaffolds in tissue engineering bone and cartilage"; *Biomaterials*; 2000; **21**; 2529-2543.
- ²² Chena, G.-Q.; Wu, Q. "The application of polyhydroxyalkanoates as tissue engineering materials"; *Biomaterials*; 2005; **26**; 6565–6578.
- ²³ Leong, K.F.; Cheah, C.M.; Chua, C.K. „Solid Freeform Fabrication of three-dimensional scaffolds for engineering replacement tissues and organs"; *Biomaterials*; 2003; **24**; 2363-2378.
- ²⁴ Hutmacher, D.W.; Sittering, M.; Risbud, M.V. „Scaffold-based tissue engineering: rationale for computer-aided design and solid freeform fabrication systems"; *Trends in Biotechnology*; 2004; **22**; 354-362.
- ²⁵ Yana, Y.; Xionga, Z.; Hub, Y.; Wangc, S.; Zhanga, R.; Zhang, C. "Layered manufacturing of tissue engineering scaffolds via multi-nozzle deposition"; *Materials Letters* ;2003; **57**; 2623– 2628.
- ²⁶ Yeong, W.-Y.; Chua, C.-K.; Leong, K.-F.; Chandrasekaran, M. "Rapid prototyping in tissue engineering: challenges and potential"; *Trends in Biotechnology*; 2004; **22**; 643-652.
- ²⁷ Landers, R.; Mühlhaupt, R. „Desktop manufacturing of complex objects, prototypes and biomedical scaffolds by means of computer-assisted design combined with computer-guided 3D plotting of polymers and reactive oligomers"; *Macromolecular Materials and Engineering*; 2000; **282**; 17-21.
- ²⁸ Lam, C.X.F.; Moa, X.M.; Teoh, S.H.; Hutmacher, D.W. "Scaffold development using 3D printing with a starch-based polymer"; *Materials Science and Engineering C*; 2002; **20**; 49–56.
- ²⁹ Porter, N.L.; Pilliar, R.M.; Grynepas, M.D. "Fabrication of porous calcium polyphosphate implants by solid freeform fabrication: A study of processing parameters and *in vitro* degradation characteristics"; *Journal of Biomedical Materials Research Part A*; 2001;**56**;504-515
- ³⁰ Yang, S.; Leong, K.-F.; Du, Z.; Chua, C.-K. „The design of Scaffolds for Use in Tissue Engineering. Part II. Rapid Prototyping Techniques"; *Tissue Engineering*; 2002; **8**; 1-11.
- ³¹ Fouassier, J.P. "Photoinitiating Systems"; Vol II, Elsevier: Amsterdam, 1993.
- ³² Schlie, S.; Ngezahayo, A.; Ovsianikov, A.; Fabian, T.; Kolb, H.-A.; Haferkamp, H.; Chichkov, B. "Three-Dimensional Cell Growth on Structures Fabricated from ORMOCER® by Two-Photon Polymerization Technique"; *Journal of Biomaterials Applications*; 2007; **22**; 275-287.
- ³³ Moszner, N.; Salz, U. "New developments of polymeric dental composites"; *Prog. Polym. Sci.*; 2001; **26**; 535-576.
- ³⁴ Ifkovits, J.L.; Burdick, J.A. "Review: Photopolymerizable and Degradable Biomaterials for Tissue Engineering Applications"; *Tissue Engineering*; 2007; **10**; 2369-2385.

- ³⁵ Hill-West, J.L.; Chowdhury, S.M.; Sawhney, A.S.; Pathak, C.P.; Dunn, R.C.; Hubbell, J.A. "Prevention of Postoperative Adhesions in the Rat by In Situ Photopolymerisation of Bioresorbable Hydrogel Barriers"; *Obstetrics and Gynecology*; 1994; **83**; 59-64.
- ³⁶ Burkoth, A.K.; Burdick, J.; Anseth, K.S. "Surface and bulk modifications to photocrosslinked polyanhydrides to control degradation behavior"; *Journal of Biomedical Materials Research Part A*; 2000; **51**; 352-359.
- ³⁷ Tessmar, J.K.; Göpferich, A.M. "Customized PEG-Derived Copolymers for Tissue Engineering Applications"; *Macromolecular Bioscience*; 2007; **7**; 23-39.
- ³⁸ Bryant, S.J.; Anseth, K.S. "The effects of scaffold thickness on tissue engineered cartilage in photocrosslinked poly(ethylene oxide) hydrogels"; *Biomaterials*; 2001; **22**; 619-626.
- ³⁹ Burdick, J.A.; Anseth, K.S. "Photoencapsulation of osteoblasts in injectable RGD-modified PEG hydrogels for bone tissue engineering"; *Biomaterials*; 2002; **23**; 4315-4323.
- ⁴⁰ DeLong, S.A.; Moon, J.J.; West, J.L. "Covalently immobilized gradients of bFGF on hydrogel scaffolds for directed cell migration"; *Biomaterials*; 2005; **26**; 3227-3234.
- ⁴¹ Nuttelman, C.R.; Tripodi, M.C.; Anseth, K.S. "*In vitro* osteogenic differentiation of human mesenchymal stem cells photoencapsulated in PEG hydrogels"; *Journal of Biomedical Materials Research Part A*; 2004; **68A**; 773-782.
- ⁴² Arcaute, K.; Mann, B.K.; Wicker, R.B. "Stereolithography of Three-Dimensional Bioactive Poly(Ethylene Glycol) Constructs with Encapsulated Cells"; *Annals of Biomedical Engineering*; 2006; **34**; 1429-1441.
- ⁴³ Davis, K.S.; Burdick, J.A.; Anseth, K.S. "Photoinitiated crosslinked degradable copolymer networks for tissue engineering applications"; *Biomaterials*; 2003; **24**; 2485-2495.
- ⁴⁴ Rice, M.A.; Sanchez-Adams, J.; Anseth, K.S. "Exogenously triggered, enzymatic degradation of photopolymerized hydrogels with polycaprolactone subunits: experimental observation and modeling of mass loss"; *Biomacromolecules*; 2006; **7**; 1968-1975.
- ⁴⁵ Han, D.K.; Hubbell, J.A. "Synthesis of Polymer Network Scaffolds from L-Lactide and Poly(ethylene glycol) and Their Interaction with Cells"; *Macromolecules*; 1997; **30**; 6077-6083.
- ⁴⁶ Hiemstra, C.; Zhou, W.; Zhong, Z.; Wouters, M.; Feijen, J. „Rapidly in situ forming biodegradable robust hydrogels by combining stereocomplexation and photopolymerization"; *J.Am.Chem.Soc.*; 2007; **129**; 9918-9926.
- ⁴⁷ Dhariwala, B.; Hunt, E.; Boland, T. "Rapid Prototyping of Tissue-Engineering Constructs, Using Photopolymerizable Hydrogels and Stereolithography"; *Tissue Engineering*; 2004; **10**; 1316-1322.
- ⁴⁸ Burkoth, A.K.; Burdick, J.; Anseth, K.S. "Surface and bulk modifications to photocrosslinked polyanhydrides to control degradation behavior"; *Journal of Biomedical Materials Research Part A*; 2000; **51**; 352-359.
- ⁴⁹ Anderson, D.G.; Tweedie, C.A.; Hossain, N.; Navarro, S.M.; Brey, D.M.; Van Vliet, K.J.; Langer, R.; Burdick, J.A. "A Combinatorial Library of Photocrosslinkable and Degradable Materials"; *Advanced Materials*; 2006; **18**; 2614-2618.

- ⁵⁰ Matsuda, T.; Mizutani, M. "Liquid acrylate-encapped biodegradable poly(ϵ -caprolactone-co-trimethylene carbonate). II. Computer-aided stereolithographic microarchitectural surface photoconstructs" *Biomed. Mater. Res.*; 2002; **62**; 395-403.
- ⁵¹ Popov, V.K.; Evseev, A.V.; Ivanov, A.L.; Roginski, V.V.; Volozhin, A.I.; Howdle, S.M. "Laser stereolithography and supercritical fluid processing for custom-designed implant fabrication"; *Journal of Materials Science: Materials in Medicine*; 2004; **15**; 123-128.
- ⁵² Lee, K.-W.; Wang, S.; Fox, B.C.; Ritman, E.L.; Yaszemski, M.J.; Lu, L. "Poly(propylene fumarate) Bone Tissue Engineering Scaffold Fabrication Using Stereolithography: Effects of Resin Formulations and Laser Parameters"; *Biomacromolecules*; 2007; **8**; 1077-1084.
- ⁵³ Fishera, J.P.; Deanb, D.; Mikos, A.G. "Photocrosslinking characteristics and mechanical properties of diethyl fumarate/poly(propylene fumarate) biomaterials"; *Biomaterials*; 2002; **23**; 4333-4343.
- ⁵⁴ Cooke, M.N.; Fisher, J.P.; Dean, D.; Rinnac, C.; Mikos, A.G. "Use of Stereolithography to Manufacture Critical-Sized 3D Biodegradable Scaffolds for Bone Ingrowth"; *J. Biomed. Mater. Res. B*; 2003; **64B**; 65-69.
- ⁵⁵ Chandra, R.; Rustgi, R. "Biodegradable Polymers"; *Prog. Polym. Sci.*; 1998; **23**; 1273-1335.
- ⁵⁶ Weber, L.M.; Hayda, K.N.; Haskins, K.; Anseth, K.S. "The effects of cell-matrix interactions on encapsulated b-cell function within hydrogels functionalized with matrix-derived adhesive peptides"; *Biomaterials*; 2007; **28**; 3004-3011.
- ⁵⁷ Mann, B.K.; Gobin, A.S.; Tsai, A.T.; Schmelden, R.H.; West, J.L. "Smooth muscle cell growth in polymerized hydrogels will cell adhesive and proteolytically degradable domains: synthetic ECM analogs for tissue engineering"; *Biomaterials*; 2001; **22**; 3045-3051.
- ⁵⁸ Hern, D.L.; Hubbell, J.A. "Incorporation of adhesion peptides into nonadhesive hydrogels useful for tissue resurfacing"; *J. Biomed. Mater. Res.*; 1998; **39**; 266-276.
- ⁵⁹ Benoit, D.S. W.; Anseth, K.S. "The effect on osteoblast function of colocalized RGD and PHSRN epitopes on PEG surfaces"; *Biomaterials*; 2005; **26**; 5209-5220.
- ⁶⁰ Müh, E.; Zimmermann, J.; Kneser, U.; Marquardt, J.; Mühlhaupt, R.; Stark, B. "LysineurethanedimethacrylateFa novel generation of amino acid based monomers for bone cements and tissue repair" *Biomaterials* 2002; **23**; 2849-2854.
- ⁶¹ Brinkman, W.T.; Nagapudi, K.; Thomas, B.S.; Chaikof, E.L. "Photo-Cross-Linking of Type I Collagen Gels in the Presence of Smooth Muscle Cells: Mechanical Properties, Cell Viability, and Function"; *Biomacromolecules*; 2003; **4**; 890-895.
- ⁶² Schacht, E. "New medicaments based on polymers composed of methacrylamide modified gelatin"; *WO Pat. Appl.* 1998, WO 98/55161, 21.
- ⁶³ Zimmermann, J.; Bittner, K.; Stark, B.; Mühlhaupt, R. "Novel hydrogels as supports for in vitro cell growth: poly(ethylene glycol)- and gelatine-based (meth)acrylamidopeptide macromonomers"; *Biomaterials*; 2002; **23**; 2127-2134.
- ⁶⁴ Gonen-Wadmany, M.; Oss-Ronen, L.; Seliktar, D. "Protein-polymer conjugates for forming photopolymerizable biomimetic hydrogels for tissue engineering"; *Biomaterials*; 2007; **28**; 3876-3886.

- ⁶⁵ Bencherif, S.A.; Srinivasan, A.; Horkay, F.; Hollinger, J.O.; Matyjaszewski, K.; Washburn, N.R. "Influence of the degree of methacrylation on hyaluronic acid hydrogels properties"; *Biomaterials*; 2008; **29**; 1739-1749.
- ⁶⁶ Poon, Y.F.; Zhu, Y.B.; Shen, J.Y.; Chan-Park, M.B.; Ng, S.C. "Cytocompatible Hydrogels Based on Photocrosslinkable Methacrylated *O*-Carboxymethylchitosan with Tunable Charge: Synthesis and Characterization"; *Adv. Funct. Mater.*; 2007; **17**; 2139-2150.
- ⁶⁷ Kim, J.; Lee, K.-W.; Hefferan, T.E.; Currier, B.L.; Yaszemski, M.J.; Lu, L. "Synthesis and Evaluation of Novel Biodegradable Hydrogels Based on Poly(ethylene glycol) and Sebacic Acid as Tissue Engineering Scaffolds"; *Biomacromolecules*; 2008; **9**; 149-157.
- ⁶⁸ Rodriguez, G.; Gallardo, A.; San Roman, J.; Rebuelta, M.; Bermejo, P.; Bujan, J.; Bellon, J.M.; Honduvilla, N.G.; Escudero, C. "New resorbable polymeric systems with antithrombogenic activity"; *Journal of Materials Science: Materials in Medicine*; 1999; **10**; 873-878.
- ⁶⁹ Koepff, P.; Bräumer, K.; Babel, W. "Biodegradable, water-resistant polymer material"; *US Pat. Appl.* 1998; US 5.733.994, 3.
- ⁷⁰ Sorensen, W.R.; Sweeny, F.; Campbell, T.W. "Preparative Methods of Polymer Chemistry"; Third Edition; 73. ISBN 0-471-58992-6.
- ⁷¹ Bauer, B. "Synthese und Prüfung von Betonadditiven auf Basis nachwachsender Rohstoffe"; *Dissertation*; 1998; 69.
- ⁷² Wong, K.K.W.; Cölfen, H.; Whilton, N.T.; Douglas, T.; Mann, S. "Synthesis and characterization of hydrophobic ferritin proteins"; *Journal of Inorganic Biochemistry*; 1999; **76**; 187-195.
- ⁷³ Sengonul, M.; Ruzicka, J.; Attygalle, A.B.; Libera, M. "Surface modification of protein nanocontainers and their self-directing character in polymer blends"; *Polymer*; 2007; **48**; 3632-3640.
- ⁷⁴ Kushibiki, T.; Matsuoka, H.; Tabata, Y. "Synthesis and Physical Characterization of Poly(ethylene glycol)-Gelatin Conjugates"; *Biomacromolecules*; 2004; **5**; 202-208.
- ⁷⁵ Toledano, O.; Magdassi, S. "Emulsification and Foaming Properties of Hydrophobically Modified Gelatin"; *Journal of colloid and interface science*; 1998; **200**; 235-240.
- ⁷⁶ Montheard, J.P.; Chatzopoulos, M.; Chappard, D. "2-Hydroxyethyl methacrylate (HEMA): chemical properties and applications in biomedical fields"; *Journal of Macromolecular Science, Reviews in Macromolecular Chemistry and Physics*; 1992; **C32**; 1-34.
- ⁷⁷ Brandrup, J., Immergut, E.H. and Grulke, E.A. In *Polymer Handbook* 4th Ed.; John Wiley & Sons Inc: New York, 365-381, 1999.
- ⁷⁸ Davis, K.A.; Burdick, J.A., Anseth, K.S. „ Photoinitiated crosslinked degradable copolymer networks for tissue engineering applications"; *Biomaterials* 2003; **24**; 2485-2495.
- ⁷⁹ Lee, T.Y.; Roper, T.M.; Jönsson, E.S.; Guymon, C.A.; Hoyle, C.E. "Influence of Hydrogen Bonding on Photopolymerization Rate of Hydroxyalkyl Acrylates"; *Macromolecules*; 2004; **37**; 3659-3665.
- ⁸⁰ Kasuga, T.; Ota, Y.; Nogami, M.; Abe, Y. "Preparation and mechanical properties of polylactic acid composites containing hydroxyapatite fibers"; *Biomaterials*; 2001; **22**; 19-23.
- ⁸¹ Koenig, M.F; Huangt, S.J. "Biodegradable blends and composites of polycaprolactone and starch derivatives"; *Polymer*; 1995; **36**; 1877-1882.

- ⁸² Gibson, L.; Ashby, M.F. In: Cellular solids – structures and properties, 2nd edition, Cambridge University Press, 1997.
- ⁸³ Geiss, M. „Mechanische Eigenschaften partikelverstärkter Biopolymere“; diploma thesis; 2006; 40.
- ⁸⁴ Yeung, T.; Georges, P.C.; Flanagan L.A.; Marg B.; Ortiz M.; Funaki M.; Zahir, N.; Ming, W.; Weaver, V.; Janmey, P.A. „Effects of Substrate Stiffness on Cell Morphology, Cytoskeletal Structure, and Adhesion“; Cell Motil Cytoskeleton; 2005; **60**; 24-34.
- ⁸⁵ Kong, H.J.; Polte T.R.; Alsberg E.; Mooney D.J.; “FRET measurements of cell-traction forces and nano-scale clustering of adhesion ligands varied by substrate stiffness”; Proc Natl Acad Sci USA; 2005; 102; 4300-4305.
- ⁸⁶ Keselowsky, B.G.; Collard, D.M.; Garcia, A.J. “Surface chemistry modulates focal adhesion composition and signaling through changes in integrin binding”; Biomaterials; 2004; **25**; 5947-5954.
- ⁸⁷ Keselowsky, B.G.; Collard, D.M.; Garcia, A.J. “Integrin binding specificity regulates biomaterial surface chemistry effects on cell differentiation”; Proc Natl Acad Sci USA; 2005; **102**; 5953-5957.
- ⁸⁸ Fukazawa, H.; Nakano, S.; Mizuno, S.; Uehara, Y. “Inhibitors of Anchorage-Independent Growth Affect the Growth of Transformed Cells on Poly(2-hydroxyethyl methacrylate)-coated Surfaces”; Int J Cancer; 1996; **67**; 876-82.
- ⁸⁹ Crivello, J., Dietliker V. In: Chemistry & Technology of UV-EB Formulation for Coatings, Inks & Paints. Bradley, G., London: Sita Technology Ltd., Vol. 3, 268, 1998.
- ⁹⁰ Heller, C.; Pucher, N.; Seidl, B.; Kuna, L.; Satzinger, V.; Schmidt, V.; Lichtenegger, H.; Stampfl, J.; Liska, R. „One- and two-photon activity of cross-conjugated photoinitiators with bathochromic shift“; J. Pol. Sci. Part A: Polym. Chem.; 2007; **45**; 3280-3291.
- ⁹¹ Fisher, J.P.; Holland, T.A.; Dean, D.; Mikos, A.G. ”Photoinitiated Cross-Linking of the Biodegradable Polyester Poly(propylene fumarate). Part II. In Vitro Degradation” Biomacromolecules; 2003; **4**; 1335-1342.
- ⁹² Williams, C.G., Malik, A.N., Kim, T.K., Manson, P.N., Elisseff, J.H. “Variable cytocompatibility of six cell lines with photoinitiators used for polymerizing hydrogels and cell encapsulation”; Biomaterials; 2005; **26**; 1211-1218.
- ⁹³ Kolyagina, G.F., Glazunova, N.P., Meshcheryakov, V.I., Gavrilov, L.D., Vereshchagin, L.I. “Therapeutic activity of ethynyl ketones during experimental trichophytia” Pharmaceutical Chemistry Journal; 1981; **15**; 103-105.
- ⁹⁴ Wei, J.; Wang, H.; Jiang, X.; Yin, J. „Novel Photosensitive Thio-Containing Polyurethane as Macrophotoinitiator Comprising Side-Chain Benzophenone and Co-Initiator Amine for Photopolymerization“; Macromolecules; 2007; **40**; 2344-2351.
- ⁹⁵ Angiolini, L.; Caretti, D.; Salatelli, E. “Synthesis and photoinitiation activity of radical polymeric photoinitiators bearing side-chain camphorquinone moieties”; Macromol Chem Phys; 2000; **201**; 2646-2653.

- ⁹⁶ Chen, Y.; Loccufier, J.; Vanmaele, L.; Barriau, E.; Frey, H. "Novel Multifunctional Polymeric Photoinitiators and Photo-Coinitiators Derived from Hyperbranched Polyglycerol" *Macromol Chem Phys*; 2007; **208**; 1694-1706.
- ⁹⁷ Chen, Y.; Loccufier, J.; Vanmaele, L.; Frey, H. "Novel multifunctional hyperbranched polymeric photoinitiators with built-in amine coinitiators for UV curing"; *J Mater Chem*; 2007; **17**; 3389-3392.
- ⁹⁸ Handbook of Metathesis; Grubbs, R. H., Ed.; Wiley-VCH: Weinheim, Germany, 2003.
- ⁹⁹ Slugovc, C. "The Ring Opening Metathesis Polymerisation Toolbox"; *Macromol Rapid Commun*; 2004; **25**; 1283-1297.
- ¹⁰⁰ Slugovc, C.; Riegler, S.; Hayn, G.; Saf, R.; Stelzer, F. "Highly Defined ABC Triblock Cooligomers and Copolymers Prepared by ROMP Using an N-Heterocyclic-Carbene-Substituted Ruthenium Benzylidene Initiator"; *Macromol Rapid Commun*; 2003; **24**; 435-439.
- ¹⁰¹ Buchmeiser, M. R. "Homogeneous Metathesis Polymerization by Well-Defined Group VI and Group VIII Transition-Metal Alkylidenes: Fundamentals and Applications in the Preparation of Advanced Materials"; *Chem Rev*; 2000; **100**; 1565-1604.
- ¹⁰² Neckers, D.C. "Rose Bengal"; *J Photochem Photobiol A*; 1989; **47**; 1-29.
- ¹⁰³ Grotzinger, C.; Burget, D.; Jaques, P.; Fouassier, J.P. "Photopolymerization Reactions Initiated by a Visible Light Photoinitiating System: Dye/Amine/Bis(trichloromethyl)-Substituted-1,3,5-Triazine"; *Macromol Chem Phys*; 2001; **202**; 3513-3522.
- ¹⁰⁴ Neumann, M.G.; Schmitt, C.C.; Maciel, H.J. "The photopolymerization of styrenesulfonate initiated by dyes The effect of monomer aggregation"; *Photoch Photobiol A*; 2005; **175**; 15-21.
- ¹⁰⁵ Satoh, M.; Shirai, K.; Saitoh, H.; Yamauchi, T.; Tsubokawa, N. "Photografting of Polymers onto Nanosized Silica Surface Initiated by Eosin Moieties Immobilized onto the Surface"; *J Polym Sci A*; 2005; **43**; 600-606.
- ¹⁰⁶ Schaap, P.A.; Thayer A.L.; Blossey, E.C.; Neckers, D.C. "Polymer-Based Sensitizers for Photooxidations. II"; *J Am Chem Soc*; 1975; **97**; 3741-3745.
- ¹⁰⁷ Burget, D.; Fouassier, J.P.; Amat-Guerri, F.; Mallavia, R.; Sastre, R. "Enhanced activity as polymerization photoinitiators of Rose Bengal and Eosin esters with an *O*-benzoyl- α -oxoimine group: The role of the excited state reactivity"; *Acta Polym*; 1999; **50**; 337-346.
- ¹⁰⁸ Jing, B.; Zhang, M.; Shen, T. „An Unusual Photosensitizer: Dyad of Eosin-Tris(2,2'-bipyridine)Ru(II)“ *Org Lett*; 2003; **5**; 3709-3711.
- ¹⁰⁹ Farsari, M.; Filippidis, G.; Sambani, K.; Drakakis, T.S.; Fotakis, C.J "Two-photon polymerization of an Eosin Y-sensitized acrylate composite"; *Photochem Photobiol A*; 2006; **181**; 132-135.
- ¹¹⁰ Jordan, O.; Desmangles, A.-I.; Marquis-Weible, F. "Interfacial Photopolymerization of b-Cell Clusters: Approaches to Reduce Coating Thickness Using Ionic and Lipophilic Dyes"; *Biotechnol Bioeng*; 2001; **72**; 634-641.
- ¹¹¹ Chaikof, E.L.; Orban, J.M.; Faucher, K.M.; Dluhy, R.A. "Cytomimetic Biomaterials. 4. In-Situ Photopolymerization of Phospholipids on an Alkylated Surface"; *Macromolecules*; 2000; **33**; 4205-4212.
- ¹¹² Fuassier, J.P.; Chesneau E. "Polymérisation induite sous irradiation laser visible, 4. Le système éosine/photoamorceur ultra-violet/amine"; *Macromol Chem*; 1991; **192**; 245-260.

- ¹¹³ Padon, K.S.; Scranton, A.B. "A Mechanistic Investigation of the Three-Component Radical Photoinitiator System Eosin Y Spirit Soluble, NMethyl-diethanolamine, and Diphenyliodonium Chloride"; *J Polym Sci A*; 2001; **39**; 715-723.
- ¹¹⁴ Sandholzer, M.; Lex, A.; Trimmel, G.; Saf, R.; Stelzer, F.; Slugovc, C. "Xanthene dye functionalized norbornenes for the use in ring opening metathesis polymerization"; *J. Polym. Sci. Part A: Polym. Chem.*; 2007; **45**; 1336-1348.
- ¹¹⁵ Sanford, M.S.; Love, J.A.; Grubbs, R.H. "A Versatile Precursor for the Synthesis of New Ruthenium Olefin Metathesis Catalysts"; *Organometallics*; 2001; **20**; 5314-5318.
- ¹¹⁶ Timpe, H.-J.; Jokusch, S.; Körner, K. Radiation curing in polymer science and technology; Fouassier, J. P.; Rabek, J. F. Eds. Elsevier Applied Science, London and New York, 1993, Vol II, p.580.
- ¹¹⁷ Schuster, M. „Photopolymerisierbare Biopolymere für Knochenersatzmaterialien“; diploma thesis; 2005.
- ¹¹⁸ Neumeister, A.; Himmelhuber, R.; Temme T.; Stute, U. "Generation of micro mechanical devices using stereolithography"; 17th Solid Freeform Fabrication Symposium 2006; University of Texas, Austin, 12-24.
- ¹¹⁹ Sun, H.-B.; Kawata, S. "Two-Photon Laser Precision Microfabrication and its Applications to Micro-Nano Devices and Systems"; *Journal of Lightwave Technology*; 2003; **21**, 624-33.
- ¹²⁰ Uzulina, I.; Abele, S.; Zicmanis, A.; Guyot, A. "Methacrylic maleic bifunctional stabilizer in emulsion Polymerization"; *Macromol. Rapid Commun.*; 1998; **19**; 397-402.
- ¹²¹ Pöchlauer, P.; Hendel, W. „One-Pot Formation of Succinimidyl Esters by the System Chlorophosphate/Hydroxysuccinimide/Base“; *Tetrahedron*; 1998; **54**; 3489-3494.
- ¹²² Hern, D.L.; Hubbell, J.A.; "Incorporation of adhesion peptides into nonadhesive hydrogels useful for tissue resurfacing"; *Journal of Biomedical Materials Research Part A*; 1998; **39**; 266-276.
- ¹²³ Li, J.; Kao, W.J. "Synthesis of Polyethylene Glycol (PEG) Derivatives and PEGylated-Peptide Biopolymer Conjugates"; *Biomacromolecules*; 2003; **4**; 1055-1067.
- ¹²⁴ Kushibiki, T.; Matsuoka, H.; Tabata, Y.; "Synthesis and Physical Characterization of Poly(ethylene glycol)-Gelatin Conjugates"; *Biomacromolecules*; 2004; **5**; 202-208.
- ¹²⁵ Toledano, O.; Magdassi, S. "Formation of Surface Active Gelatin by Covalent Attachment of Hydrophobic Chains"; *Journal of colloid and interface science*; 1997; **193**; 172-177.
- ¹²⁶ Maier, L. "Organic Phosphorus Compounds 60. The direct synthesis of tris(N-substituted carbamoyl) phosphine oxides"; *Helvetica Chimica Acta*; 1973; **56**; 1252-1257.
- ¹²⁷ Sandholzer, M.; Schuster, M.; Varga, F.; Liska, R.; Slugovc, C. "ROMP Based Photoinitiator-Coinitiator Systems with Improved Migration Stability"; *Journal of Polymer Science: Part A: Polymer Chemistry*; 2008; **46**, 3648-3661.
- ¹²⁸ Sandholzer, M. "Functionalized polymers and polymer particles prepared by ROMP"; Dissertation; 2008
- ¹²⁹ Seybold, P.G.; Gouterman, M.; Callis, J. "Calorimetric, photometric, and lifetime determinations of fluorescence yields of fluorescein dyes"; *Photochem Photobiol*; 1969; **9**; 229-242.
- ¹³⁰ Du, H.; Fuh, R.A.; Li, J.; Corkan, A.; Lindsey, J.S. "PhotochemCAD[‡]: A Computer-Aided Design and Research Tool in Photochemistry"; *Photochem Photobiol*; 1998; **68**; 141-142.

Curriculum Vitae – Monika Schuster

Margaretenstrasse 56/2/20

A-1050 Vienna, Austria

monika.m.schuster@gmx.at

Personal Details

Marital status single

Date and Place of Birth: November 26th 1980; Vienna, Austria

Nationality: Austrian

Education

PhD at the Vienna University of Technology, March 2005 – June 2008

Vienna University of Technology, M.Sc. in Chemistry, 2005

High School Degree, Gymnasium Baden, 1999

Work Experience

01/2007 – 06/2008 Project Assistant at the Vienna University of Technology, Institute of Applied Synthetic Chemistry

03/2005 – 12/2006 Project Assistant at the Vienna University of Technology, Institute of Materials Science

08/2002 Industrial training at Novartis

1999 - 2001 Industrial training at Siemens

Achievements

01/2007 DOC-fFORTE fellowship of the Austrian Academy of Sciences

04/2006 Poster award, Junior Scientist Conference 2006

01/2006 TU-BioMed award 2005

07/2005 Poster award, Austrian Polymer Meeting 2005

10/2002 Scholarship for extraordinary achievement from the Vienna University of Technology